January 2013

Immobilization and Characterization of Physisorbed Antibody Films Using Pneumatic Spray as Deposition Technique

Jhon J. Figueroa
University of South Florida, jjfiguer22@aol.com

Immobilization and Characterization of Physisorbed Antibody Films Using Pneumatic Spray as Deposition Technique

by

Jhon Figueroa

A dissertation submitted in partial fulfillment
of the requirements of the degree of
Doctor of Philosophy
Department of Chemistry
College of Arts and Sciences
University of South Florida

Major professor: Rudy Schlaf, Ph.D.
Xiao Li Ph.D.
Li-June Ming Ph.D.
Abdul Malik Ph.D.

Date of approval:
November 14, 2013

Keywords: Biosensors, avidin-biotin bridge, surface morphology, antibody Immobilization

DEDICATION

This dissertation is dedicated principally to God who gave the strength to achieve the unachievable. I want to honor Him in all that I did and in all that I would do after this stage. I also dedicate this to my dear wife Ruth Mary who was able to accept all the hard conditions that brought the challenge of pursuing a PhD degree. I have to recognize you nena as inherent part of this achievement and thank you for your commitment, support, appreciation, patience, love and overall thank you for being my friend, I love you.

ACKNOWLEDGMENTS

The first person that I want to acknowledge is Dr. Schlaf who with his guidance, advice, trust and support has helped me to complete all the requirements to achieve this dissertation. There are many words to express feelings, but two can summarize well what I feel towards him: gratitude and admiration for what he has done through these years.

I also want to thanks the committee members for their time and guidance making it possible to achieve this dream.

I would like to thanks Dr. Lim and his team in the Advanced Biosensor Laboratory for all the technical support given to me and especially to Sonia Magana who has been an invaluable asset to this project and an incomparable source of knowledge; thank you Sonia for all the fructiferous scientific discussions.

Thank you to all the members of the surface science laboratory for their support and unconditional help especially Eric Tridas and Daniel Gomez. Finally, I want to thank my parents, family, church members and friends who in one way or another were a crucial part of this achievement by their patience and understanding.

TABLE OF CONTENTS

LIST OF TABLES

LIST OF FIGURES

LIST OF ABBREVIATIONS

ABB	Avidin-biotin bridge
AF647	Alexa Fluor 647 dye
AFM	atomic force microscope
ATR-FTIR	attenuated total reflectance-Fourier transform infrared spectroscopy
CCD	charge-coupled device
Fab	Fragment of antigen binding
Fc	Fragment crystallizable
FM	Frank-van der Merve
GFP	Green fluorescent protein dye
ICP-MS	Inductively coupled plasma mass spectrometry
IgG	Immunoglobulin G
IR	Infrared
kDa	Kilodaltons
LBAA	Luria-Bertani, arabinose, ampicillin
NaPCl	Sodium Phosphate / Sodium Chloride buffer
PBS	Phosphate Buffered Saline
PS	Pneumatic spray
PVDF	polyvinylidene difluoride

ROI	Region of interest
Rq	Root mean square average
SD	Standard deviation
SNR	Signal to noise ratio
Tbkg	Total background
TSA	Tryptic Soy Agar
UV/vis	Ultraviolet visible spectroscopy
XPS	x-ray photoemission spectroscopy

ABSTRACT

The immobilization of antibodies on silica surfaces has been a wide and common practice via crosslinking with the formation of covalent bonds between surface and antibody. The formation of antibody thin films on solid surfaces using pneumatic spray (PS) as the deposition technique and the analysis of the surface morphology of these films were investigated during this study. The pneumatic spray method was compared with the covalent bonding method Avidin-Biotin Bridge (ABB). The intensities and capture efficiency tests showed similar results for both techniques with a lower signal-to-noise ratio (SNR) for the PS deposited films. Specificity tests suggested that the bio-sensitivity of the antibody films that were pneumatically sprayed maintained their capture abilities after the immobilization process. Analysis obtained from the attenuated total reflectance Fourier transform infrared ATR-FTIR support these results indicating that the antibodies retained their native structure and chemical stability thorough the induced physisorption process. The pneumatic spray films also preserve mechanical stability by adhering to the surface after the rinsing procedures.

Capture efficiency was tested for both immobilization techniques, the results of which were similar. The pneumatic spray technique was also tested using a diverse range of deposition times. It was shown that a 2 minute deposition time was sufficient to produce a film with similar capture efficiency to the avidin-

biotin bridge technique. The surface density obtained for the 2 minute deposition was 9.05 ng/mm^2, which is higher than the range of 2.2 to 4.74 ng/mm^2 reported for the avidin-biotin bridge technique[1-3]. The contact angle measurements for the pneumatic spray films showed a higher hydrophobicity compared with the avidin-biotin bridge films. This is due to the higher surface roughness obtained for the avidin-biotin bridge films, a higher surface density for the PS and the random orientation of the antibodies in the pneumatic spray films. A study of shelf life showed that the pneumatic spray technique produces stable films that can be used for as long 100 days (study performed only up to 100 days) with similar capture efficiency to those prepared in the same day.

To further understand the improvement in capture efficiency of the pneumatic spray films, the surface morphology was investigated to determine its influence in the cell adhesion process. The surface was characterized by several different techniques: ellipsometry to determine the thickness of the films, atomic force microscopy (AFM) to calculate the surface roughness, optical microscopy to identify particle formation during antibody immobilization process, fluorescent microscopy and sandwich fluorescent immunoassay to observe the immobilization patterns of antibodies and antigens on the surface, contact angle measurements to analyze the wettability of the antibody films and X-ray photoelectron spectroscopy (XPS) to confirm the presence of antibody on both deposition methods and to propose a growth model for the pneumatic spray deposition technique.

A possible explanation for the similar results of capture efficiency for both techniques can be attributed to three main factors. First, the antibodies retained their native structure thorough the induced physisorption process allowing then to capture antigen normally. Second, the lack of orientation of the antibodies in the pneumatic films was compensated by high surface density thereby offering more binding sites to capture antigens. Third, hydrophobic surfaces are favorable to cell adhesion, therefore the high hydrophobicity of the pneumatic spray films increases the capture efficiency. It is important to mention that the time that it takes to produce the immunoassay surfaces was reduced dramatically from more than twenty four hours for the avidin-biotin bridge films to only a few minutes for the pneumatic spray films. In addition, pneumatic spray films significantly reduce the amount of materials and chemicals used in the deposition process. These factors make the pneumatic spray technique an excellent technique for the immobilization of antibodies on glass slides for commercial biosensor devices.

CHAPTER 1. INTRODUCTION AND FUNDAMENTALS

1.1 Outline and motivation

The use of biosensors has become an important part of many industries due to the importance of pathogen monitoring. Quality assurance in food, agriculture and pharmaceutical industry, monitoring the environment for contaminants, developing new methods for the detection of biological agents in warfare and the identification of important biomolecules in medical diagnostics are some of the common uses of biosensors[4-7]. Desirable properties for these biosensors include high sensitivity and specificity to a variety of pathogens, cheap mass production and easy operation in the field. One of the most popular and well known sensor devices is the evanescent wave biosensor[8]. Evanescent waves are formed when electromagnetic waves go from a medium of a high refractive index to one with a less refractive index. If the incidence angle is greater than the critical angle, the wave undergoes total internal reflection. At its boundary, the energy of the wave is totally reflected but an electromagnetic field extends from the interface into the medium with the lower refractive index. This field is the evanescent wave which decays exponentially with the distance from the interface. The materials used to fabricate planar array evanescent wave biosensors must comply with some minimum criteria with respect to the refractive index. Glass complies with almost all of those criteria (especially when doped)[9].

The biological capture agent (i.e. antibody) of the biosensor must be attached to the sensor in a way that the biomolecules preserve their biological activity and chemical attributes. Planar waveguides designed specifically for the evanescent wave technique are based on a variety of methods such as covalent bonding or physical adsorption[10]. The immunoassay used in many current protocols immobilizes antibodies onto a glass surface via covalent bonds with the most common being the Avidin-biotin bridge (ABB) technique. This process involves many steps and can take days complete. Due to the high number of steps and the complexity of the process, the ABB technique is error prone. The ABB procedure also uses a variety of hazardous chemicals resulting in a less environmentally friendly protocol.[11-13]

The presented research explores a new methodology for the fabrication of immunoassays targeting the common pathogen *E. coli* O157:H7 using a low flow pneumatic nebulizer to immobilize the antibody to planar waveguides. A short spray deposition of the antibodies creates a thin film that is adsorbed on the surface of the glass with an interaction force strong enough to withstand the rigors of the rinsing procedures carried out during the immunoassay process. The film also keeps the functionality and specificity of the antibodies at the same level of the avidin-biotin bridge process. This unexpected result warranted further investigation of the physical properties of the sprayed films with experiments examining the surface morphology in the context of the excellent chemical and mechanical stability of the films.

The thickness and film composition was investigated by ellipsometry and XPS. Sandwich immunoassay and ATR-FTIR experiments showed that the films well preserve to preserve their native chemical structure and their biological activity. Fluorescent microscopy and AFM showed that physical adsorption was facilitated through rapid evaporation of the solvent during the nebulization process and complete solvent removal from the droplet at the surface. A central feature of the pneumatic spray process is its non-equilibrium characteristics which allowed direct control over the thickness and density of the adsorbed material. This is in contrast to immersion/ incubation based physisorption processes, where usually an equilibrium-based deposition state results.

In general, the spray process offers a number of practical advantages over the avidin-biotin bridge immunoassay method that include a high process speed, an almost chemical-free protocol, consistent coverage of the surface, and easy set up suggesting that large scale manufacturing should be possible. Additionally, the relative low cost and easy maintenance of the equipment makes the pneumatic spray technique an inexpensive and efficient immunoassay preparation process.

1.2 Immobilization methods

The biological component of the biosensor is introduced by immobilization onto a solid surface (waveguide). An essential characteristic of the immobilized biomolecule is that its biological activity has to be preserved in order to get maximum interaction with the target molecule.

There are many methods to immobilize the biomolecules on the wave guides, the most common being covalent attachment, entrapment within polymer matrices, indirect attachment via intermediate bimolecular species and physical adsorption[9].

The direct covalent attachment of molecules to glass is performed mainly with the use of organoheterosilanes with functionalized chemical groups like COOH-, NH2-, SH-. Then, a cross-linker molecule is used to bond the biomolecule (i.e. antibody) to the silane modified glass surface. One of the reported drawbacks for this technique is the lack of control over the orientation of the antibody at the surface thus reducing the amount of available binding sites for the antigen to interact[11, 14].

The attachment of antibodies through an intermediate protein layer is another approach. Proteins like avidin and its derivatives (Figure 1) have been used resulting in improved sensitivity over direct attachment. However these results were dependent on the type of antibody used[15]. Protein A and protein G were also used to immobilize antibodies to the surface. The advantage of this approach is the orientation of the outer layer molecules. This resulted in an improvement of the sensitivity compared to the direct attachment method[3, 16].

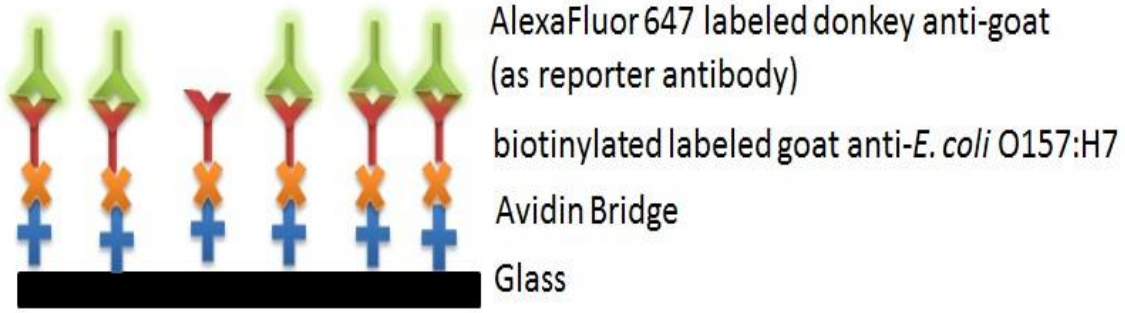

Figure 1. Schematic of attachment through intermediate layer immobilization method. Goat-anti-*E coli O157:H7*antibody and donkey anti-goat reporter antibody were used for the immunoassay.

Static physical adsorption (using a solid–liquid interface) has been used as a simple and rapid option to immobilize biomolecules on various surfaces[17-20] to overcome some of the drawbacks involved with chemical bonding[20-24]. The use of glass surfaces as substrates is not a popular approach for the physical adsorption technique. This is due to the chemical instability of the molecular interaction on the surface at low and high pH values[17, 25, 26]. Other often claimed drawbacks are high non-specific adsorption, and that adsorbed proteins can leach or wash off from the surface if the coated substrate is exposed to a high liquid flow. Furthermore, it has been mentioned that proteins can suffer denaturation after adsorption due to the surface-protein interaction[27] leading to non-specific binding of the antibodies to the target.

The equilibrium process carried out during the immobilization of the protein by static or non-active adsorption (liquid-solid interface) limits the total amount of material that can be attached to the surface, thereby limiting the density of the film[28]. From a kinetic standpoint the adsorption of a biomolecule at the solid-liquid interface can be

divided into two main steps; the first is the transport of the molecules to be adsorbed toward the interface by diffusion and convection and the second is the interaction between the solute and the surface[29] until equilibrium is reached. On the other hand, the non-equilibrium spray deposition process carried out via pneumatic spray (Figure 2), allows to define the surface density. The mass transfer of the biomolecules to the surface via pneumatic spray induces physisorption directly through the evaporation of the solution in a solid-liquid-air interface allowing the tuning of the thickness and the density of the films.

Figure 2. Schematic of pneumatic spray immobilization of antibody on glass surface. Goat-anti-*E coli O157:H7*antibody and donkey anti-goat reporter antibody were used for the immunoassay.

1.3 Pneumatic spray

Pneumatic spray is a widely used technique for the generation of aerosol from biological and chemical solutions. The diverse use of pneumatic nebulizers demonstrates the versatility of the spray technique on which this research work is based.

The performance and characteristics of nebulizers depends on the geometric design as well as the solution characteristics and velocity field of the gas carrier. In

analytical chemistry there are many techniques that require conversion of a sample from liquid to aerosol for analysis. These techniques include flame and electrical plasmas used for atomic absorption, emission, mass and fluorescence spectroscopy [30-33]. Pneumatic nebulization is one of the most widely used techniques for sample introduction of solution or slurry due to its relatively low cost, simplicity of operation, high efficiency and no "dead volume" of solution[34-36]. As shown in Figure 3 the process of pneumatic spray used for the formation of an antibody film involves evaporation of the solvent, and concentration of the antibody inside the drop, the deposition of concentrated antibody solution at the surface, surface diffusion and finally the physisorption of the antibody to the surface.

The type of nebulizer used during these experiments was a low flow concentric nebulizer with a polyvinylidene difluoride (PVDF) body and fused silica capillary (CETAC model DS5) used for ICP-MS applications (Figure 4. Low flow concentric pneumatic nebulizer DS5). Pneumatic spray also has been used as a deposition technique creating inorganic transparent electrically conducting thin films (CdO, In_2O_5Sn, In_2S_3, ZnO) [37-40]. Deposition using a nebulizer to make thin films is improved by the use of a heated substrate, a technique called spray pyrolysis. This technique increases the evaporation rate of the solvent, allowing a dry particle to react with the surface or another particle in a dry state[41]. Biomolecules films also benefit from heating the substrate to control de evaporation of the solvent. In such applications lesser temperatures compatible with the solute (typically in the 40-70 ˚C range) are used[42, 43].

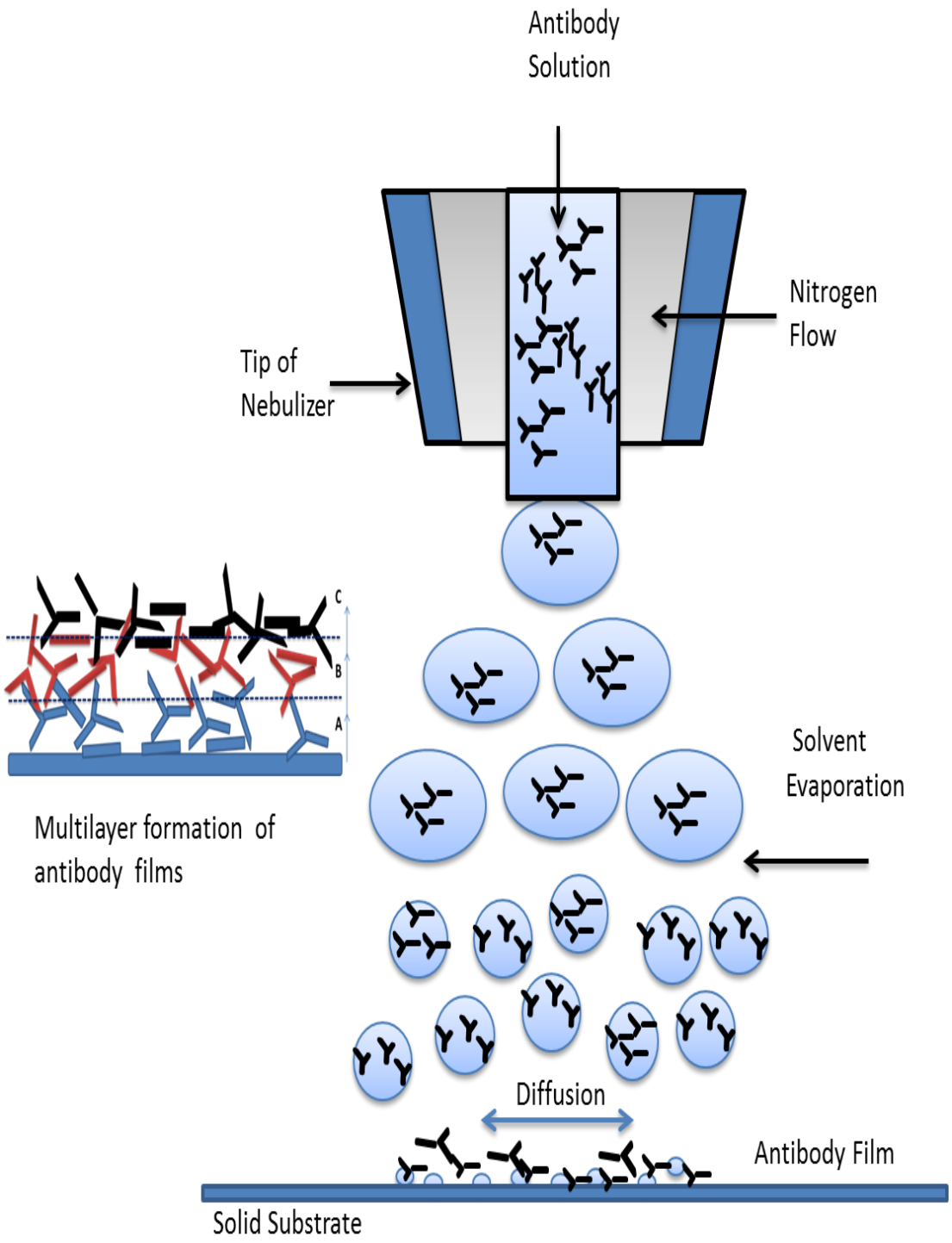

Figure 3 Schematic of pneumatic spray process during deposition of antibody solution on glass surface. A suggested multilayer formation of pneumatic spray antibody films with randomly oriented antibody.

Figure 4. Low flow concentric pneumatic nebulizer DS5

Furthermore, there are biomedical thin film uses for pneumatic spray that further enhance the versatility of the technique. For instance pneumatic spray matrix deposition was used to coat tissue samples for matrix-assisted laser desorption/ionization (MALDI) based molecular imaging of peptides and proteins in biological samples.

This technique has demonstrated a high degree of reproducibility from different investigation sites within a sample as well as results from sample to sample since is able to produce homogeneous thin films that can easily be reproduced[44].

To create a functional antibody film from liquid samples it is necessary to control the amount of solvent evaporation from the aerosol before it reaches the surface. Factors including distance, flow rate, air pressure and ambient temperature have to be investigated to achieve the optimum parameters for the task. The presence of an adjustable stage that can be positioned to control the distance between the emitter of the pneumatic nebulizer and the substrate is an important key for the creation a dry deposited film. As the distance between emitter and substrate is decreased the solvent contained in the aerosol droplets has less time to evaporate. If not properly controlled, this can result in large liquid droplets forming at the surface which will prevent the formation of a dry homogenous film and result in loss of material.

The solution flow rate through the nebulizer must also be carefully controlled in order to generate a fine aerosol. The carrier gas of the nebulizer, which is applied at higher than atmospheric pressure, creates the aerosol by shearing the solution into an unstable liquid film which subsequently breaks down into smaller droplets[45]. The size of the drops in the mist will depend of the ratio between flow rate and air pressure[32]. Some studies suggested that there is a positive correlation between the size of the droplet and the survival of the biomolecule. As the drop size becomes larger more microorganisms can pack together and survive longer upon drying. Because the aerosol

plume emitted from the nebulizer is ejected in a conical shape, the resulting area of deposition will increase as the distance increases. Figure 5 shows a schematic of the relationship between emitter and substrate distance and the diameter of the resulting deposition area using the pneumatic spray method.

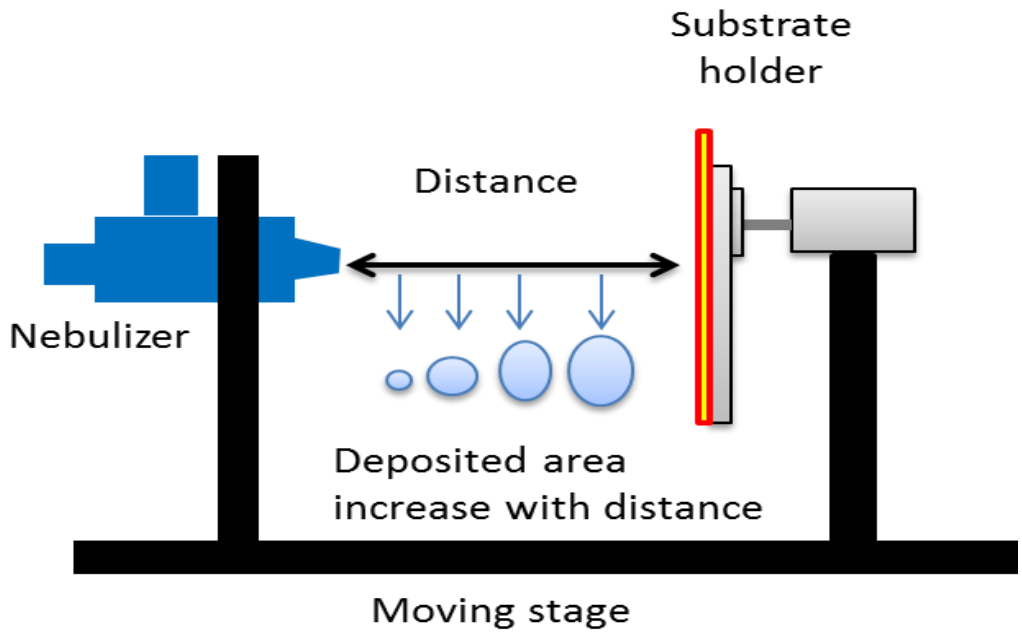

Figure 5. Representative diagram. Effects on the sprayed area by changing the distance between the nebulizer and substrate

1.4 Proteins, structure and importance

The basic component of any protein is the amino acid, which forms polymers via peptide bonds. These polymers form the primary structure of proteins. Each protein has a specific amino acid sequence that defines its main functions and physical characteristics. The secondary protein structure arises from a spatial organization of the linear chain via internal crosslinks such as hydrogen bonds, turns, ß sheets or α helices are formed creating a new geometry. The ß sheets and α helices are periodic structures that create

inner hydrogen bonds to stabilize the protein shape. For example, the α helices turns in clock-wise forms due to the dipoles present in the turns. These hydrogen bonds are almost in parallel to each other and close enough to allow Van der Waals interaction to take place in the helices. ß sheets, on the other hand, form when polypeptides chains are close forming packs of adjacent linear chains via hydrogen bonds. These sheets can be antiparallel (when the chains alternate) or parallel (when the chains have identical orientation). Finally, the tertiary protein structure is formed when secondary structures pack into a three-dimensional structure that is held together by various interactions like hydrophobic/hydrophilic, salt bridges, disulfide bonds or hydrogen bonds.

Proteins can denature under many circumstances based on parameters such as temperature, pressure, shear forces, interaction with other proteins, lyophilization etc. It is very important to keep the basic chemical structure of the antibody intact, especially in the Fab region where the immobilization of the antigen occurs. For this reason it is necessary to test the antibody for specificity after immobilization on a solid surface using a biological test (different antigens) or chemical analysis (ATR-FTIR) and confirm the biological activity of the antibody used.

Antibodies like the goat anti-*E.coli O157:H7* used for these experiments are immunoglobulin or gamma globulin proteins found in the blood or other corporal fluids of vertebrates. Immunoglobulin or IgG is a glycoprotein that has four polypeptide chains linked through disulfide bonds. The total molecular weight of this molecule is approximately 150 kDa with two of these chains being light weight (25 kDa) while the

other two are heavier (50kDa). In a specific antibody the two heavy chains are identical as well as the two light chains, giving to the molecule two identical binding sites for the antigen. Figure 6 shows the basic structure of an immunoglobulin with the two pairs of chains. Each pair of chains has a constant and a variable part (CH,VH) for the heavy and (CL, VL) for the light chain[46, 47]. The antigen binding site is formed by the two variable sections of the heavy and the light chains. There are two types of light chains: lambda (λ) and kappa (κ), and in a given immunoglobulin only one of the two species is present. The heavy chain has five classes or isotypes depending of the structure: immunoglobulin M or IgM, immunoglobulin D or IgD, immunoglobulin G or IgG, immunoglobulin A or IgA, and immunoglobulin E or IgE[48].

The antibody basic structure has a shape of a "Y" with a hinge formed by disulfide bridges in the intersection of the "Y". The section of the molecule where the variable section of the heavy and light chains is located is referred as Fab (Fragment of antigen binding). The other section which does not interact with the antigen was observed to crystallize and for this reason is called Fc (fragment crystallizable) see Figure 6. The antibody-antigen interaction occurs in the Fab region or paratope. The chemical composition of this section (Fab) determines the type of interaction with the antigen and it can vary among subclasses (Idiotype) making the interaction antibody-antigen very specific. The type of heavy chains (sequences of amino-acids) determines the class of the antibody and each one is correlated to a class of immunoglobulin. Gamma chain (ɣ) is IgG, mu (μ) is IgM, alpha (α) is IgA, delta (δ) is IgD and epsilon (ε) is IgE.[49]

The antibody recognizes a region of the antigen called epitope or antigenic determinant (chemical constituents like proteins or carbohydrates) which is a small section of the antigen but enough to be detected. The interaction antibody-antigen is strong but non-covalent in nature and is composed of a variety of interactions like hydrogen bonds, hydrophobic bonds, electrostatic bonds, Van der Waals forces. The unique interaction between one antigenic determinant (epitope) regions of the antigen with the paratope of the antibody is called specificity. The antibody can recognize the antigen with three types of identification: the primary structure of the antigen, isomeric forms of the antigen, and finally by the secondary and tertiary structure of the antigen. The cross reactivity of an antibody is the ability to interact with more than one epitope from different antigens. [50]

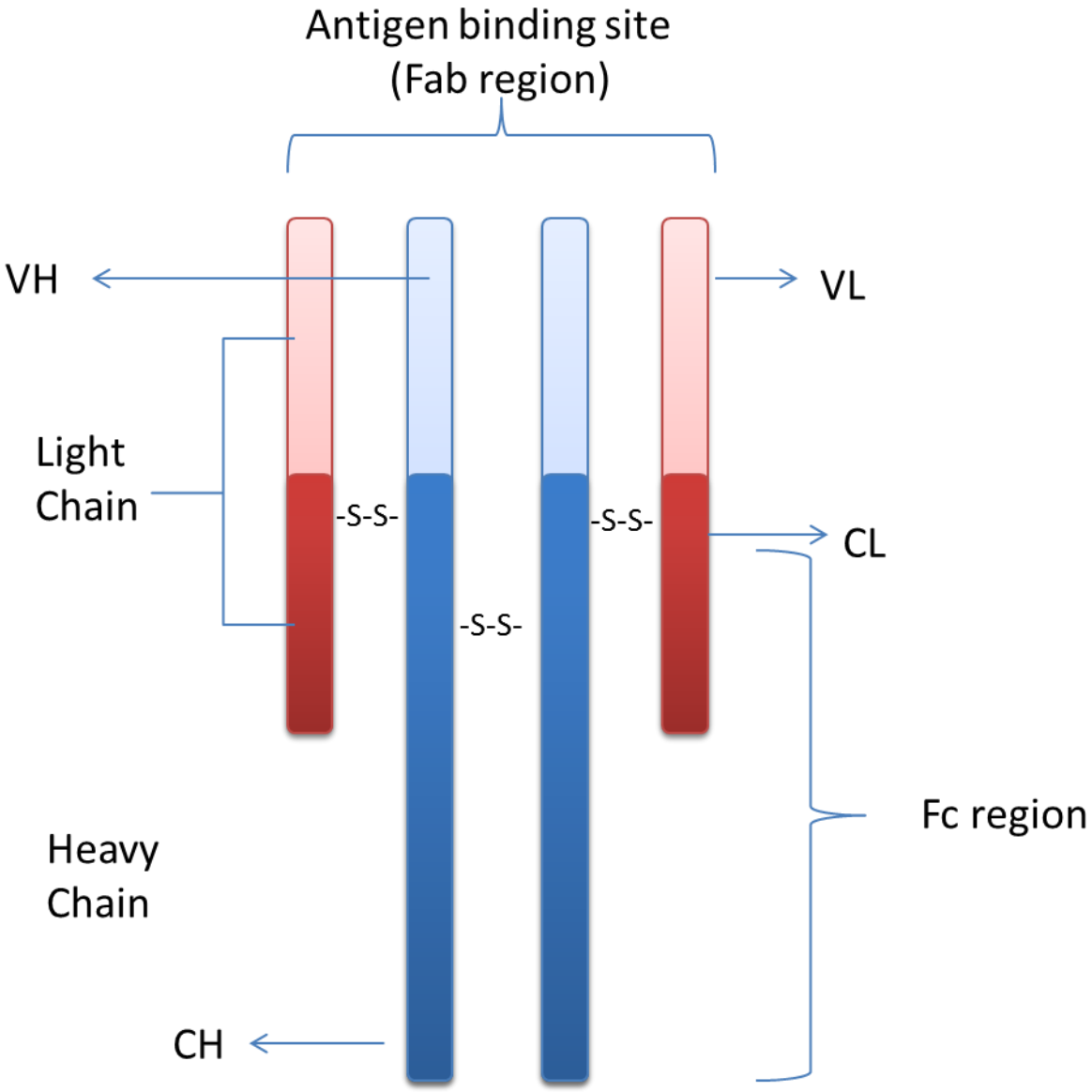

Figure 6. . Antibody basic structure. Each heavy (H) part has a constant (C) and a variable (V) section (VH, CH). The light chain has also two parts one constant and one variable (VL, CL). The chains are linked by disulfide bonds (s-s). Antibody main two regions are fragment antigen binding (Fab) and fragment crystallizable (Fc).

CHAPTER 2. EXPERIMENTAL METHODOLOGY

2.1 Analysis performed by fluorescent microscopy

2.1.1 Visualization of antibody and bacteria patterns

Fluorescent microscopy was initially developed to identify the natural fluorescence emitted by many plant and animal molecules. Over time however, the technique was improved upon and researchers now frequently attach fluorescent molecules to specimens to allow for observation using this technique. When excited, fluorescent molecules (fluorochromes) emit monochromatic light. Typically the fluorochrome chemical structure has a base of aromatic molecules bound with conjugated π bonds. Fluorochromes can be bonded to a macromolecule such as an antibody or bacterium in order to be used as a marker or label[51]. A simple schematic of a fluorescent microscopy is shown in Figure 7.

In fluorescence microscopy a sample containing fluorochromes is illuminated with light of a specific wavelength. An incident photon excites a fluorochrome on the surface, which fluoresces (emits photons with a wavelength of a lower energy).These fluorescent photons are detected through a microscope objective. Two filters are necessary for the technique to function properly. The first monochromatizes the incident wavelength, while the second blocks photons reflected off of the surface from the exciting light source. This technique can be used for the detection of microorganisms that

emit fluorescent light[51, 52]. Labeled molecules with fluorescent tags or fluorochromes[53-57] have been used to develop a variety of techniques to identify and quantify microorganisms including crystal violet assay, direct enumeration and microtiter assay[58].

The well-known antibody-antigen intermolecular interaction and the use of fluorochromes to label them have become a useful tool for a wide range of uses from medical diagnosis to pathogen detection in microbiology [59, 60]. In this project, the bio-recognition properties of antibodies and fluorochromes were used to identify, visualize and calculate a concentration of immobilized biological samples on solid surfaces.

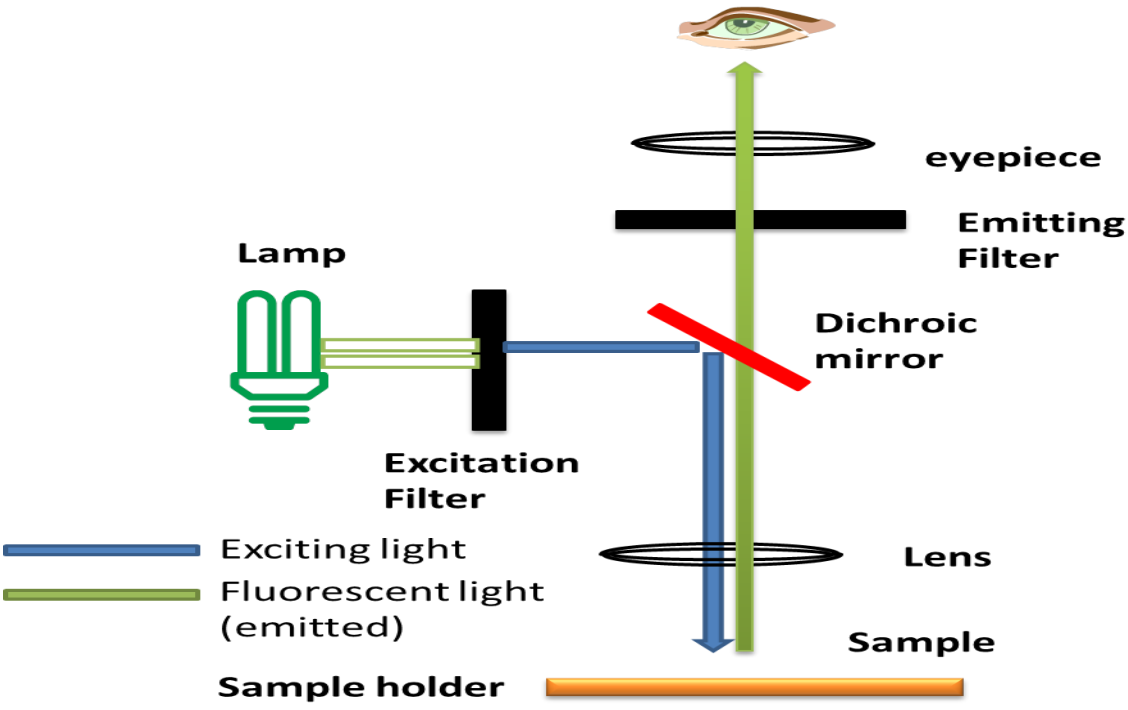

Figure 7. Diagram of the basic components of a fluorescence microscope.

There are many bio-labels used in fluorescent microscopy, however for the experiments performed on this research only three fluorochrome molecules were used. Green fluorescent protein (GFP), as its name states, is a protein that emits green light when excited by ultraviolent light. GFP is often used as a biomarker in immunoassays and attached to pathogens like Escherichia coli O157:H7 allowing researchers to investigate and visualize many characteristics of such bacteria[61]. One of the most important characteristics of GFP is that it has been demonstrated that when attached to other molecules it does not change the natural behavior or biological activity of the labeled molecule, allowing for diverse in vivo analysis.

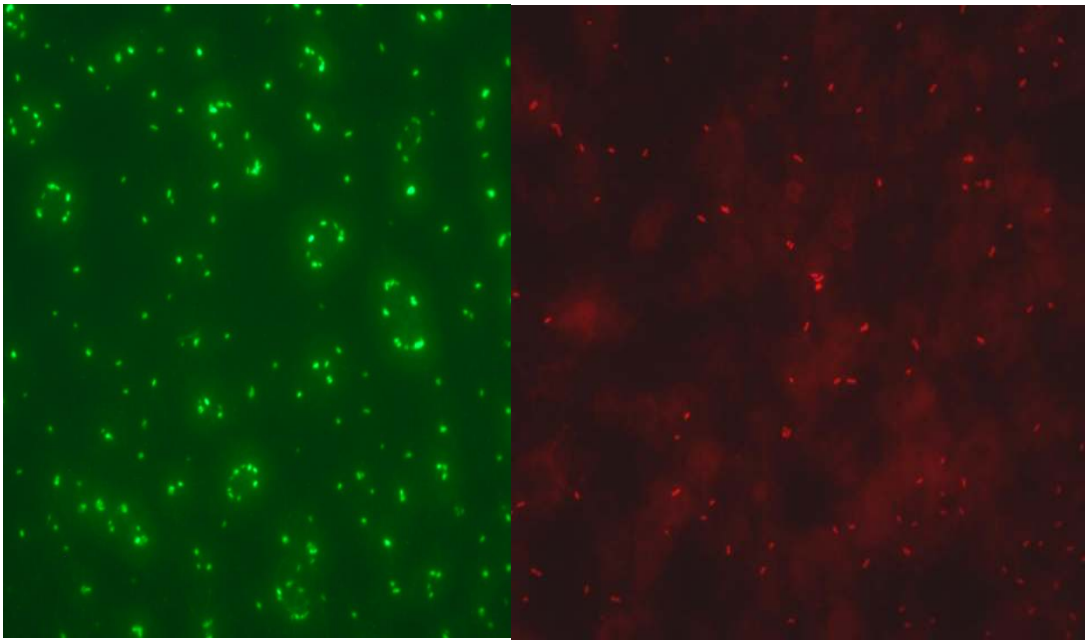

Figure 8. Representative sample of fluorescent biomarkers on antibody and bacteria. Images of E. coli O157: H7. The left image shows GFP- E. coli O157: H7 (green particles) immobilized on an AF647 conjugated anti-E. coli O157: H7 IgG antibody film. The right image shows E. coli O157: H7 immobilized on goat anti-E. coli O157: H7 IgG after being incubated with Rhodamine red conjugated donkey anti goat-E. coli O157:H7 IgG.

The second type of bio-label or fluorochrome molecule used for the immunoassays was Alexa Fluor 647. This fluorochrome is a small dye with good staining capabilities on antibodies and whose emitted light is green when illuminated with ultraviolet light (Figure 8, green background of left image). The final fluorochrome used was Rhodamine red, used as a label for biomolecules including antibodies. As its name suggests the excitation light is red (Figure 8Figure 8, left image).

2.1.2 Specificity, shelf life, capture efficiency and sensitivity test

The objective of the specificity tests were to determine whether the pneumatically sprayed antibody film was able to properly detect the antigen (*E. coli* O157:H7) without any cross reactivity with other antigens. This test was also performed to test the specificity of the antibody itself, ensuring that there were no conformational changes during immobilization that could induce non-specific binding. Such conformational changes can directly affect the bioactivity of the antibody resulting in false positives during the immunoassay procedure [62-64]. Five types of bacteria (including two non- *E. coli* O157:H7 strains) were used during the specificity test, and the same assay procedure established for the target *E. coli* was followed.

The shelf life test is used to determine the length of time in which a product can be stored and still retain its original functionality. This is a very common test for different manufactured products including chemicals, food or pharmaceutical products. For the antibodies used in this project there are a variety of references indicating various

storage conditions such as in solution, frozen and lyophilized. Under these conditions the shelf life can vary from one month to years[65], however there are no references for the shelf life of antibodies immobilized on solid surfaces or in thin films. In this case the shelf life test was performed to establish a period of time in which the immobilized antibody film can be stored and then used with results similar in quality as those obtained by films prepared the same day.

Capture efficiency is a quantitative value that indicates how well a capture agent is able to immobilize a specific antigen in certain period of time. Calculations of capture efficiency for immobilized bacteria can be complex and time consuming if the number of bacteria is high and the count is performed manually. Capture efficiency is calculated by dividing the number of captured cells by the number of cells added to a specific surface area[54]. Using fluorescent microscopy to quantify bacteria with the help of specialized software is part of the research performed in this study. The software DIME[66] was used to automate and accelerate the counting process as well as increase the reproducibility of the data obtained.

A calibration curve was performed to estimate the validity of the results obtained by the use of DIME. The test was performed by spraying bacteria at known concentrations on a specific area, then manually performing the total direct counts per sample and comparing them with the numbers given by the DIME analysis. Figure 99 shows a screenshot of a window in the DIME software where parameters for counting, including shapes, sizes and the outline marks for the objects to be analyzed can be set.

The physical principle is similar to that of fluorescent microscopy however in this case the fluorescent signal was detected by a CCD camera rather than the human eye.

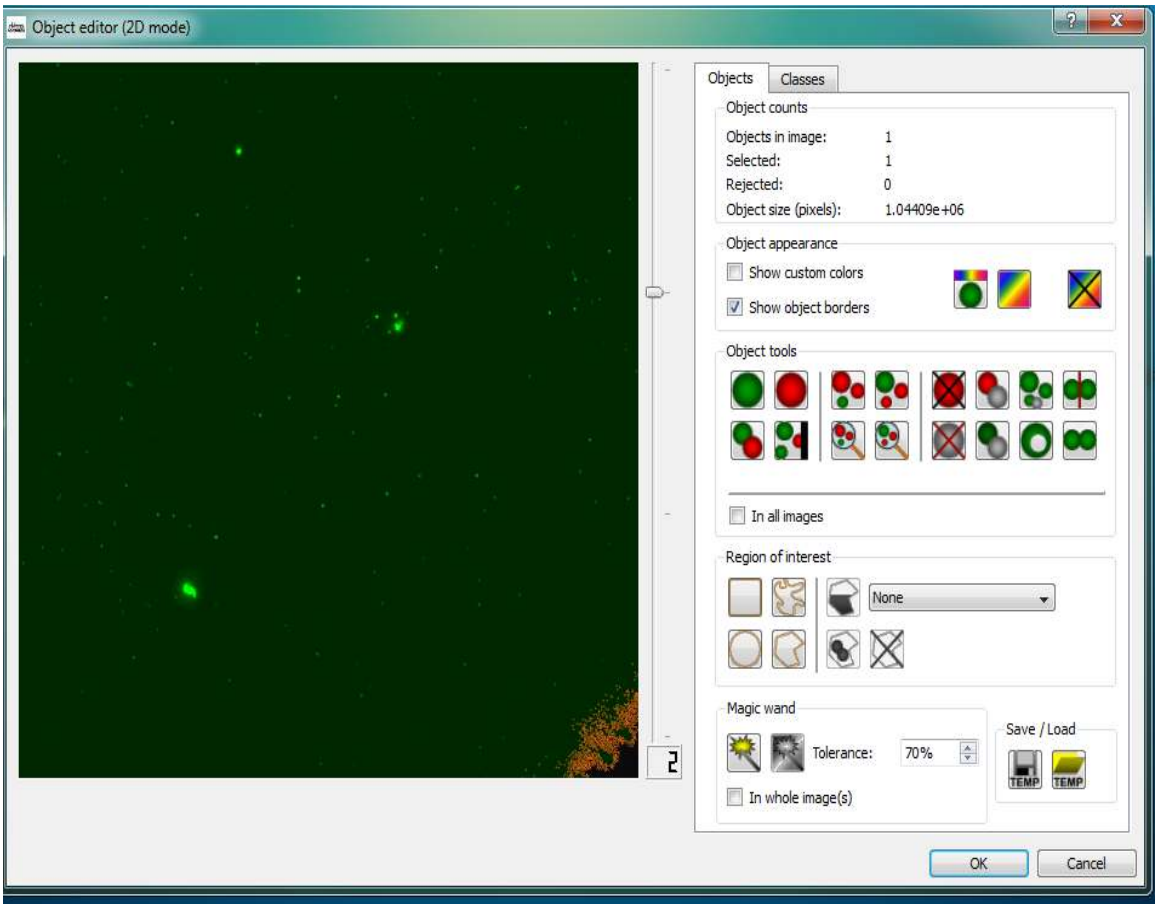

Figure 9: Screen shot of DIME 1.31, setting parameters for the images to be analyzed.

The sensitivity test was performed to determine the lowest concentration a fluorescent labeled molecule needed to be detected by equipment (signal to noise ratio >3). As the amount of material being measured becomes smaller and smaller, the noise detected increase in magnitude making it difficult to differentiate between the measured value and the noise detected[67]. To calculate the sensitivity of both deposition

techniques used in this project the parameter signal to noise ratio (SNR) was calculated. A HLAB 5000 biosensor was used to obtain the SNR from the samples.

The SNR was determined using equation 1 in which the mean background fluorescence intensity (Tbkg) is subtracted from the mean intensity of the region of interest (ROI), then dividing the result over the background standard deviation (Tbkg SD). Any SNR number below 3 is considered negative detection (no difference between the noise and the signal).

$$SNR = (ROI - Tbkg) / (Tbkg\ SD) \qquad \text{Eq (1)}$$

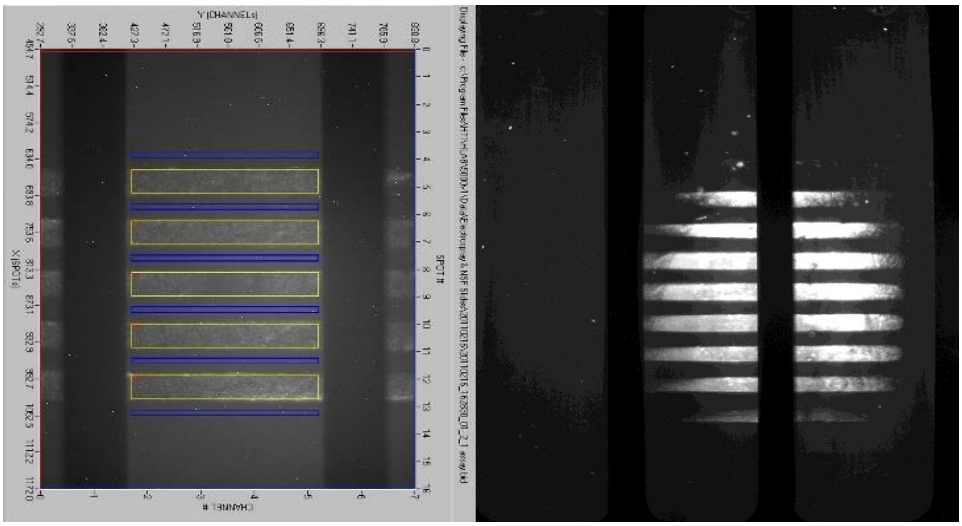

Figure 10. Representative sample of HLAB 5000 images. Left image, the blue (background) and yellow (region of interest) rectangles were used to calculate SNR and measure intensities. Right image, patterns created by pneumatic spray of unlabeled goat anti- *E. coli* O157:H7 plus detector antibody AF647 labeled Donkey Anti-Goat.

As is shown in Figure 10, the yellow rectangle highlights the fluorescent intensities of the region of interest (ROI) while the top and bottom blue outline rectangles highlight the background. The measured intensities within those rectangles were used to calculate the SNR of all the measurements performed in this experiment.

2.2 Characterization of antibody thin films

The interaction of proteins with surfaces is an important factor that determines the way that many medical devices, including biosensor devices, are built. Proteins, like antibodies, are a major component of many biosensor devices which use them as detector agents immobilized on a solid surface. In the experiments performed in this project, antibodies were immobilized on glass and then used to detect antigens in an immunoassay procedure [68].

In this study surface characterization of immobilized antibody films was performed using the following techniques: ellipsometry, ultraviolet/visible spectroscopy (UV/vis), attenuated total reflection Fourier transform infrared (ATR-FTIR), atomic force microscope (AFM), X-ray photoemission spectroscopy (XPS) and contact angle.

2.2.1 Ellipsometry and Ultraviolet visible spectroscopy

An ellipsometer was used to calculate the thickness of the films created by the two immobilization techniques used during this project. Ellipsometry is an optical, contactless technique. Because of this is well suited for in situ studies that require the sample to remain functional during and after analysis[69] (Figure 11).

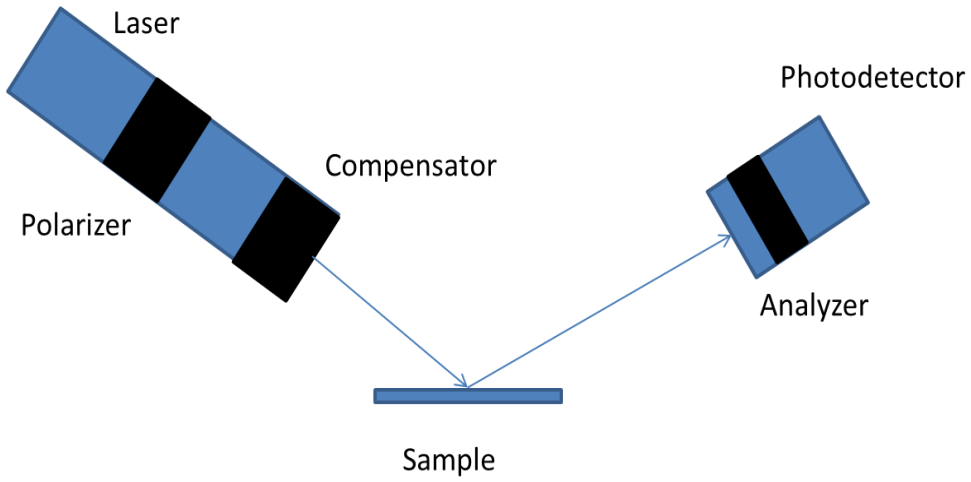

Figure 11. Schematic of Rudolph null ellipsometer used for these experiments.

The ellipsometer detects changes in the polarization of incident light caused by the interaction between the light and the sample after being reflected from the surface. That change in the linearly polarized light is quantified (Equation 2) by the ellipsometric angles tan Ψ, cos Δ and by the ellipsometric ratio ρ. R_s and R_p represent the complex coefficients of reflection in which R_s represents the perpendicular and the R_p the parallel light to the plane of incidence [26]. The value of the complex ellipsometric ratio depends directly on the wavelength of the light, the angle of incidence, and the optical properties of the surface material (i.e. refractive index).

The Eq. 2 represents the relationship between the ellipsometric ratio and the angles.

$$\rho = \tan \Psi \, e^{i\Delta} = R_p / R_s \qquad \text{Eq. (2)}$$

Monochromatic light emitted by the laser can be characterized by its amplitude, phase and incident angle relative to the interface light. The beam of light that interacts with the surface will be elliptically polarized and finally analyzed. A transparent film like the one created by immobilization of antibodies can reflect and refract the incident light, absorbing a minimal amount of light. The refractive index of the film and its thickness can be easily calculated if the refractive index of the ambient (air), substrate (Silicon wafer) and angle of incidence (70º) of the monochromatic light are known.

An ultraviolet/visible spectrophotometer was used in conjunction with the ellipsometer to detect changes in the thickness of the films after the protocol rinsing process and to determine the mechanical stability of the immobilized antibodies. The use of UV/vis to determine the concentration of proteins in solution is a common technique in many chemical laboratories[70]. The molecular absorption is based on measurement of the absorbance or transmittance of the light through solutions where the interaction between molecules and light is a quantitative process. In other words, the amount of light absorbed is proportional to the amount of molecules present in the solution. The relationship can be quantified by Beer's law[67] Eq. 3.

$$A = -\log T = \log (Po/P) = \varepsilon bc \qquad \text{Eq. (3)}$$

The simplicity and usability of this nondestructive method is based on the ability of some molecules (proteins in this case) to absorb light in the UV and visible regions of the EM spectrum. The absorbance of the collected rinse solution from the sprayed films

at a wavelength of 280 nm was measured in order to calculate the concentration of protein therein. This is the region in which the tryptophan and tyrosine amino acids strongly absorb the light due to the π-π^* electronic transition of the aromatic component[71]. The presence of these two amino acids remains fairly constant in proteins like the antibodies used in these experiments allowing the calculation of the concentration.

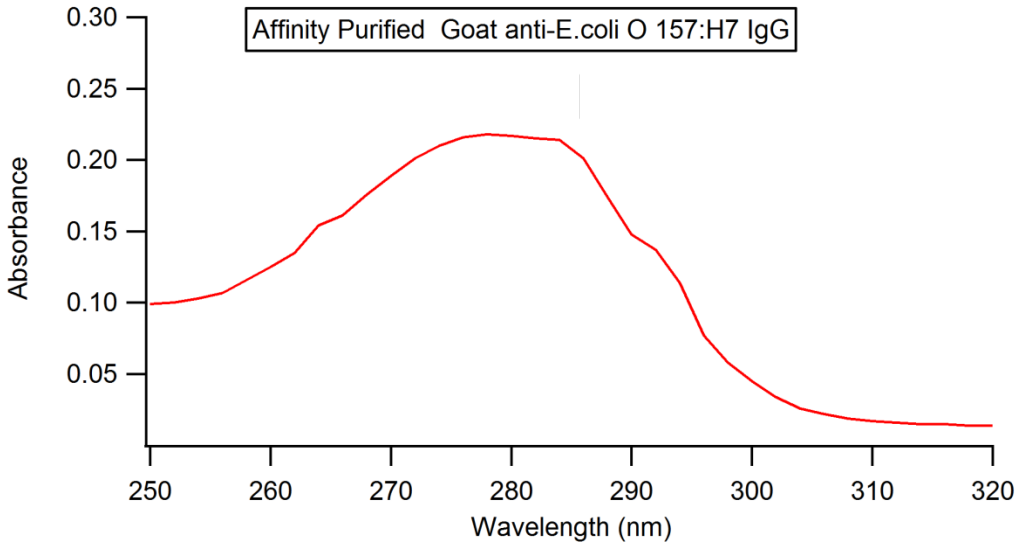

Figure 12. UV/vis representative absorption spectrum of goat anti-E.coli O157:H7 IgG in PBS solution.

In this study UV/vis was used to determine the amount of antibody that was removed from the surface after being rinsed with buffer solution. The immobilized antibody film was rinsed with phosphate buffered saline (PBS) and the wash solution collected. The solution was placed in a quartz cuvette then measured using the UV/vis spectrophotometer. A solution of antibodies in PBS as well as a bulk material were prepared and measured to observe the wavelength at the maximum absorbance (Figure

12). The spectrophotometer was calibrated by creating several solutions of known concentration and measuring their absorbance levels. A curve of known protein (antibody) concentration against absorbance was then calculated. The protein concentration of the collected wash solutions was calculated using this curve.

2.2.2 Attenuated total reflection Fourier transform infrared (ATR-FTIR)

The infrared (IR) region of the electromagnetic spectrum is divided into three sections called the near, mid and the far-IR; with each of these divisions has different applications and instrumentation. The wavelength of the IR region can extend from 0.78 to 1000 μm[67] and the energy of IR radiation is not strong enough to cause substantial electronic transitions like UV/vis. Instead the dipole moment of the molecule changes caused by rotation or vibration when absorbing energy in IR region. If a molecule has no net change in the dipole moment during the vibration or rotation, it can be inferred that such a molecule does not absorb IR radiation. Examples of this can be found in homonuclear molecules like O_2, N_2, Cl_2.

IR spectrometry has been widely used for quantitative analysis in many fields due to its inherent ability to differentiate molecules. The IR spectrometry equipment has changed dramatically over the last 30 years as the dispersive type was slowly replaced by the Fourier transform (FT) type. Dispersive instruments use grating to disperse the radiation that is to be detected by the transducer, which makes it difficult to differentiate the source signal from external radiation.

The FT type of instruments uses interferometry to detect the signal and the data is then processed using a Fourier transform resulting in a signal to noise ratio improvement of more than one order of magnitude[67].

The attenuated total reflection (ATR) devices use the phenomenon of total internal reflection in which a beam enters in a medium (crystal) with a higher refractive index than the sample at an angle in which the beam is totally reflected. The interaction of the beam with the reflective surface causes an evanescent wave that can penetrate into the sample (Figure 13). The depth of the penetration directly depends on the wavelength and can extend from 0.5 to 5µm into the sample. In the region where the sample absorbs the energy, the evanescent wave is attenuated before reaching the IR detector. This technique is commonly used to perform surface analysis, protein structure detection and many other biological applications[72].

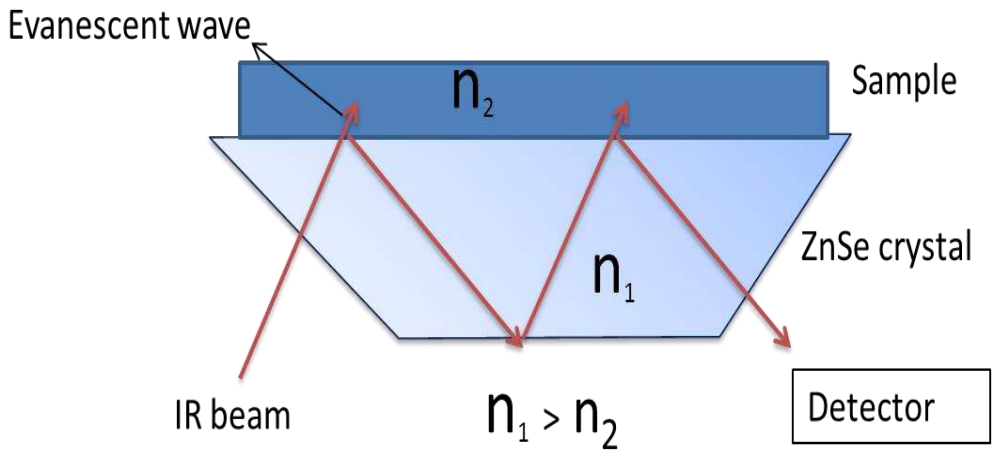

Figure 13. Schematic of attenuated total reflection system. The refractive index (n) of the zinc selenide crystal is higher than the refractive index of the sample.

Proteins are polymers in which the monomeric unit is amino acids. Amino acids are linked by the union of one amino group of one amino acid and the carboxylic group from another; such a bond is called peptide bond (Figure 14). When a protein is formed by linking of many amino acids, that chain is called a polypeptide. Not all polypeptides are considered proteins, only those that can form a three dimensional structure by the folding of its chains are considered proteins.

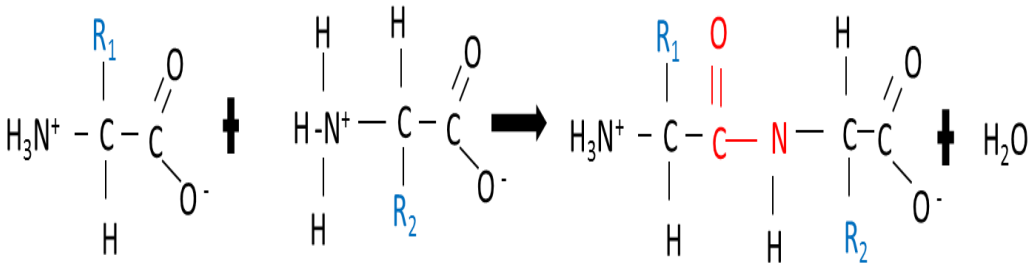

Figure 14. Two amino acids forming an amide bond (peptide bond).

Proteins are characterized by three main types of structures, primary, secondary and tertiary, each of which plays a role in the functionality of the protein. Due to the vast number of vibration modes that a polypeptide chain can exhibit, the overlapping of close peaks and the complexity of the spectrum, it is necessary to extract information from specific regions from the peptide. Repetition of chemical groups in the main molecular chain (backbone) offers an advantage due the common mode of vibration these groups will exhibit. An example of this is the carboxylic group (C=O) which is part of the backbone of the entire structure of a protein and can be localized in the amide I region (1600-1700 cm^{-1}, Figure 155).

This region is generally used to analyze the secondary structure of a protein and gives information regarding structural integrity and bioactivity[72].

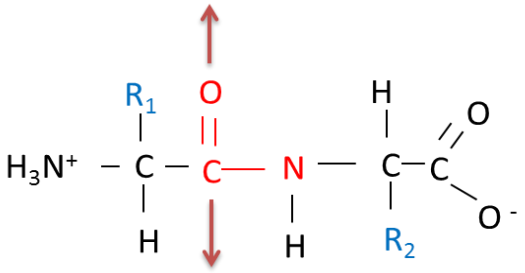

Figure 15. Stretching vibration mode of carboxylic group in the amide bond (Amide I vibration).

The use of the ATR-FTR technique in these experiments is focused on the protein structure analysis after the immobilization of the antibody by the pneumatic spray method. The protein-surface interaction, protein-protein interaction and nebulization process can denature proteins[73]. By analyzing shifts in the IR structural peaks (amide I region) any significant change in the chemical structure can be detected.

2.2.3 Atomic force microscope (AFM)

The atomic force microscope (AFM) was invented in 1989 by Calvin Quate and Christoph Gerber after its predecessor the scanning tunneling microscope, developed by Gerd Binnig and Heinrich Roher during the 1980s. The atomic force microscope or scanning force microscope is a great tool for topographic analysis or surface morphology studies. This high resolution microscope belongs to the scanning probe microscope family where a mechanical probe (cantilever) scans linearly and in a very close proximity to the sample, creating an image of the surface. Unlike optical microscopes, the scanning

force microscope reveals details in the direction perpendicular to the surface (z-axis) with a resolution close to 10 Å. The scanning probe moves in the x- and y-directions over the surface while the cantilever, held with a constant force during the scan, is forced up and down over the sample features[67].

The probe is a sharp tipped cantilever made of silicon or silicon nitride that, when brought to proximity with the sample, is forced to move in the vertical direction, displaced by features on the surface. The movement in the probe is related to the force by Hooke's law. A laser is used to detect the deflections of the probes by reflecting its beam off of the top surface of the cantilever into photo-detectors. The precision of the technique is also achieved by the use of piezoelectric materials (ceramics) that can contract or expand depending on the applied electrical current. Using these materials a highly precise three dimensional actuator can be constructed to scan the probe with the appropriate resolution[74]. An advantage of the AFM over other scanning microscopy techniques is that can be used with insulating samples such as those used in these experiments.

There are three different modes in which the AFM can operate: contact mode, tapping mode and non-contact mode. Each of these modes offers a variety of advantages that can be selected according to the needs of the experiment. The first mode is contact mode where the probe is in constant contact with the surface of the sample. This mode can damage the sample or distort the images obtained from the scan due to the contact between the cantilever and the sample. Normal AFM analysis is performed under regular

ambient conditions in which the atmospheric pressure or very small surface tensions can change the results of the scan pulling or pushing the probe. To solve this problem the next AFM mode, tapping mode, can be used. In this mode the cantilever oscillates at a few hundred kilohertz touching the sample at the bottom of each cycle. Each oscillation and amplitude is monitored continuously in order to obtain a good image. The last AFM mode and the least common is the non-contact mode. In this mode the cantilever is placed a few nanometers over the surface to be analyzed. The probe maps the surface by the attractive Van der Waals interaction forces between the surface and the tip of the cantilever[67].

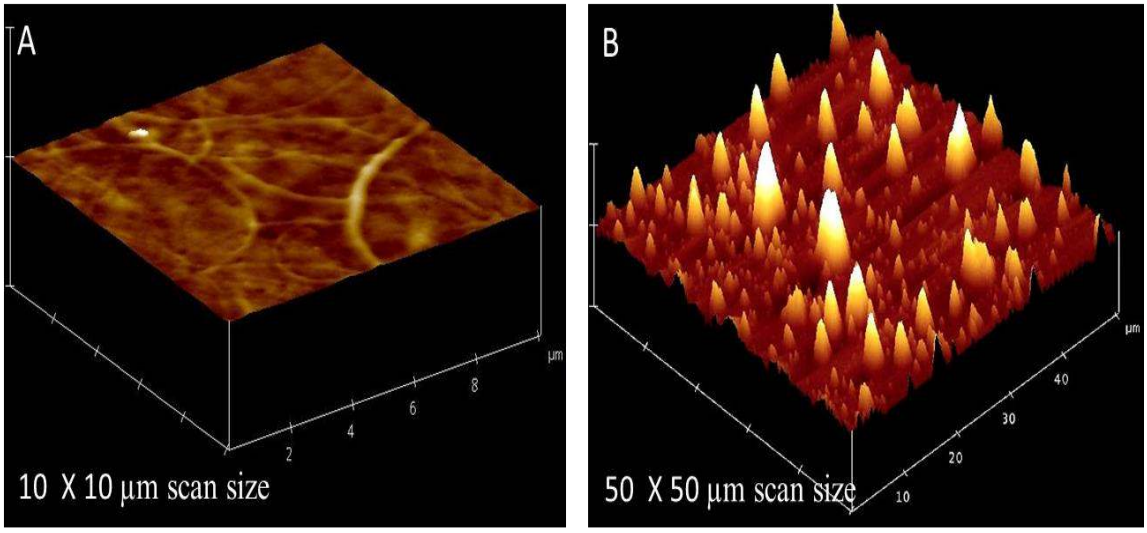

Figure 16. AFM image of immobilized antibody on glass surface. (A) Immobilization of anti-*E. coli* O157:H7 IgG using pneumatic spray method, rings from droplets formed during the spray can be noticed on the surface after drying. (B) Immobilization of anti-*E. coli* O157:H7 IgG using avidin-biotin bridge method, large particles form due to aggregation of avidin.

A sample of an AFM image can be seen in Figure 16 where anti-*E. coli* O157:H7 IgG antibody was deposited using two different immobilization techniques. Even though

the atomic force microscope cannot show the molecular structure of proteins the equipment can elucidate the morphological conformation of clusters at the surface. The topography of the surface after the antibody is immobilized is important due to its intrinsic relationship with cell adhesion. The wettability of a film will determine the ability of such a surface to interact with other surfaces or liquids directly affecting the interactions between them. A good parameter that can be measured in the topography of the surface is the roughness (Rq). Rq can be defined as the root mean square average of the total height (Z) deviation taken from the mean data plane in a given area (see eq. 4).

$$Rq = \frac{\sqrt{(Z_1^2 + Z_2^2 + Z_3^2 .... + Z_N^2)}}{N}$$

Eq. 4

The surface roughness of the two immobilization techniques employed in this project was also used as another comparison paramter. The Rq data gives a relative value to the morphology of the surface, which can be used to quantify the formation of aggregates or clusters after the immobilization of antibody at the surface.

2.2.4 X-ray photoemission spectroscopy (XPS)

In numerous studies the analysis of the bulk properties of a sample is essential to understand the characteristics of the material. However, in some circumstances the properties of the surface of a material are of greater interest. Spectroscopic surface methods provide the information required to perform not only qualitative analysis but

quantitative as well. There are many spectroscopic techniques to analyze surfaces, including Auger electron spectroscopy (AES), electron energy-loss spectroscopy (EELS), electron microprobe (EM), surface plasmon resonance (SPR), ellipsometry and X-ray photoelectron spectroscopy (XPS).

In 1981 the physicist K. Siegbahn was awarded the Nobel Prize for his work on the principles of XPS. Since then, the technique has evolved to provide chemical analysis due to its ability to obtain information not only about the atomic composition of the sample, but the oxidation state as well[75]. A schematic representation of the spectroscopic surface technique is shown in Figure 17. A primary beam (electrons, ions, photons) is used to impact a surface. The result of this impact is a secondary beam (electrons, ions, photons) caused by scattering, sputtering, or emission, which is ejected from the surface in the direction of a detector.

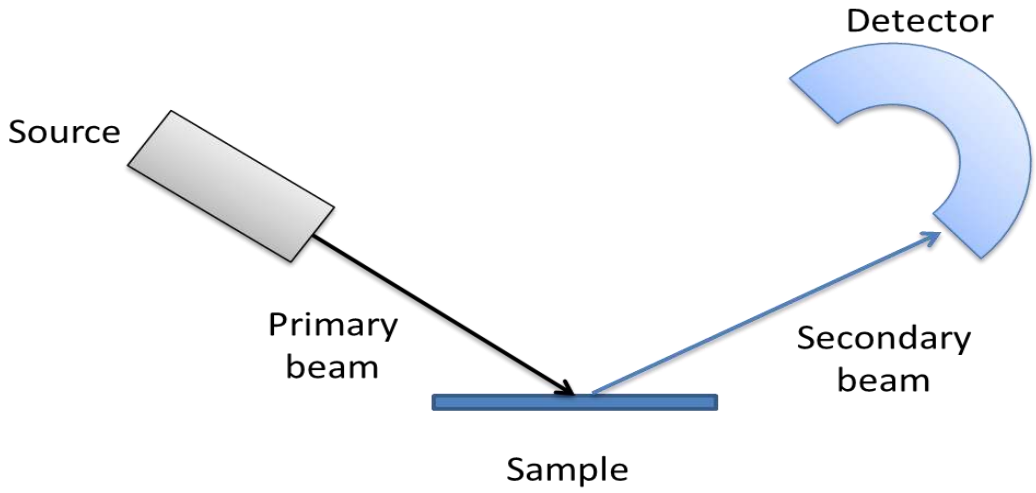

Figure 17. Basic schematic for a surface spectroscopy equipment. For the XPS the primary beam is X-ray photons and the detected secondary beam are electrons.

Contamination on the surface is one of the main problems encountered in these surface techniques. A vacuum environment is essential to avoid adsorption of contaminant molecules to the surface (rate of adsorption is reduced by increasing the vacuum). A simple XPS system consists of 5 main elements. The first is the source, an x-ray tube with magnesium or aluminum targets containing a monochromator to provide a very narrow bandwidth (0.3 eV), high signal to noise ratio and a small beam cross section at the surface. Next, is the sample holder, which must be positioned as close as possible to the source to reduce attenuation of the beam (a pressure of 10^{-5} torr or less is important). The analyzer consists of a series of lenses that discriminate the secondary beam by discriminating the kinetic energy of the emitted beam. The transducer is an electron multiplier (doped material with lead or vanadium) that improves the signal received by emitting more electrons than the one that was received (a gain of 10^6 to 10^8). The final component is the data system which analyzes the signal collected from the multiplier using computer software[67, 75].

To understand the mechanism of the XPS is necessary to imagine a prototypical atom with outer and inner shells. The binding energy of the shells decreases with the distance from the core of the atom, meaning that removing an electron from the inner shell requires more energy than removing one from an outer shell (valence electrons). Once the primary beam (with a known energy $h\upsilon$) penetrates the shells it will displace an electron from one of the orbitals if the incoming photon energy is greater than the binding energy of the electron. The energy of the emitted electron (Ek) and the binding energy

(Eb) can be calculated using Equation 5. In this equation (w) is the work function or a factor that accounts for the electrostatic environment in which the electron was measured.

$$Eb = h\upsilon - Ek - w \qquad \text{Eq. 5}$$

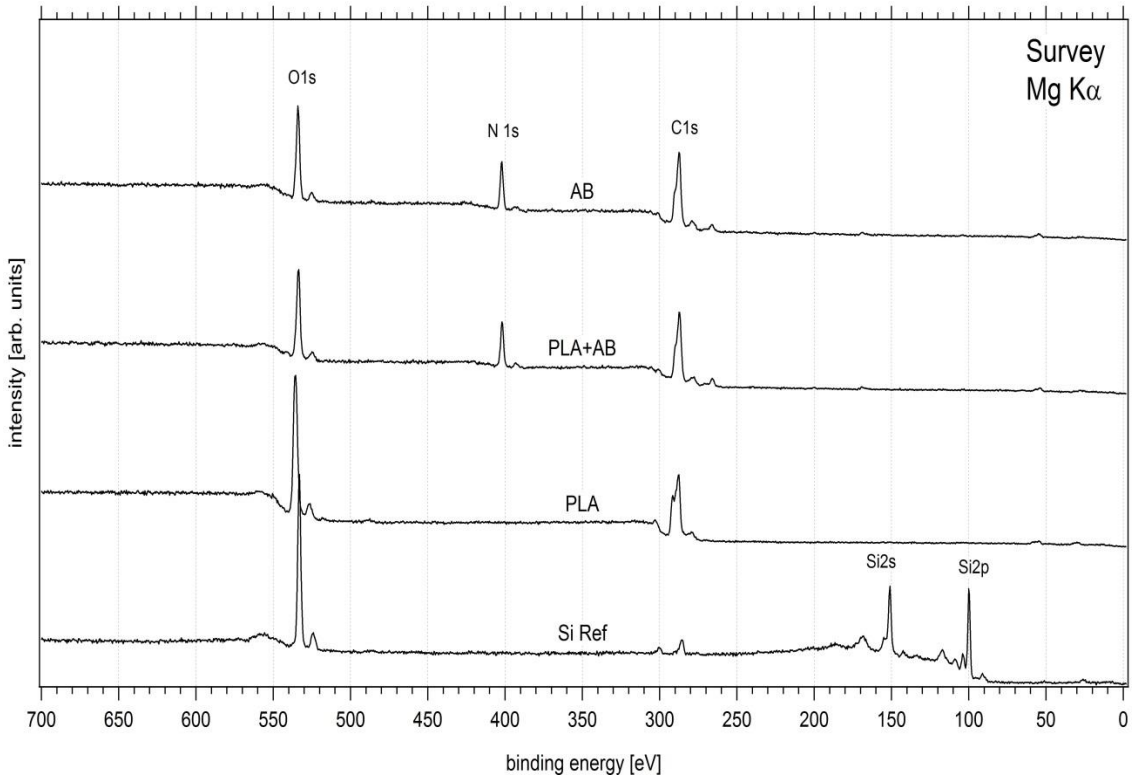

Figure 18. Representative image of a X-ray photoelectron survey spectrum. Three different films were deposited by pneumatic spray on silicon wafer: from bottom to top, silicon surface as reference, a PLA film, a film of anti *E. coli* antibody deposited on a PLA film and the top survey is a film of anti *E. coli* antibody deposited on silicon wafer. The presence of antibody (protein) is confirmed by the N1s peak in the top two surveys.

One of the basic analyses that can be performed by the XPS equipment is a survey spectrum. This spectrum normally use a range of kinetic energies from 250-1500 eV which are equivalent to about 0-1250 eV binding energy, thereby covering all the

elements in the periodic table. This spectrum elucidates the basic components of a material shown in Figure 18 where a polymer (poly-lactic acid) is deposited on the top of a silicon wafer. The two basic components of the polymer (carbon and oxygen) are detected for that survey, while the nitrogen appears only in the films that have antibody (nitrogen being a main component of proteins). The silicon survey is used as reference and to evaluate the elements present before any addition of material.

In this study the formation of a thin film of antibodies on a glass surface with a specific functionality as a capturing agent is performed under pneumatic spray conditions. XPS allows one to analyze the coverage of the surface with the protein after the deposition process. The intensity of each measured peak can be evaluated to reveal the amount of material present in the sample. The presence or absence of certain elements in a film can be detected by the survey scan which can help in the qualitative confirmation of a immobilized material on the analyzed surface[76]. In this case the solid surface on which the film was deposited was a silicon wafer. The peaks contributed from the substrate are Si2s, Si2p and from the film C1s, O1s and N1s.

For these experiments, the presence of nitrogen in the spectrum is an indication of the existence of the antibody at the surface (immobilization) as this element is only found in the immobilized antibody films. The increase in the intensity of the peak for a single element after a deposition is related to an increase in the amount of material on the surface. This value will increase until it reaches a plateau. At this point the penetration power of the x-ray has reached the maximum.

2.2.5 Contact angle (wetting properties of a film

Wetting can be described as the property of a liquid to keep contact with a surface, and the total surface area involved in the contact depends on attractive and repulsive forces at the liquid-solid interface. Surface wetting is a relevant topic due to its importance in many industries including pharmaceuticals, cosmetics, printing process, fabrics, and biomaterials (body implants, contact lenses). Many techniques have been developed to measure those interactions. The wettability property can be determined by the measurement of the contact angle (Figure 19). The relationship between contact angle and wettability is inverse, in other words when a measurement gives a high contact angle (<90º) the surface has a low wetting properties; this surface is considered hydrophobic. In the opposite case when the contact angle is low (>90º) the wetting is high and the surface is considered hydrophilic[77].

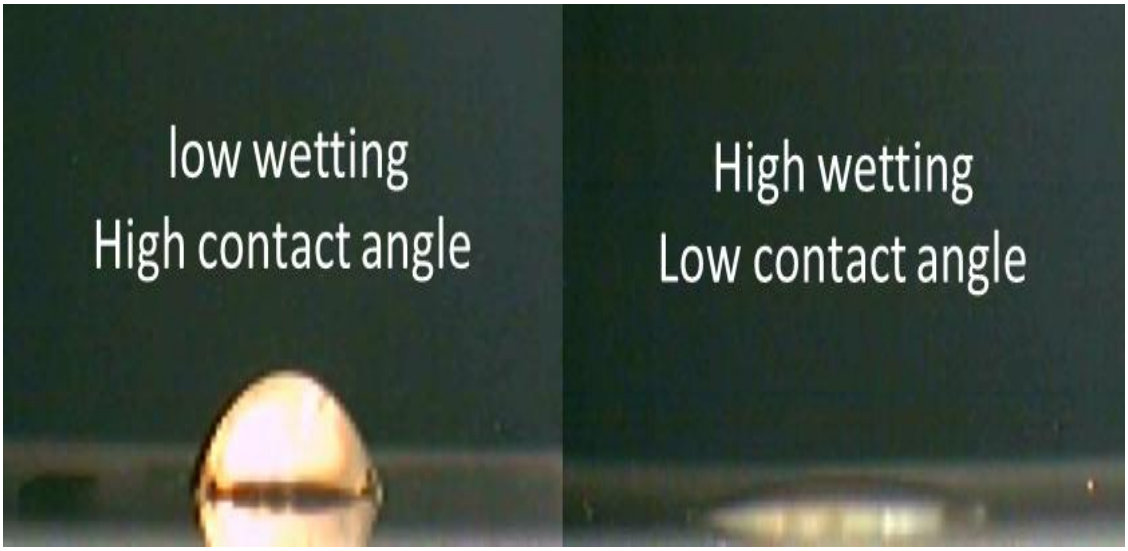

Figure 19. Inverse relationship between contact angle and wetting properties. The images show a drop of water on a poly-lactic acid coated surface (left) and drop of water on a glass surface (right).

The contact angle can be described as the angle between the liquid and substrate at the interface from the contact point as seen in Figure 20. The shape of the drop on a surface is affected by the surface tension forces that interact at the interface. To better describe these forces it is necessary to visualize the atoms within a solid broken into two sections; the bulk material and the surface. The atoms in the bulk material are packed tightly with neighboring atoms resulting in a zero net force between the atoms. The atoms present on the surface are not completely surrounded by other atoms causing a misbalance in the forces with a net attractive force pointing toward the interior of the bulk material. The excess energy gained by the atoms at the surface is called surface energy (free energy). Systems will move towards the most stable condition by reducing the amount of free energy.

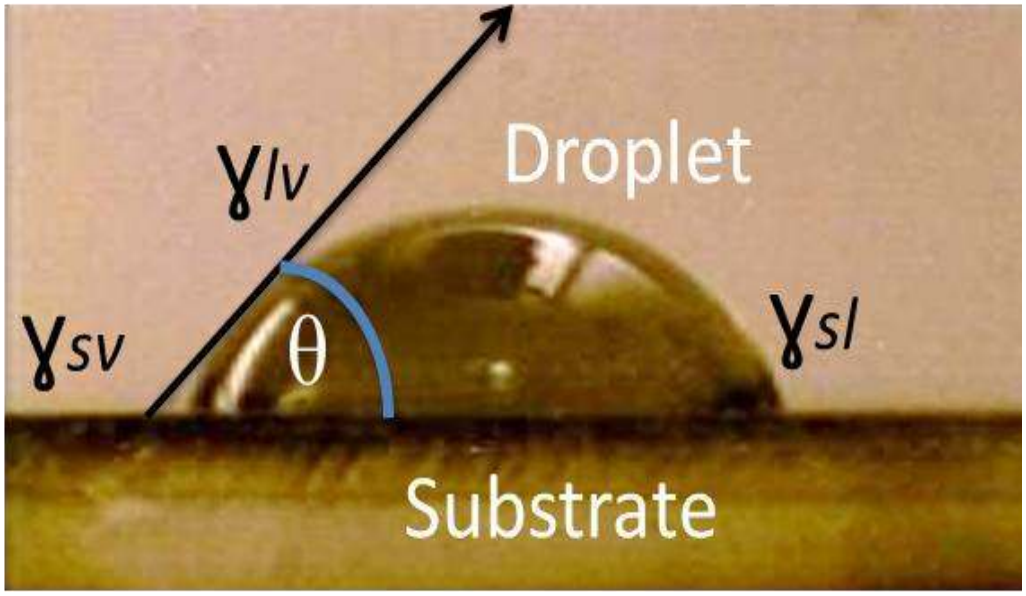

Figure 20. Image of a contact angle formed by a water drop on an antibody film immobilized on glass substrate. Three tension interfaces are shown solid-liquid (*sl*), solid-vapor (*sv*) and liquid-vapor (*lv*).

If the system is a liquid droplet, the excess energy from the surface atoms creates an attractive force towards the interior of the drop. This tendency of the system leads to a reduction of its energy, causing the drop contract thereby decreasing its surface area. The force that decreases the size of the drop in an effort to maintain the lowest energy level is called surface tension. In 1805 Thomas Young defined the mathematical relationship between the surface and drop interaction in his equation[78].

$$\gamma_{lv} \cos \theta Y = \gamma_{sv} - \gamma_{sl} \qquad \text{Eq. 6}$$

Equation 6 shows three different interfaces (*lv*) liquid-vapor, (*sv*) solid-vapor, and (*sl*) solid-liquid; (ɣ) is the tension and (θY) is the contact angle. The experimental contact angle is not always equal to the value obtained from Young's equation due to other factors including surface roughness that directly affect the measurement. Because of this characterizing the wetting properties of a surface based only in the static contact angle is not adequate. The use of dynamic contact angle and advancing and receding contact angle are more accurate approximations to the measurement. The advancing and receding angle is also called hysteresis (H) and is correlated to the heterogeneity (roughness) or topography of the surface[79]. The calculation of the contact angle in different topographic surfaces (rough and heterogeneous) is performed using the Wenzel and Cassie-Baxter angles which differ from the Young angle. The interaction of liquids at a solid surface has many applications in the biological field including biomedical implants (metal or plastic) where the wettability of the material and the exposure time are crucial due to the formation of a biofilm interface with the body [80]. Another application

is in the development of waveguides for biosensors, where antibodies are immobilized on a solid surface (glass), the wettability of the film is an important parameter that contributes to the efficiency of the interaction between the liquid containing the antigen to be captured and the antibody[81]. In these experiments the contact angle measurements were used primarily as a parameter to qualitatively analyze and compare the antibody films immobilized by the two different techniques, the pneumatic spray and the avidin-biotin bridge.

2.3 Experimental set up

2.3.1 Materials

Plain microscope glass slides used for all experiments were purchased from Globe Scientific Inc. (Paramus, NJ). Antibodies used were unlabeled goat anti-*E. coli* O157:H7 (used for pneumatic spray method), the biotinylated labeled goat anti-*E. coli* O157:H7 (for avidin-biotin bridge method), AlexaFluor 647 labeled donkey anti-goat (as reporter antibody), and Rhodamine Red conjugated AffiniPure donkey anti-goat. The first two antibodies were purchased from Kirkegaard & Perry Laboratories, Inc. (Gaithersburg, MD), the third antibody was purchased from Invitrogen (Eugene, OR), and the fourth from Jackson ImmunoResearch (West Grove, PA). Antibodies were rehydrated and stored following manufacturers' instructions. Goat anti-*E. coli* O157:H7 was labeled with Alexa Fluor 647 (AF647) using the AF647 protein labeling kit from Invitrogen (Eugene, OR) and following the manufacturer's instructions. Other reagents used were NeutrAvidin biotin binding protein from Thermo Scientific (Rockford, IL),

methanol, potassium hydroxide, sodium chloride, sodium phosphate dibasic heptahydrate, sodium phosphate monobasic, Tween 20 from Fisher Scientific (Fair Lawn, NJ), ampicillin sodium salt, L-(+)-arabinose, dimethyl sulfoxide , 4-maleimidobutyric acid N-hydroxysuccinimide ester, (3-mercaptopropyl)triethoxysilane, toluene anhydrous 99.8% from Sigma-Aldrich (St. Louis, MO), and ethanol 200 proof from AAPER Alcohol & Chemical Co. (Shelbyville, KY). Luria-Bertani and Tryptic Soy media (Becton Dickinson Company, Sparks, MD) were used for growth of bacteria.

Escherichia coli O157:H7 ATCC 35130 labeled with Green Fluorescent Protein (GFP) was used previously[61] and was employed in this study. Bacteria (GFP-*E. coli* O157:H7) were grown on a media (Luria-Bertani) containing 5 mg/mL arabinose and 100 µg/mL ampicillin (LBAA) for 18-24 h at 37˚C prior to each experiment. *E. coli* K12 ATCC 23590, *E. coli* O124:H7 CDC 3836-65, *Salmonella enterica* Typhimurium ATCC 19585, *Shigella flexneri* ATCC 12022, and *Staphylococcus aureus* ATCC 25923 were grown on (TSA) in the same conditions that the *Escherichia coli* O157:H7 mentioned before. The cell suspensions were made in a buffer solution of 10 mM Sodium Phosphate/10 mM Sodium Chloride (NaPCl) then, diluted ten-fold. All the direct counts were done with Cellometers (Nexcelom Bioscience, Lawrence, MA) to calculate concentrations followed by spread plating on LBAA agar plates (for GFP-*E. coli* O157:H7) or TSA (all other bacteria) in triplicate to determine the amount of viable cell concentrations.

2.3.2 Immobilization methods (pneumatic spray and avidin-biotin bridge)

The pneumatic spray deposition was performed using a nebulizer with a low flow rate (3-10 µl/min) (Nebulizer Model DS-5, CETAC, Omaha, Nebraska) and an in-house apparatus to hold the nebulizer and a glass slide (Figure 21). A N_2 gas line was connected to the nebulizer with a pressure regulator. A syringe pump was used to deliver the sample (Pump 11 Pico Plus Harvard apparatus, Holliston, Massachusetts) adapted with a 1 mL syringe. The syringe holding the sample was connected to the nebulizer using PVC tubing. A solution of 10% KOH in methanol was prepared and the glass slides were immersed in this solution for 30 min followed by rinsing with deionized water and drying with nitrogen flow. Individual slides were placed on the slide assembly and located at a predefined distance away from the tip of the nebulizer. The syringe was filled with unlabeled goat-*E. coli* O157:H7 antibody solution according to the amount needed for each experiment. Parameters used during the experiments were the following: antibody concentration (100 or 200 µg/mL), distance of glass slide from nebulizer (30-70 mm), outflow N_2 pressure (20-60 PSI), rotational rate of the moving glass slide sample holder (7.5-17 RPM) and amount of time sprayed (2-32 min).

The flow rate was the only constant parameter throughout the experiments and was set at 4 µl/min. The antibody pattern on the glass was established using a metal mask with dimensions of 25 x 75 mm with 15, 1 x 9 mm rectangular openings (rows). The patterns created by these parameters yield at least 6 rectangular rows with immobilized antibody. Finally, the prepared pneumatic spray slides were stored at 4°C if they were not used the same day.

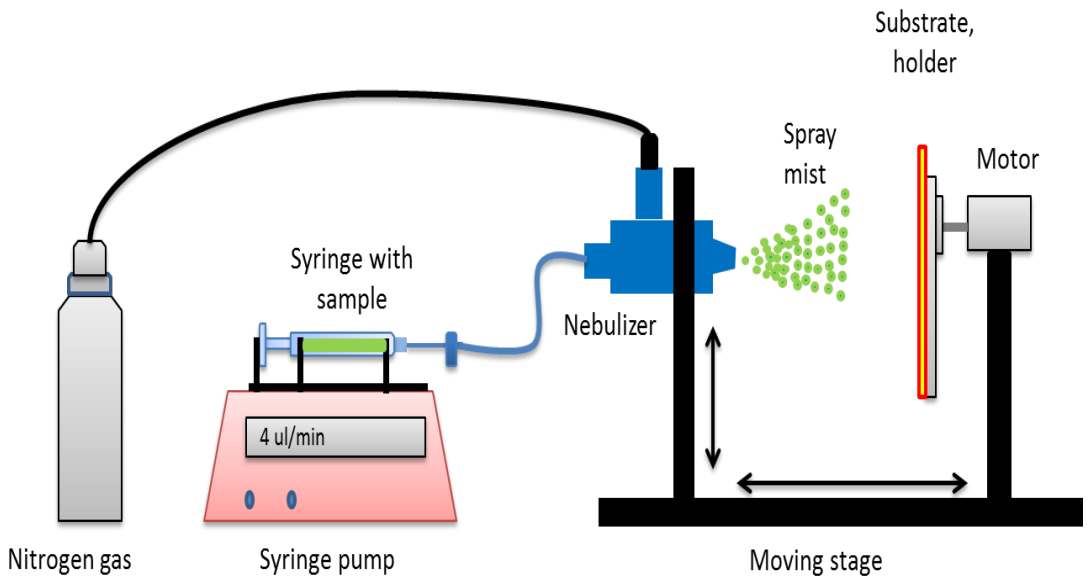

Figure 21. Pneumatic spray setup for immobilization of antibodies on solid substrate.

The covalent immobilization method of antibodies via avidin-biotin bridge has previously been described in detail by other groups[12, 82]. Briefly, glass slides were immersed for 30 min in a solution of 10% KOH in methanol, then rinsed vigorously with deionized water and dried under nitrogen flow. The following procedure was performed under nitrogen environment inside a glove bag: the cleaned slides were treated for 1 h with a 2% solution of (3-mercaptopropyl) triethoxysilane in toluene, and then incubated in a 2.1 mM, 4-maleimidobutyric acid N-hydroxysuccinimide ester in 200 proof ethanol solution for 30 min. Slides were rinsed with deionized water then incubated for 2 h in a solution of 33mM NeutrAvidin in NaPCl buffer at 27°C. Slides were rinsed with buffer solution and air dried, then placed in patterning templates (Hanson Technologies, Inc., Carlisle, PA). Each template consists of an acrylic holder and a poly-dimethylsiloxane (PDMS) flow module termed patterning gasket. A biotinylated goat anti-*E. coli* O157:H7

solution of 10 µg/mL in NaPCl buffer was injected into the flow chamber. Slides were incubated for 18-22 h at 4°C and then rinsed using a plastic pipette with NaPClT buffer (mixed with 0.5% tween 20). Slides were dried with a flow of nitrogen then used or stored at 4°C.

2.3.3. Reproducibility and visualization of patterns of immobilized antibody

The reproducibility of pneumatic sprayed antibody pattern was determined after establishing spray parameters. Ten slides were sprayed and treated with reporter antibody against the immobilized goat anti-*E. coli* O157:H7 antibody to illuminate the spray patterns. Pneumatic spray prepared slides were placed horizontally on a slide holder and 1 mL of 5 µg/mL AF647 donkey anti-goat antibody solution was added to the top surface of the slide and allowed to incubate for 15 min at 27°C. Slides were rinsed with NaPClT buffer and air dried. The visualization of antibody patterns was performed via fluorescent microscopy. PS and avidin-biotin bridge prepared slides were processed for visualization of antibody patterns. One milliliter of a 5 µg/mL Rhodamine red anti-goat IgG solution was added to each slide and incubated for 15 min at 21˚C. Slides were then rinsed three times (0.5 mL each time) with NaPClT buffer using a transfer pipette and allowed to dry. Slides were interrogated with a 635 nm laser and visualized with a CCD camera. Visualization was performed using an Olympus BX60 Epifluorescent microscope (Olympus America Inc., Center Valley, PA) with a UPlanFl 10x and a UIS2 LUCPlan FLN 40x objectives. Digital images were obtained with an attached SPOT Flex color CCD camera (Diagnostic Instruments Inc., Sterling Heights, MI). Image adjustments and

ruler measurements were done with the SPOT Advanced version 4.6 software (Diagnostic Instruments Inc., Sterling Heights, MI).

2.3.4 Testing capture efficiency, specificity and shelf life of immobilized antibody

Pneumatic spray and avidin-biotin bridge prepared slides were assayed with GFP-*E. coli* O157:H7 to determine the immobilized antibody's functionality. Five assay replicate experiments were done in which each experiment consisted of 3 slides of each deposition method (total of 6 slides) with one sample concentration (10^5, 10^6, 10^7 cells/mL) per slide. Slides were warmed to 21˚C and placed inside acrylic holders with silicon gaskets. The gaskets had a 17.4 x 16.8 mm open area (292.32 mm^2) for sample application. One hundred microliters of sample was added to the 292.32 mm^2 area and incubated for 30 min at 21˚C on the Belly Dancer shaker (Stovall Life Science, Greensboro, NC). Slides were then rinsed three times (0.5 mL each time) with NaPClT buffer using a transfer pipette. One half of one milliliter of 10 µg/mL AF647 anti-*E. coli* O157:H7 detector solution was added and incubated for 15 minutes at 21˚C on the Belly Dancer shaker. Slides were rinsed three times (0.5 mL each time), removed from the acrylic holder and air dried. Slides were then interrogated with a 635 nm laser and visualized with a CCD camera thereafter and viewed under fluorescent microscopy to determine GFP cell counts and calculate percent capture efficiencies. Slides from 3 different experiments (3 sets) were then subjected to the procedure for visualization of antibody patterns via fluorescent microscopy as mentioned above.

To determine if the immobilized antibody was still specific for *E. coli* O157:H7, pneumatic spray and avidin-biotin bridge prepared slides were assayed with non-target bacteria. *E. coli* K12, *E. coli* O124:H7, *S. enterica* Typhimurium, *S. flexneri*, *S. aureus*, and GFP- *E. coli* O157:H7 (positive control) suspensions at 10^7 cells/mL were added to slides (one bacterial strain per slide) following the same procedure performed for the functionality of immobilized antibody experiments found in the previous paragraph. Slides were interrogated with a 635 nm laser and visualized with a CCD camera. Data analyses were done on the resulting images. To estimate the shelf-life of PS slides, twelve slides were prepared via the PS process on the same day (day 0) and stored at 4˚C. On day 1 (24 h after slide prep) one slide was assayed with a GFP-*E. coli* O157:H7 sample at 10^7 cells/mL following the procedure done for the functionality of immobilized antibody experiments. Thereafter, one slide was assayed each week for 12 weeks. Slides were interrogated with a 635 nm laser, visualized with a CCD camera and thereafter viewed under fluorescent microscopy to determine GFP cell counts and calculate percent capture efficiencies. Data analyses were done on images.

2.3.5 Testing sensitivity of immobilized antibody films

Images captured with the CCD camera were analyzed using the HLAB 5000 analysis software (Hanson Technologies, Inc., Carlisle, PA). A 6 x 6 array grid was used to read the target areas (the antibody rows at the center of the slide), termed region of interest area (ROI, ~4.37 mm^2), as well as non-target areas to the left and right of the ROIs, termed the left and right background areas (LBA, RBA ~1.09 mm^2 each) see Figure 10. Signal to noise ratios (SNRs) were determined by subtracting the background

fluorescent intensity (mean of LBA and RBA) from the mean intensity of the ROI and then dividing by the background standard deviation (LBA and RBA). Antibody rows with SNRs ≥ 3 were evaluated as positive for detection in the GFP-*E. coli* O157:H7 assays.

Percent capture efficiencies of each ROI were determined by placing each GFP-*E. coli* O157:H7 assayed slide on the Epifluorescent microscope containing a UIS2 LUCPlan FLN 40x objective and generating a digital image. The total area of the image was 0.09486 mm^2. GFP-*E. coli* O157:H7 and the cells on the images were counted using DIME 1.31 software[66]. The calculation of percent capture efficiency is performed by dividing the number of GFP cells counted per image by the theoretical number of GFP cells per image and multiplying by 100. Theoretical number was calculated by dividing the number of cells applied by the antibody pattern area in contact with cell sample. Each antibody pattern row created by the pneumatic spray was approximately (based on mask dimensions) 16.80 mm^2 and the area for the avidin-biotin bridge was estimated to be 14.94 mm^2. The unpaired t-test or the Mann-Whitney test for sample groups with non-Gaussian distributions (GraphPad InStat v3.0, GraphPad Software, Inc., La Jolla, CA) was used to estimate the differences in fluorescent intensity values, SNRs, and percent capture efficiencies for pneumatic spray and avidin-biotin bridge techniques. Differences were considered statistically significant for P being less than or equal to 0.05 (95% confidence level).

2.3.6 Equipment (ellipsometry, UV/vis spectroscopy and ATR-FTIR)

For the ellipsometry measurements silicon, in the form of a wafer, was chosen as the substrate to perform the antibody deposition instead of glass due to the transparent characteristics of the antibody film. Wafers were cut to 2.5 cm by 4 cm then immersed in a solution of 10% KOH in methanol and incubated for 30 min followed by extensive rinsing with deionized water and drying with nitrogen. Ten silicon samples were pneumatically sprayed with goat anti-*E. coli* O157:H7 as described in section 2.3.2. Each sample was sprayed using different deposition times (from 2 min to 14 min) per duplicate. For comparison purposes, antibody was immobilized via the avidin-biotin bridge following the same process described on section 2.3.2 onto two silicon samples. The thickness of the deposition layer was analyzed by the ellipsometer (Null point Ellipsometer Rudolph AutoEL III) with a single wavelength of 632.8 nm and a resolution of 3-10 Å at a fixed angle of 70º. A clean silicon sample without immobilized antibody was kept as a reference for the two film making techniques.

After thickness measurements were performed (using ellipsometry) the slides were rinsed with 3 mL of PBS per slide. The rinsed solution was collected and measured using Uv/vis spectroscopy (Thuramed T60 UV/VIS spectrophotometer version 1.10) at a wavelength of 280 nm for protein detection with wavelength accuracy of +/- 1nm, a photometric range of absorbance -0.3-3Abs (Louisville, KY). The rinsed slides were dried with nitrogen flow and again measured on the ellipsometer to obtain the difference in thickness after washing. Glass slides were cut into 7 x 7 mm squares, cleaned and pneumatically sprayed as described in section 2.3.2 with a deposition time ranging from

2-14 min. Each sample was placed inside the UV/vis cuvette filled with 3 mL of buffer solution and measured for a period of time (0-48 h) to detect any desorption of the protein from the surface. Each deposition time was performed in triplicate. To analyze the samples using the ATR-FTIR a zinc selenide (ZnSe) crystal was cleaned with methanol and dried by a flow of nitrogen. Antibodies were deposited on the ZnSe crystal at each deposition time using the same parameters described on section 2.3.2. After each deposition the film deposited on the crystal was measured and then removed by rubbing the surface with a wipe soaked with methanol before the next deposition. Experiments for each deposition time were made in duplicate. The ATR-FTIR equipment used was a Nicolet 6700 spectrometer from Thermo Electron (Madison, WI) equipped with the ATR accessory and a ZnSe ATR crystal. The spectra were analyzed using the OMNIC software version 7.2.a (Thermo Electron Corporation). The spectrometer was purged with nitrogen continuously to reduce contamination form H_2O and CO_2 vapors.

2.3.7 Equipment (AFM, XPS and contact angle)

For AFM analysis, glass slides were cleaned then pneumatically sprayed (both procedures described in section 2.3.2). Every deposition was done in triplicate and each deposition was scanned in three different areas. The AFM measurements were performed using a Digital Instruments - Dimension 3100. The AFM was operated under tapping mode with a piezoelectric scanning probe microscope head and silicon probe tip. The thin film samples were examined at a scan rate of 1 Hz over an area of 50 μm × 50 μm and 1 μm x 1 μm.

For XPS analysis, silicon wafers were cut into 10 mm x 10 mm squares and cleaned with a solution of 10% KOH/Methanol for 30 min and then dried with nitrogen. Each slide was pneumatically sprayed according to procedure described on section 2.3.2. The XPS measurements were taken using a SPECS UVS 10/35 ultraviolet source and a SPECS XR 50 X-ray gun. The X-ray emission line used for standard core level XPS was the Mg KR ($h\nu$ = 1235.6 eV), with a 20 mA emission current. The calibration was carried out to yield the standard Cu 2p3/2 line at 932.66 eV and the Cu 3p3/2 line at 75.13 eV. All the data obtained was analyzed using Igor Pro software (WaveMetrics, Inc.).

For the contact angle measurement a 250 µl syringe was filled with deionized water and clamped above the location of the test slide. Each glass slide was cleaned and pneumatically sprayed with an antibody film as described in section 2.3.2 then positioned under the water drop system. To find the contact angle of all the antibody films, an in-house physical water-drop system apparatus (Figure 22) was built, a digital microscope camera (Amscope MD 600, v 3.0.12, Irvine, CA) was attached to the system to image the drop. The free open source image processing software program ImageJ and the plugin, dropSnake, was used to analyze the images of the drops[83]. The syringe plunger was controlled manually by pressing down to release a single drop of water 15µl in volume. After each drop an image was taken using the Amscope MD600 camera, and then the contact angle was calculated using the ImageJ software. Each deposition sprayed in duplicate and three drops per slide were performed.

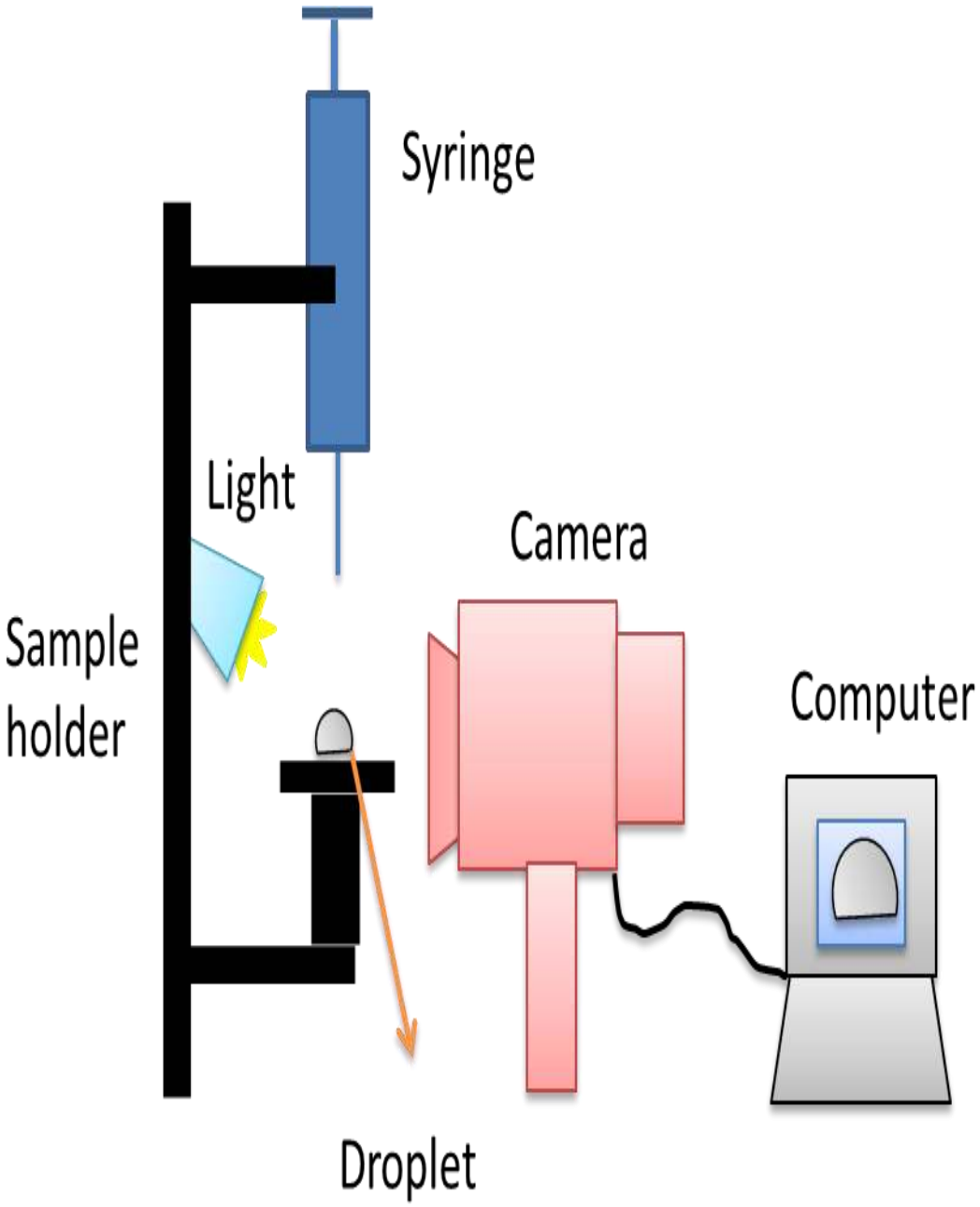

Figure 22. Schematic of an in-house physical water-drop apparatus to measure contact angle on solid surfaces.

CHAPTER 3: ANTIBODY IMMOBILIZATION USING PNEUMATIC SPRAY: COMPARISON WITH THE AVIDIN-BIOTIN BRIDGE IMMOBILIZATION METHOD

This chapter summarizes the results of the publication "Antibody immobilization using pneumatic spray: Comparison with the avidin-biotin bridge immobilization method". Results were published in the Journal of Immunological Methods and can be found in the appendix B.

3.1 Introduction

The detection of pathogens in the food industry, the detection of biological molecules that can be used in bioterrorism, or the detection of biomarkers for medical diagnostics have been a topic of growing interest in the scientific community in the past years. Biosensors are the preferred tool to achieve those tasks due to their ability to detect biomolecules selectively. Many biosensors use selectively bonding biological molecules (i.e. antibodies, oligonucleotides, enzymes) to enhance the selectivity of the device.[1-4]. One of the most sensitive and reliable devices currently used in the detection of biomolecules is the evanescent wave biosensor[5]. This type of sensor is usually used with antibodies as the detecting entity due to their high specificity for targeting biomolecules.

The immobilization of the detector entity (i.e. antibody) is a crucial step in the preparation of biosensors for the recognition of the captured biomolecules. Many

different methods to immobilize the antibody onto a solid surface (while preserving bio-sensitivity) have been developed in recent decades leading to a variety of choices for immobilization. Among the most common methods to immobilize biomolecules onto solid surfaces are direct covalent attachment, attachment through an intermediate layer and physical adsorption.[6,7]

The direct covalent attachment procedure immobilizes antibodies on a glass surface via silanes, which provide a chemical interface that is easily adapted for specific molecules. The attachment of the silanes can be done through amine-and thiol terminated silane groups. The antibody is immobilized directly to the silane group[8-11] via an intermediate layer which is the most common technique to immobilize antibodies on solid surfaces. One example for an intermediated layer is the Avidin-Biotin Bridge (ABB) where a protein (i.e. avidin) is the intermediate molecule to immobilize the antibody. This method of immobilization is very efficient due to the high degree of orientation of the antibody that can be achieved during the immobilization process. However, this technique involves many intricate and complicated steps leading to a long multi-step process which is prone to errors. These issues lead to losses in materials and time due to an inheriting slow feedback loop for the detection of unsuccessful steps[12-14].

The physical adsorption method has not been very popular among researchers due to the perceived issues such as non-specific adsorption, chemical instability interaction at low or high pH[16-18] and the probability that adsorbed proteins can leach or wash off from the surface if the coated substrate is exposed to a liquid flow[19]. Some studies also

suggested that the adsorption of proteins can lead to denaturation of the biomolecule through surface-protein interaction[5,20,21] producing non-specific binding of the antibodies. Despite these potential issues the simplicity of the physical adsorption technique also offers advantages[22,23]. The results of this study show that physically adsorbed films deposited via pneumatic spray are compatible with the requirements of biosensor, suggesting that physical adsorption is a viable alternative for the immobilization of antibodies.

The presented research explores the immobilization of affinity purified, goat anti *E. coli* O157:H7 antibody on glass using a low flow concentric nebulizer. The spray apparatus nebulizes the solution into microscopic droplets. This enables an almost dry deposition of the antibody on the surface. This process creates a compact antibody thin film of high density, which increases the capture efficiency. The spray process offer advantages that include the fast fabrication of patterns, an almost chemical free process, consistent coverage of the sprayed surface, easy set up, and low cost and maintenance of the equipment, which makes the pneumatic spray an inexpensive and efficient immobilization technique.

The results obtained during these experiments for comparison purposes of both deposition techniques, showed a lower sensitivity for the sprayed slides which was not related to a decrease in functionality of the films but rather to the spraying process. For the specificity, shelf life and capture efficiency results suggested no significant differences for both techniques. The thickness for both types of deposited films were

similar, but the thickness of the spray slides is based only on antibody while the avidin-biotin technique used cross linkers and intermediates before the antibody.

3.2 Results

The first step for the comparison of both deposition techniques was to determine the pattern reproducibility of the pneumatic spray films on glass and its use for immunoassays. Figure 23 shows representative images (A-C) of the antibody immobilization patterns of pneumatic spray slides assayed for repeatability; for comparison purposes an avidin-biotin bridge immobilization pattern was also included (D). All slides have well defined patterns with at least 6 usable rows for immunoassays. The mechanical stability of the films was tested by rinsing the slides with buffer solution (as performed during immobilization protocol) which did not lead to a degradation of the pneumatic spray patterns. Two of the slides showed a higher background as shown by the resulting fluorescence between the rows of each slide (Figure 23 C). Some of the antibody patterns were slightly off-centered (apparatus set-up was adjusted to center patterns in preceding experiments) and some of the rows were slightly wider than others due to the custom made metal mask used. Overall, all slides had defined multi-row patterns suitable for the testing of the functionality of the patterns.

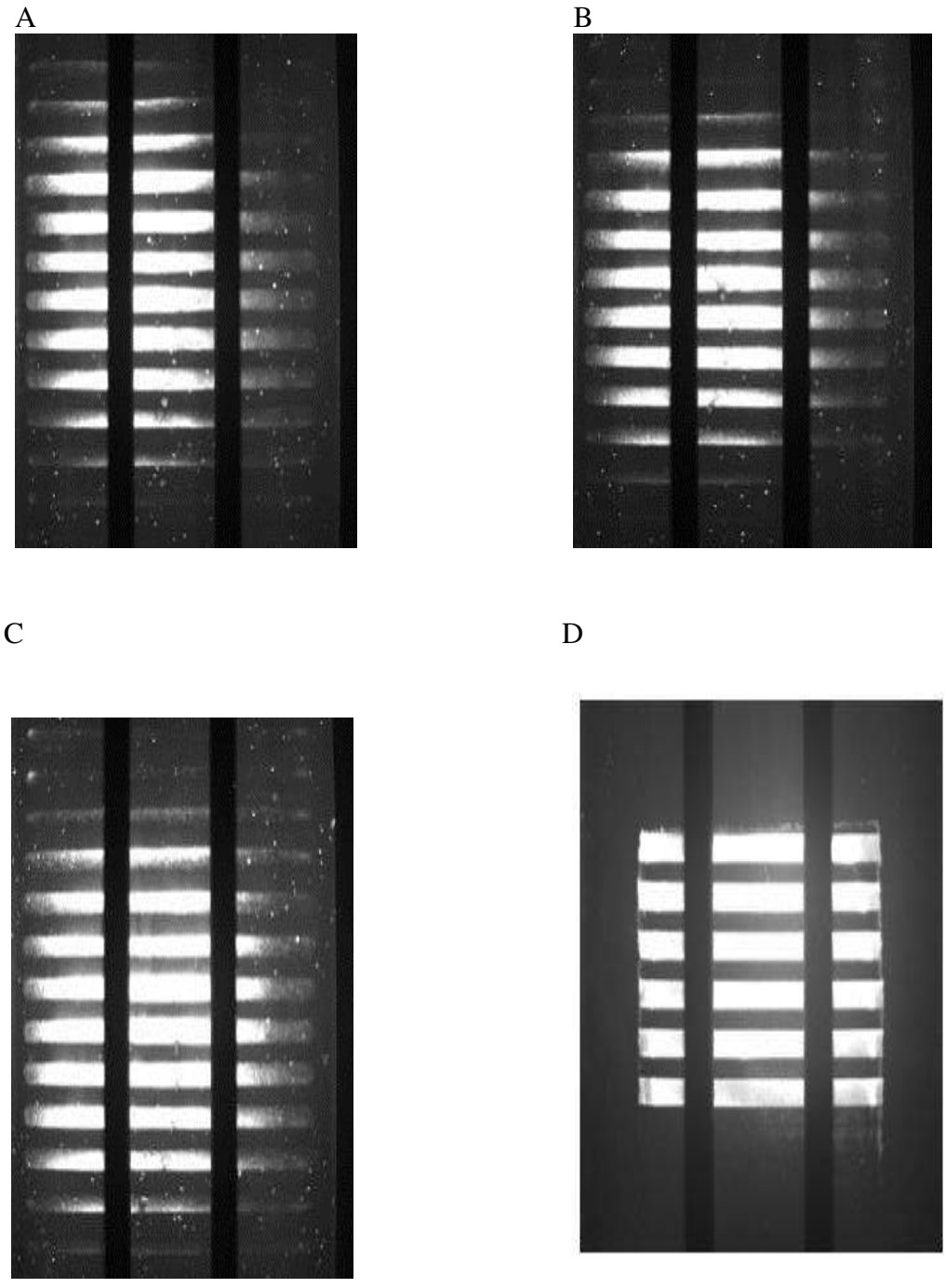

Figure 23. Representative images (A-C) of the ten slides sprayed with established parameters of 200 µg/mL goat anti-E. coli O157:H7 IgG with 60 PSI N2 outflow, 7 min spraying time, 30 mm distance from slide to nebulizer, and slide rotation at 12 RPM. Slides were

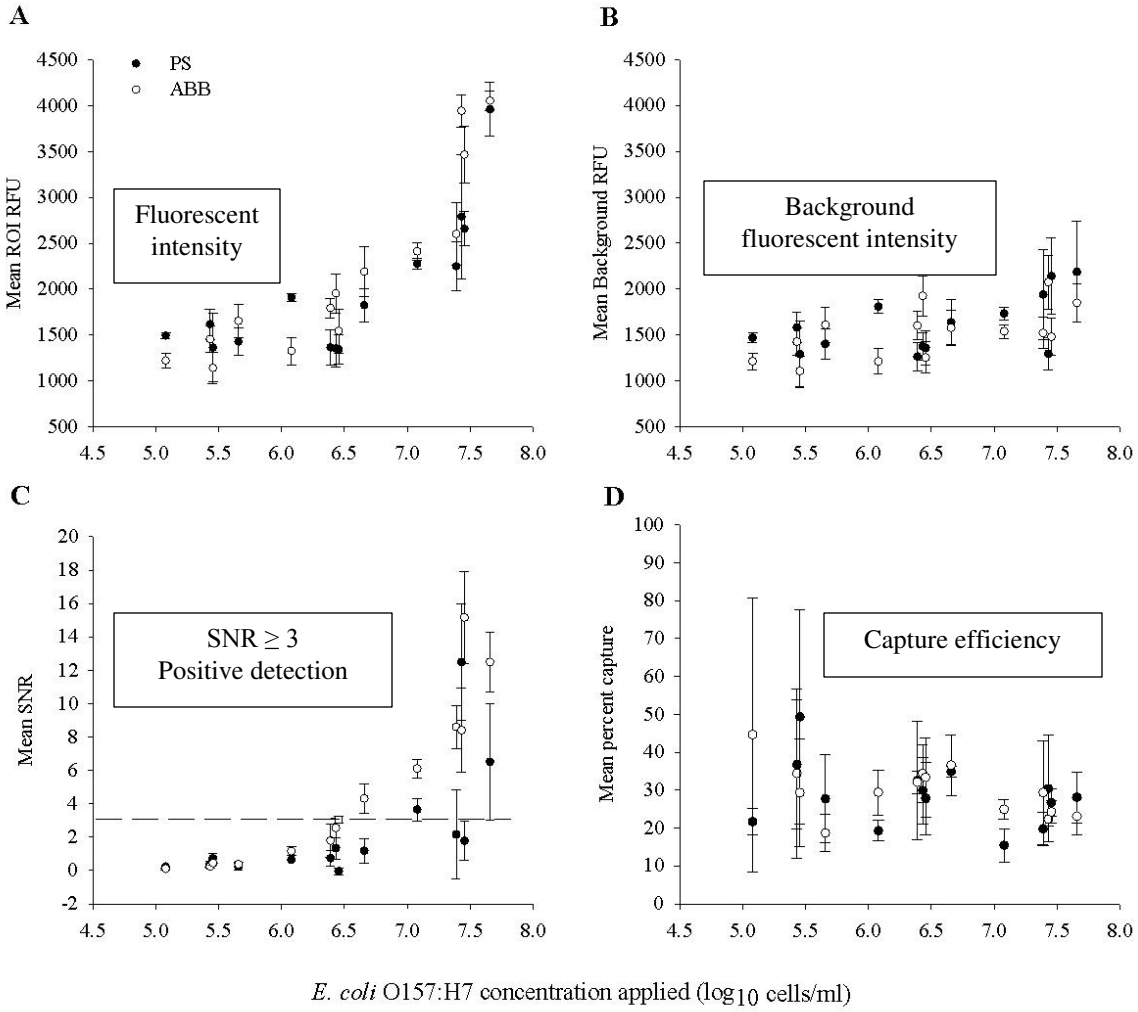

Figure 24. Comparison of mean (A) fluorescent intensities, (B) background relative fluorescent units, (C) signal to noise ratios, and (D) percent capture efficiencies for multiple samples of E. coli O157:H7. ROI denotes region of interest, RFU is relative fluorescent units.

The sensitivity of the deposited films created via spray and covalent bonding was tested by the analysis of fluorescence intensities and signal to noise ratio. Figure 24 A and B display the mean fluorescent intensity values as relative fluorescent units (RFU) obtained for *E. coli* O157:H7 samples assayed on pneumatic and avidin-biotin bridge prepared slides. The mean RFU values at 5 $\log_{10}$ cells/mL were similar for both slide

immobilization processes with no significant difference (P=0.1581) but were significantly different at 6 $\log_{10}$ cells/mL (P=0.0072) and 7 $\log_{10}$ cells/mL (P=0.0104) in which the avidin-biotin bridge slides had higher values. Mean SNR values (Figure 3C) yielded no detection at 5 $\log_{10}$ cells/mL for pneumatic spray and avidin-biotin bridge slides, 0% and 40% detection at 6 $\log_{10}$ cells/mL and 60% and100% detection at 7 $\log_{10}$ cells/mL for pneumatic spray and avidin-biotin bridge, respectively. There was no significant difference (P=0.1175) between the 5 $\log_{10}$ cells/mL mean SNR but there were significant differences (P<0.0001) at the 6 and 7 $\log_{10}$ cells/mL concentrations where avidin-biotin bridge slides had higher values. The lower ROI (Figure 24 A) and higher background RFU values (Figure 24 B) in comparison to avidin-biotin bridge slides caused the low pneumatic spray slides SNR values.

The main characteristic of a waveguide used in a biosensor is the ability of the immobilized antibody films to capture antigens. These characteristic is tested by calculating its capture efficiency. The mean percent capture efficiencies (Figure 24D) were similar for both slide immobilization processes at each concentration. There were no significant differences between the two techniques at 5 (P=0.5600), 6 (P=0.1673), or 7 $\log_{10}$ cells/mL (P=0.9964). The specificity experiments yielded no detection of any of the non-*E. coli* O157:H7 strains tested. The mean SNR values of all pneumatic spray and avidin-biotin bridge assayed slides were $\leq$ 0.2 ±2. In comparison, the *E. coli* O157:H7 positive control yielded a mean SNR of 15.2 ±10.5 for the pneumatic and 14.6 ±6.4 for the avidin slides.

To test the shelf life of the pneumatic sprayed films some slides were deposited and stored for a set period of time. Figure 25 displays the mean fluorescent intensities, SNR values, and percent capture efficiencies for pneumatic spray slides stored for different number of days at 4˚C and then assayed with GFP-*E. coli* O157:H7 at 7 $\log_{10}$ cells/mL. RFUs (Figure 25A) were similar to those generated by the antibody functionality experiments (Figure 24A) at the same concentration with no significant difference (P=0.7155). Mean SNR values (Figure 25C) yielded positive detection of *E. coli* O157:H7 at 7 $\log_{10}$ cells/mL; showing that there was no loss of detection for the pneumatic spray slides stored up to 100 days. There was a significant difference (P<0.0001) between the SNR values for the stored slides and the antibody functionality experiments (Figure 24C).

The SNRs for the stored slides were higher. This was due to the lower background RFUs (Figure 25B) achieved for the stored slides in comparison to the significantly higher (P<0.0001) values for the antibody functionality experiment slides (Figure 24B). The mean background RFU values were between 1400-2500 in the first 3 slides but then went down to 900-1700 range for the rest of the slides (Figure 25B). Mean percent capture efficiencies against time stored ranged from 11 - 73% with the median range at 10 - 40 % (Figure 25D). There was no significant difference (P=0.6599) between these percent capture efficiencies and those generated by the antibody functionality experiments (Figure 24D). The slides had defined multi-row patterns until day 71 when loss of pattern approximately 1/3 of a row for 1-3 rows was observed (images not shown).

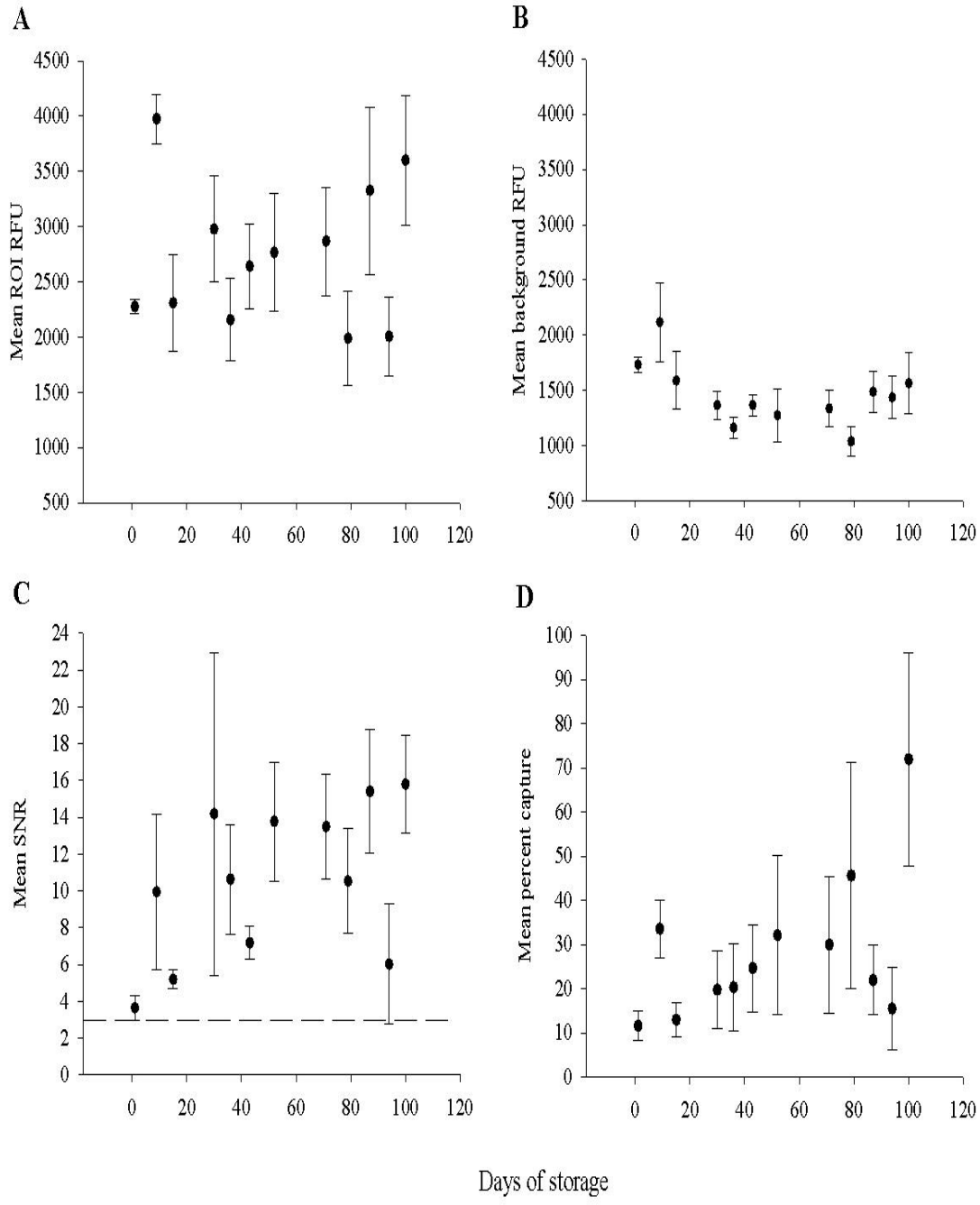

Figure 25. Mean (A) fluorescent intensities, (B) signal to noise ratios, and (C) percent capture efficiencies for PS slides stored for different number of days at 4°C and then assayed with E. coli O157:H7 at 7 log10 cells/mL.

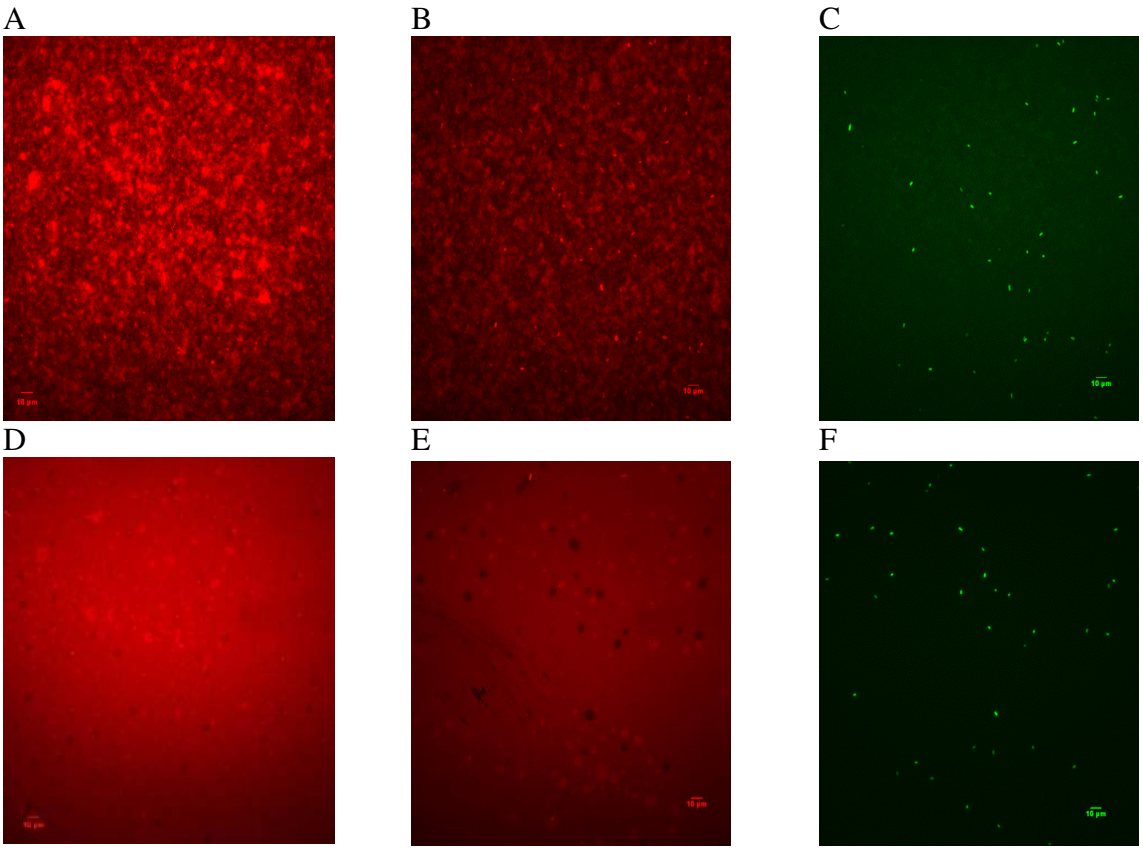

Figure 26. Epifluorescent microscopy representative images of (A, B, D, E) immobilized antibody patterns visualized by treatment with Rhodamine Red donkey anti-goat IgG and (B, C, E, F) captured GFP-*E. coli* O157:H7 cells. Images on the left are (A) pneumatic and (D) avidin-biotin immobilized goat anti-*E.coli* O157:H7 patterns with no cells using a 535-550 excitation filter. Images in the middle are (B) pneumatic spray and (E) avidin-biotin immobilized goat anti-*E.coli* O157:H7 patterns with GFP-*E. coli* O157:H7 cells using a 535-550 excitation filter. Images on the right (C, F) are the corresponding areas of (B) and (E) but using a 470-490 excitation filter to view the GFP cells (fluorescing green dots).

The purpose of this experiment was to visualize the morphology of the antibody film through labeling the deposited antibodies with a fluorophore (Rhodamine Red) tagged IgG antibody, which selectively binds to the deposited goat IgG (i.e. goat anti-*E. coli* O157:H7) on the slides. This allows the visualization and identification of the immobilized antibody on the surface. The pictures above (Figure 26) are a representative

of the fluorescent microscopy images of immobilized antibody patterns measured on glass. In these experiments GFP-*E. coli* O157:H7 cells were captured on the pre-treated immobilized goat anti-*E. coli* O157:H7 antibody surfaces and treated with Rhodamine Red donkey anti-goat IgG. Comparison of the pneumatic spray and the avidin-biotin bridge patterns (Figure 26, A and B to D and E) showed that the spray deposited patterns were less homogeneous than the patterns generated with the standard wet-chemical method. These films exhibited a more homogeneous fluorescent signature. Similar measurements were performed on slides that were assayed with GFP-*E. coli* O157:H7 cells, and similar results were obtained. However, an interesting observation was made when assayed slides (i.e with cells present) were viewed after tagging with Rhodamine Red IgG: The GFP-*E. coli* O157:H7 cells that had been captured (showing green fluorescence in Figures 26 C and F) showed up as fluorescent red dots on the Rhodamine Red tagged images (Figure 26B) of the sprayed slides, while they are not visible on standard slides (Figure 26E). Since the Rhodamine Red IgG only tags the antibody, this suggests that some antibody on the sprayed slides dislodged during the incubation process and bonded to the immobilized *E. coli* O157:H7 cells during sample incubation, making them visible through Rhodamine Red IgG tagging. Note that these slides did not have primary reporter antibody (AF647 conjugated goat anti-*E.coli* O157:H7 IgG) added prior to pattern visualization.

Fluorescent microscopy was used to visualize the immobilized antibody and captured GFP bacteria on the deposited films. Images showing the area between rows were included to describe the differences between the two immobilization techniques.

Images on slides treated with the reporter antibody are shown in Figure 27. These slides were incubated with GFP-*E. coli* O157:H7 at 7.4 $\log_{10}$ CFU/mL followed by addition of primary reporter antibody (AF647 conjugated goat anti-*E. coli* O157:H7 IgG) and then treated with Rhodamine Red donkey anti-goat IgG. Rhodamine Red IgG bound to the immobilized antibody on the surface and to primary reporter antibody on the surface of the cells. Another observational difference was that the pneumatic spray slides had "blotchy" fluorescence observed at the surface of the slide with the captured bright red cells (Figure 27B). The blotchy signature is due to the formation of antibody aggregation during the spraying process which created an inhomogeneous morphology. This was not seen on the avidin-biotin bridge slides which had minimal fluorescence at the slide surface (Figure 27D). This indicates that there is less immobilized antibody than what is on the pneumatic spray slides.

The analysis of the film thickness for the two deposition techniques used in these experiments and the potential influence in the capture ability was performed using ellipsometry. A linear relationship between the thickness of the film and the deposition time using the spray method was found based on the ellipsometer data. A linear regression yielded of 0.9874. The standard deposition time of 7 min for the pneumatic spray process showed an average thickness of 155.25 ± 11.78 Å, while the average thickness calculated for the avidin-biotin bridge method was 183.16 ± 8.54 Å. The corresponding mass for the deposited antibody was calculated to be around 9.05 ng/mm^2 for the pneumatic spray slides while the deposited mass for the covalent technique avidin-biotin bridge was reported to be between 2.2 ng/mm^2 [12,21] and 4.74 ng/mm^2 [15,18].

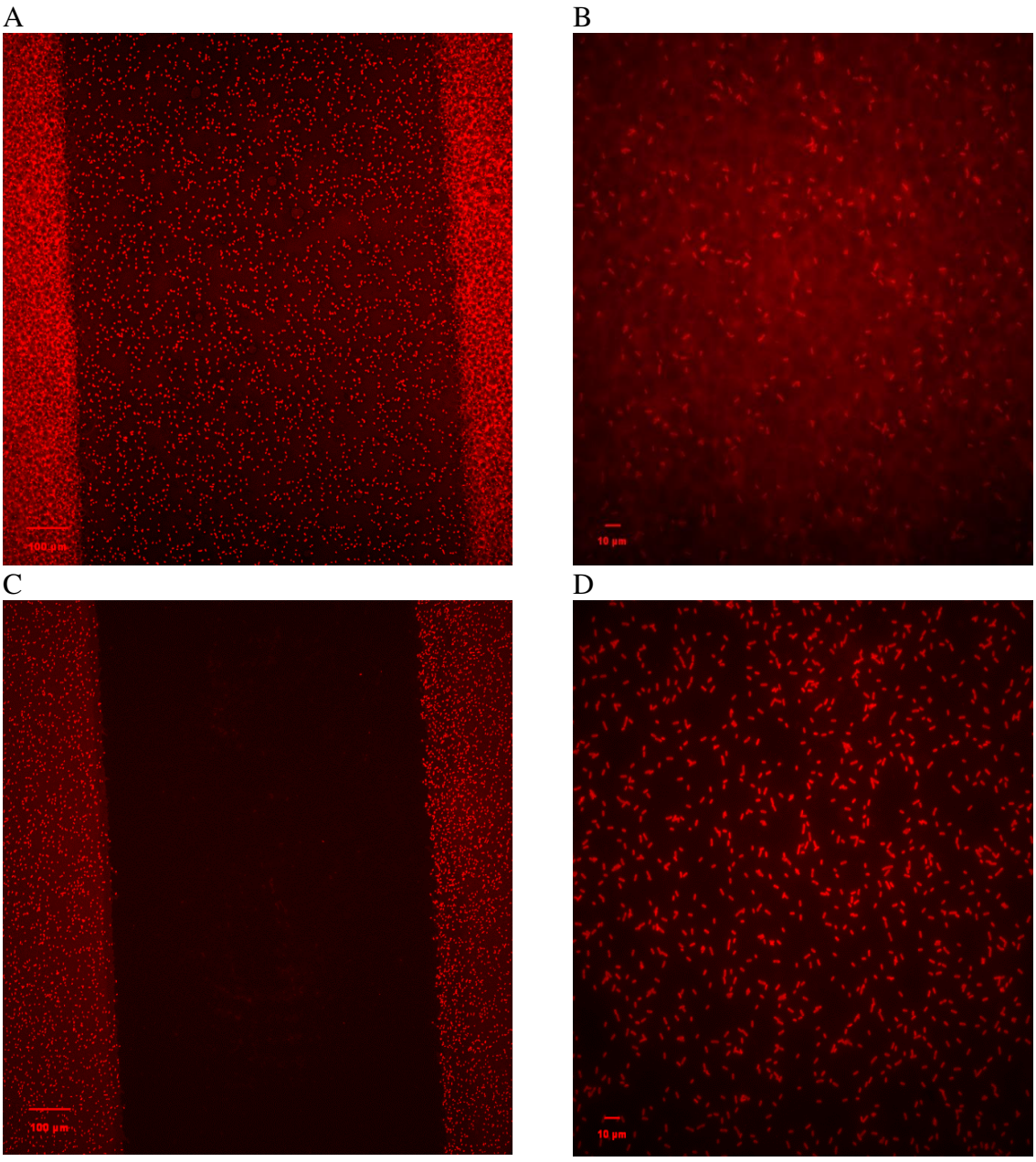

Figure 27. Epifluorescent microscopy representative images of slides immobilized by pneumatic spray and avidin-biotin bridge. All the slides were treated with Rhodamine Red conjugated donkey anti-goat IgG. Pneumatic spray slides (A) had immobilized antibody and captured cells in between the pattern rows (B) immobilized E. coli O157:H7 on goat anti-E. coli O157:H7 IgG . Avidin-biotin bridge slides (C) no cell detected between rows and (D) immobilized E. coli O157:H7 on goat anti-E. coli O157:H7 IgG.

3.3 Discussion

Two immobilization methods were investigated in this study. Spray based dry physical adsorption was compared against the standard covalent attachment method using several quantitative parameters.

The stability and durability of the film strongly depends on what happens to the adsorbed protein at the surface but there is still no agreement among researchers regarding that matter. It appears that most reports can be divided into two groups who either claim that physical attachment leads to denatured films or show in contrast that physical attachment works well. Moulin et al., for example, mentions low stability of films and the denaturation of the adsorbed protein at the surface[21] as a disadvantage for the immobilization method of physical adsorption. However, other studies showed that adsorption of antibodies onto glass in the monolayer region let the antibody conserve their native structure with minor perturbations, [27,28] allowing the antibody to keep its specificity and reactivity towards a target. Similarly, Rabbany et al. concluded that increasing the density of the immobilized antibody at the surface reduces the apparent dissociation rate[29] giving more stability to the antibody.

The results presented here suggest good chemical and biological characteristics for the pneumatic spray films. This is supported for example by the retention of the capture efficiency even after a long storage period, i.e. the sprayed (physical absorption) and the wet-chemical (covalently attached) films have both comparable shelf lifes.

Another sign for high stability of the sprayed films is their excellent stability during the applied vigorous rinsing process during the film fabrication protocol.

Another important result demonstrating the viability of the spray method is the outcome of a specificity test where the two immobilization techniques were tested on different bacteria commonly found in water and food samples[30-33] . Both techniques yielded substrates that showed no significant cross reactivity. The negative detection for the non-*E. coli* O157:H7 bacteria on all of the slides immobilized by both techniques, and the positive detection with the *E. coli* O157:H7 (used as reference) clearly demonstrate that the antibodies do not suffer significant damage through the spray process nor are they harmed by the physical adsorption on the glass surface, which intrinsically, is prone to non-specific binding to a range of types of bacteria.

It is interesting to compare the thicknesses of the active films on both sprayed and covalent-attachment films. Ellipsometry measurements on both types of films showed that the thickness of both films was similar. However, it must be considered in this context that the thickness of the sprayed slides corresponds entirely to sprayed antibody, whereas in the case of the covalently attached films, the thickness is a result of the multi-layer molecular buildup during the covalent attachment process (i.e. silane linker, avidin-biotin bridge plus the capping antibody layer). This may explain the very close performance of both film types despite the principally different attachment strategy. While the random orientation of the sprayed antibody likely disables a certain percentage of the antibody on the surface, their higher density compensates for this disadvantage.

This hypothesis is supported by results presented by Peluso et al. who found that the oriented antibody immobilization achieved with the covalent attachment method usually results in a collateral decrease of the surface coverage when compared with random attachment.

Another aspect of the presented results is that the sprayed patterns exhibited a higher background signal than the wet chemically prepared slides. During the standardized evaluation of the measured intensities during the assay this phenomenon lead to a lower signal-to-noise ratio for the sprayed films compared to the wet chemically prepared ones. The reason for this difference, however is not intrinsic to the spray process, it is rather an artifact resulting from the masking technique used in these explorative experiments. The mask that was used did not fully conform to the glass substrate since it was made from aluminum, which slightly deformed during the machining process. This resulted in some degree of penetration of sprayed antibody aerosol underneath the masked area. This caused a low-density antibody coating in these areas with resultant antigen capture capability during the tests. A solution in future experiments will be to employ rubberized masks or similar to prevent this artifact from happening. It can be expected that this will completely alleviate this issue, and that comparable signal-to-noise ratios to the covalent attachment method will be seen.

A comparison of the absolute intensities between the sprayed and wet-chemically deposited films yielded a slightly higher intensity on the standard covalently attached antibody layers. The data shown in Fig. 26 B/E suggests an explanation for this

phenomenon. The images in Fig. 26 demonstrate that cells immobilized on sprayed substrates are coated by a certain amount of antibody during the assay. This has most likely the consequence that a number of bonding locations on their surface are blocked by antibody, preventing the reporter antibody used to tag immobilized antigens from attaching. This phenomenon appears absent on assays prepared on covalently attached films, i.e. more reporter antibody per number of cells can be attached. Hence, the observed intensity will be higher. However, at this point this is only a qualitative observation and further experiments will need to be performed to quantify this process.

With regard to capture efficiency the presented data shows that both techniques have similar performance. This is most likely the result of a compensatory process between antibody orientation and antibody density. The above discussed film thickness analysis clearly suggests that the sprayed films have a higher density than the wet-chemically attached ones. This is not surprising since the spray process is a non-equilibrium technique, while the covalent attachment in solution is equilibrium controlled. In other words the spray technique can load the surface with antibodies practically without limit, while the chemical attachment in solution has a maximum density that is governed by the rate constants of the participating chemical reactions. However, there is a limit with regard to increasing the antibody layer thickness to increase the capture efficiency since buried antibodies do not participate in the capture process. Separate experiments (not shown here) confirmed this by demonstrating that there is a thickness threshold for the spray method after which no further improvement can be achieved through thickness increase.

While at a disadvantage with regard to antibody density, the wet-chemically prepared films clearly have a higher degree of orientation[9]. Results by Smyth et al. [26] and Xu et al.,[35,36] for example support this hypothesis. They showed that random orientation reduces the ability of the antibody to react with the antigen due to the impact of steric hindrance generated by the arbitrary alignment of the antibodies. In the same vein, Peluso et al. found an average increase of 33% in binding activity for specifically oriented antibodies when compared with randomly oriented antibodies[38] with the same antibody density at the surface. However, Spitznagel et al. suggested that despite the favorable orientation of the antibody at the surface of covalently attached films, molecular crowding can denature the Fab region making it necessary to find an optimal maximal coverage, which is not necessarily achieved by the wet-chemical method[37]. In summary, it appears that oriented attachment represents an advantage, but a disadvantage results from the need of a covalent attachment scheme that usually does not yield an optimum coverage.

The inhomogeneous morphology of the sprayed films is a result of the spray process. The spray head creates an aerosol containing small droplets of antibody solution. These droplets decrease in size with the distance traveled from the nebulizer to the surface of the glass as the solvent evaporates. This increases the concentration of antibody in the droplet. In the extreme, this process can even result in dry antibody clusters before they reach the substrate surface. The films for the presented experiments were prepared in a mode where it was ensured that some solvent was still present during surface contact to enable some mobility for the antibodies on the surface to smoothen the

resulting film. Nonetheless, the random distribution of droplets across the surface clearly causes an inhomogeneous coverage formed by overlapping droplet residues. This is clearly visible in the Rhodamine Red IgG images shown in Fig.26 where the sprayed film yielded a spotty image, while the covalently attached film produced a much more homogeneous result.

The morphology of the sprayed films is important since not only the number of available antibodies is crucial for good capture efficiency, but also their microscopic environment. This is supported by the results of several groups: Xu et al. noted that having a dense antibody surface reduces the structural unfolding and thereby increases the antigen binding capacity[39]. Kamyshny et al. suggests that the formation of aggregates can favor the adsorption at the surface and that an increase in antigen binding activity is expected with a denser antibody layer[40]. Cui et al. developed a layer-by-layer (LBL) film composed of avidin-biotin labeled antibody and concluded that as the number of layers of ABB increase from one to three, the amount of antigen that can be captured increases as well enhancing the binding ability compared with the covalently immobilized monolayer antibody[15]. In light of these results the high density of the antibody films created by the spray technique clearly has the potential to increase the stability of antibody films and it potentially also results in an increased shelf life. However, further experiments are needed to demonstrate these hypotheses.

3.4 Conclusions

The immobilization of antibodies on silica surfaces using cross-linkers it is a well-known method providing stability through a covalent attachment to the surface. However, the process is long, tedious and is achieved with the use of several different and hazardous chemicals. Protein adsorption as a method of immobilization of antibodies was not fully developed before because of the belief that there was a partial denaturation of the antibodies in addition to a low attaching force that caused the antibodies to leach off during the process[17]. The results presented in this report suggested that a simple method using pneumatic spray can be employed to effectively immobilize antibodies to silica surfaces without any prior chemical treatment and give equal or better results than the avidin-biotin bridge method. The capture efficiency for both methods were in comparable ranges however, intensities for the pneumatic spray were lower because mask/surface seal issues. This issue can likely be corrected by using masks with a gasket seal. The specificity test proved that no significant denaturation occurred during the spray process leaving the antibody intact and able to bind specifically to the bacteria. The shelf life results showed that the thin films were essentially stable over time when stored properly. The optimized thickness of the pneumatic spray film is comparable with avidin-biotin bridge process films. The pneumatic spray film was also able to resist the strong rinsing process suggesting that the thin film created by the pneumatic spray technique is attached to the surface by an irreversible adsorption. The high reproducibility of the spraying method, the good stability and capture efficiency of the film, and the enormous reduction in preparation time and material cost makes this new technique a valid, useful and efficient way to produce bio-assays for commercial biosensor devices.

CHAPTER 4. CHARACTERIZATION OF FULLY FUNCTIONAL SPRAY-ON ANTIBODY THIN FILMS

This chapter summarizes the results of the publication "Characterization of fully functional spray-on antibody thin films". Results will be published in a scientific journal and can be found in the appendix C.

4.1 Introduction

The authors' previous work demonstrated that sprayed antibody films can have a similar capture efficiency as films deposited using chemical bonding based avidin-biotin bridge films methodology [84]. This result warranted an investigation of the structural properties of sprayed films in comparison to covalently bonded ones with the goal to better understand the origin of their remarkable performance. Understanding the morphological characteristics of the films is especially important as surface properties strongly influence the immobilization of biomolecules onto solid surfaces and cell adhesion[85, 86].

Proteins (i.e. antibodies) immobilized on solid surfaces are commonly used for analysis and detection of specific target molecules using biosensors[87]. The IgG antibody is an immunoglobulin protein that has been widely used as a capture agent for detection of pathogens with sensor devices[88]. The immobilization method used to attach proteins to solid surfaces can vary with the type of analysis performed. There are

two principal approaches to these immobilization techniques: covalent boding and physical adsorption (Figure 28). The immobilization technique applied to the substrate as well as chemical and mechanical characteristics of the film (i.e. hydrophobic/hydrophilic, roughness, surface density) directly influence the morphology of the resulting surface and structural stability of the films.

Covalent bonding (i.e. avidin-biotin bridge) is the most widely used method, where chemical reactions attach the biomolecule via chemical bonds. This method is an equilibrium controlled process that limits the amount of molecules deposited on the surface. In the case of antibodies this can produce a film with a high degree of oriented molecules, high levels of coverage and a homogeneous surface resulting in chemical and mechanical stability[12, 89]. Physisorption on the other hand uses physical interaction (i.e. no chemical bonding occurs) to immobilize biomolecules to the solid surface. The pneumatic spray adsorption process is a non-equilibrium physisorption technique that can load the surface with a tunable antibody density. However this type of immobilization produces a randomly oriented antibody surface. Random orientation is often cited as the main reason for the poor mechanical stability and protein denaturation (chemical and biological alteration) in physisorbed films[1, 90]. In difference to incubation (covalent bond) based immobilization techniques, spray deposition offers a variety parameters that can be controlled for the optimization of film thickness and morphology. Ambient temperature, flow rate, emitter-to-substrate distance and carrier gas pressure can be varied to control the solvent content at the substrate and the spray coverage area while adjustments of the deposition time allows for the control of the surface density.

This chapter aims to identify and establish the influence of morphological and chemical characteristics of the pneumatically sprayed films on the overall performance and capture efficiency. Sandwich immunoassay, fluorescent microscopy and ellipsometry were used to determine the influence of the thickness of the pneumatic spray films on capture efficiency[91, 92]. The chemical and mechanical stability of the deposited films were studied by ellipsometry, UV-Vis spectrometry and ATR-FTIR [93, 94]·[95, 96]. Surface wettability, coverage and a possible film-growth method for the pneumatic spray films were studied by contact angle, atomic force microscopy and XPS[97, 98]·[99, 100]·[101, 102].

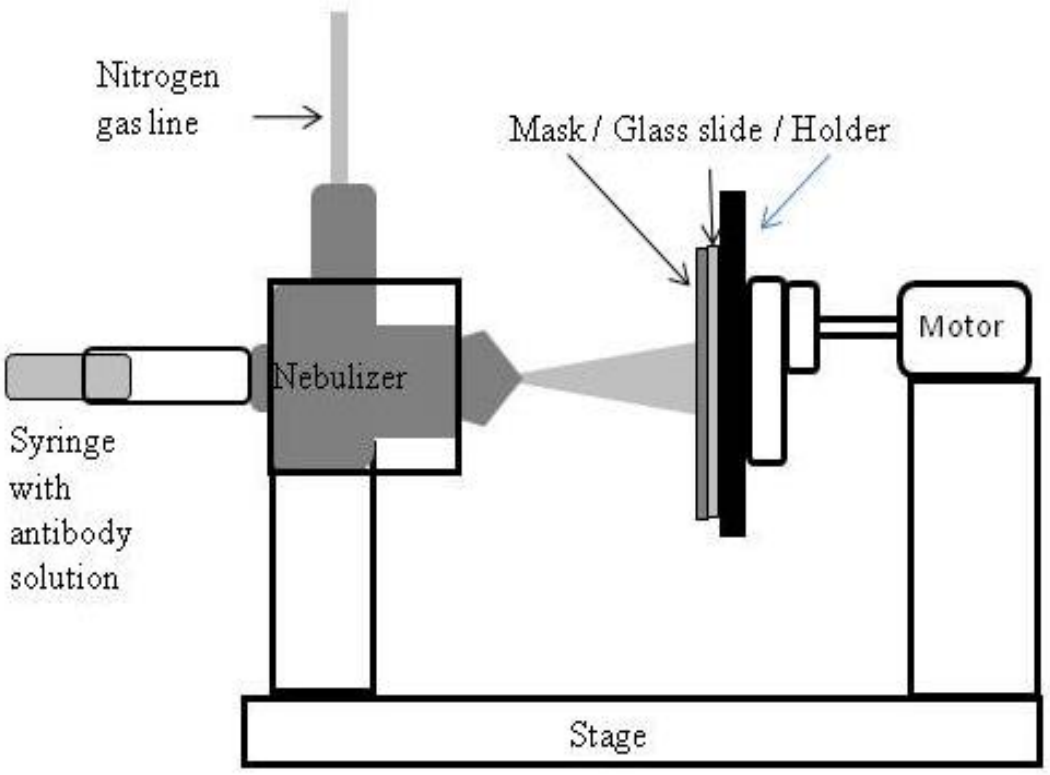

Figure 28. Pneumatic spray set-up for deposition of antibody onto glass slides. The nebulizer used was model DS-5.

4.2 Results

4.2.1 Ellipsometry, UV-Vis spectroscopy and ATR-FTIR

The thicknesses, mechanical and chemical stability of the pneumatically sprayed films were analyzed by ellipsometry, UV-Vis and infra-red spectroscopy. The ellipsometry data showed a linear relationship between the thickness of the film made by pneumatic spray and the deposition time with a linear regression of 0.9935. The average thickness determined for the avidin-biotin bridge technique was 183.16 ± 8.54 Å. After a minimum deposition time of 2 min, the pneumatic spray films had a similar cell capture performance as the avidin-biotin samples. A 2 min deposition corresponds to an average thickness of 55.62 ± 4.35 Å. The corresponding antibody surface density was calculated to be approximately 9.05 ng/mm^2, which is close to double the amount reported for the avidin-biotin bridge technique (4.74 ng/mm^2)[54]. The calculations were based a deposited diameter of 15 mm. The results shown in Figure 29 show that only about 5% or less of the antibody film was lost during the rinsing process.

The greatest percentage loss occurred on the 7 minute deposition sample. No protein was detected in the wash solutions by UV-Vis spectroscopy. This may be due to the fact that the diluted antibody solution had a concentration that was below the effective detection limit of the instrument. The 7-minute deposition had a total deposited antibody amount of 5.6 µg with a maximum antibody loss of approximately maximum of 5%. According to these results 0.28 µg was removed in the wash solution. The volume of the wash solution was 3 mL resulting in a concentration of 0.093 µg/mL an amount that is below the detection limit of the calibration curve (0.1 µg/mL). A different analytical

technique may have to be used in the future to better assess the amount of antibody concentration in the wash solution.

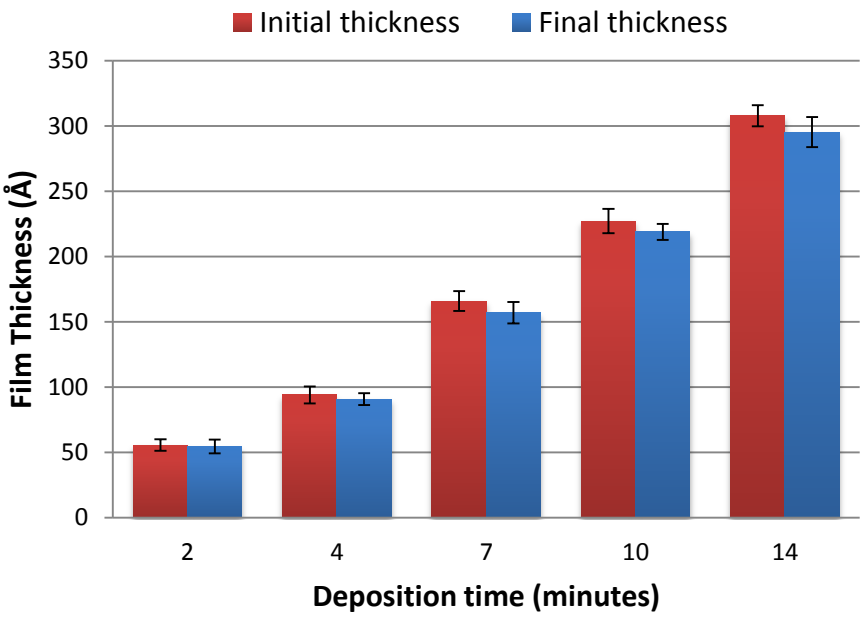

Figure 29. Film thickness change after rinsing process. Different deposition times of goat-*E. coli* O157:H7 antibody films by pneumatic spray followed by rinsing using PBS. Thickness determined by ellipsometry before and after rinsing.

ATR-FTIR spectra analysis was performed on pneumatically sprayed antibody films with varying deposition times of 60, 50, 40, 30, 20, 14, 10, 7, 4, and 2 minutes. The region shown in Figure 30 displays the infra-red absorbance between the wavelengths of 1540 and 1720 cm^{-1}. The amide I band has wavelengths in the range between 1600 and 1700 cm^{-1} [94]. The amide I peak position (average 1640.66 ± 0.51 cm^{-1}) did not change with the increased deposition time. The baseline spectra obtained from the bulk antibody

solution showed the amide I band at 1639.5 cm^{-1}. This is very close to the peak observed with the pneumatic spray films, suggesting that the deposited antibodies are still intact.

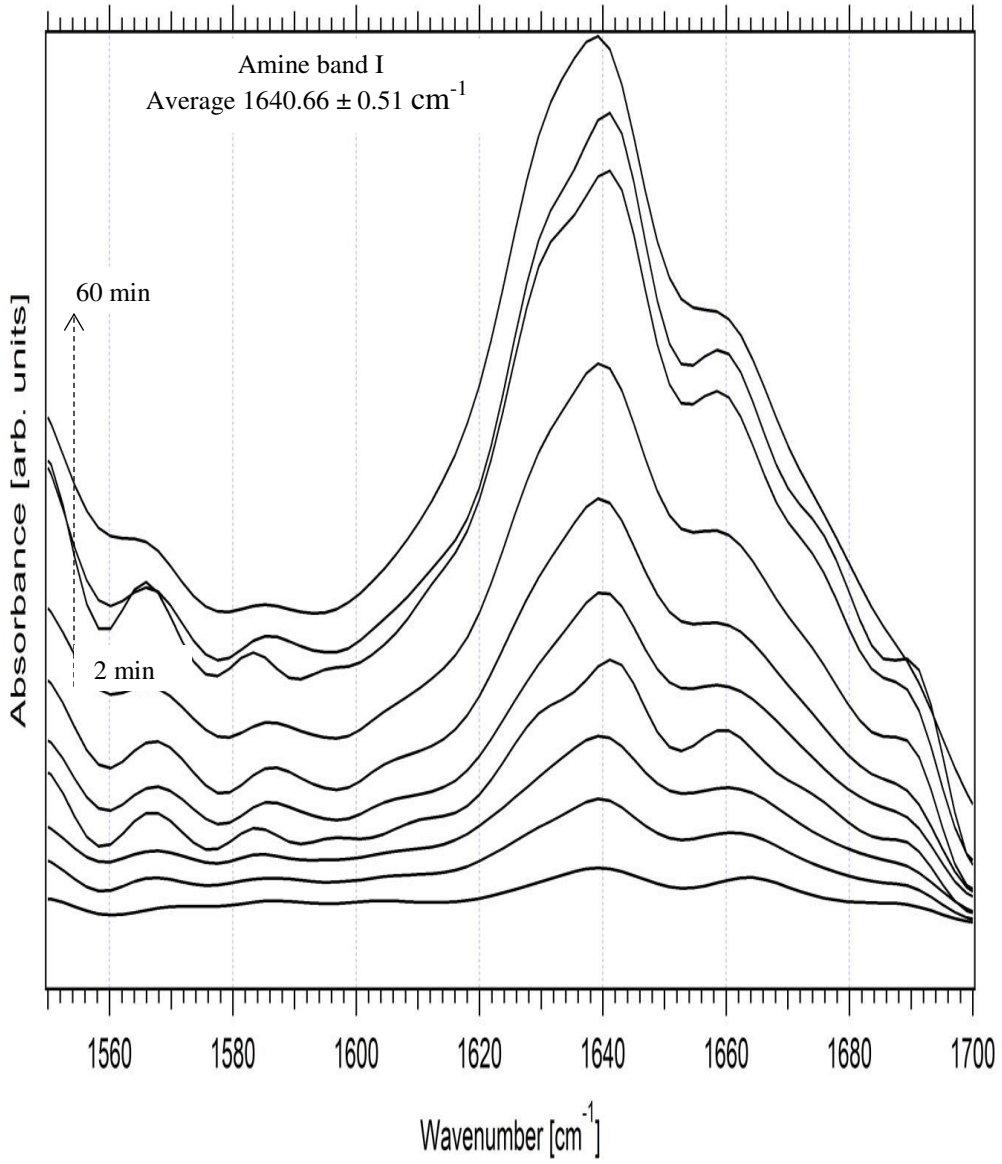

Figure 30. ATR-FTIR spectra of goat-*E*.coli O157:H7 antibody pneumatically sprayed at different deposition times. The deposition times are (2,7,10,14,20,30,40,50,60 min) from bottom to top in the same order. Amine band I vibration at 1640.66 ± 0.51 cm^{-1} average.

4.2.2 AFM, XPS and contact angle measurements

The surface morphology of the antibody films was studied by atomic force microscopy (AFM), the confirmation of the antibody deposited material performed by X-ray photoemission spectroscopy (XPS) while surface wettability was studied by contact angle measurements.

The AFM images in Figure 31 show the surface morphology for representative pneumatic spray and avidin-biotin films at 1 and 50 μm^2 scan sizes. The pneumatic spray film was deposited for 7 minutes (image a) whose appearance is similar to the avidin-biotin film (image c) when the scanned surface was 1 μm^2. Images of same samples but at different scan size (50 μm^2) can be seeing in (b) pneumatic spray and (d) avidin-biotin which showed particle formations. The images suggested that the avidin-biotin bridge slides have a similar roughness Rq (root mean square average) like the pneumatic spray films when the scan was 1 μm^2 size. The wet chemistry films show residues with an average diameter of 3 to 5µm; therefore, the small area scanned was performed in area where those formations were not present. To reveal the morphology of the flat areas, a large area scans were performed over 50μm^2. Areas of the films of the avidin-biotin bridge showed a higher roughness (Figure 31b) in comparison to the pneumatic spray film.

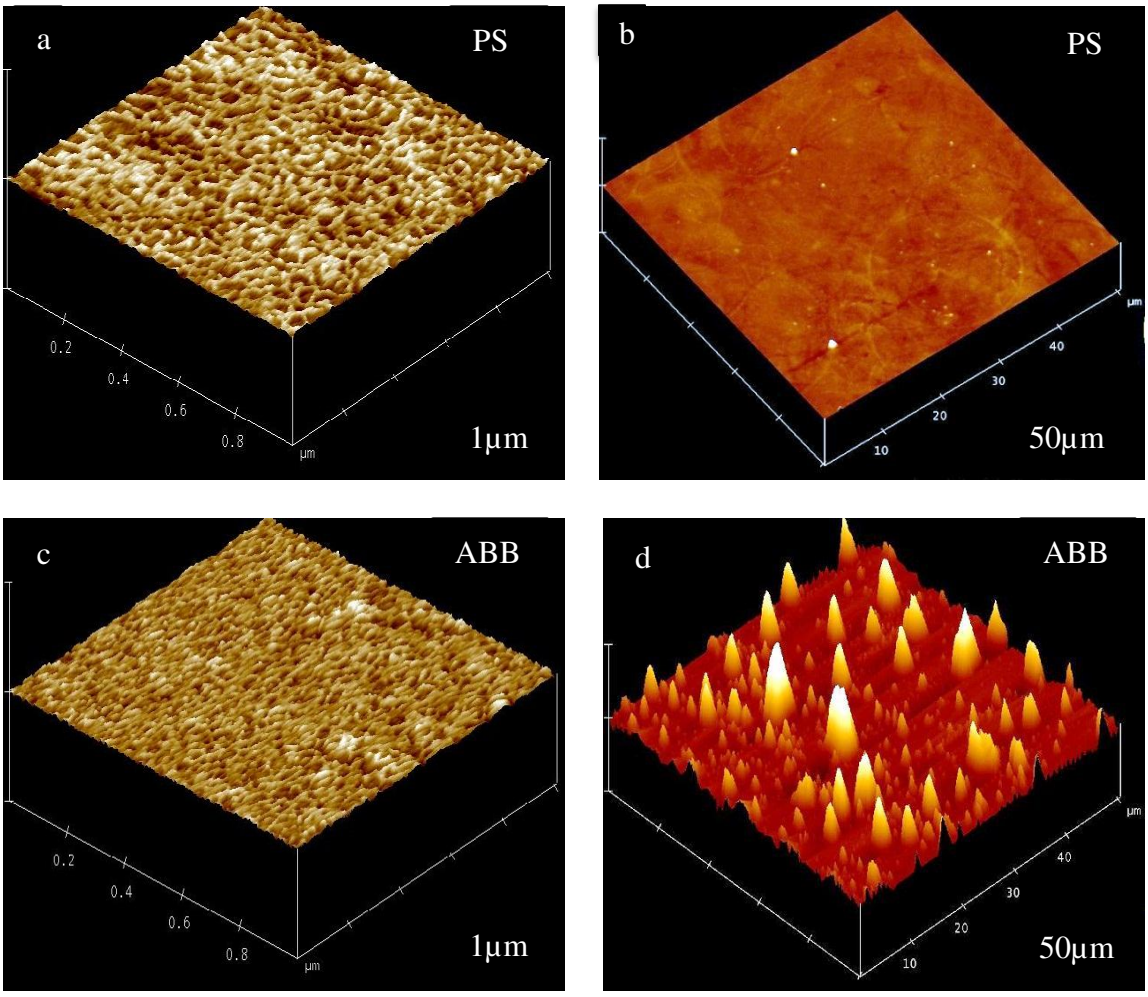

Figure 31. AFM images of pneumatic spray film and avidin-biotin bridge film. (a, b) Pneumatic spray film at 7 minutes deposition time, (a)1 µm scan size, Rq= 1.379±0.2 nm and (b) 50 µm scan size, Rq= 3.318±0.6 nm (c, d) ABB film, (c) 1 µm scan size, Rq= 2.657±0.4 nm and (d) 50 µm scan size, Rq= roughness root mean square average.

The optical images of representative pneumatic spray films and avidin-biotin bridge films. These features clearly show that aggregates form in the avidin-biotin bridge films appeared after the addition of the avidin to the intermediate layer. However, no aggregates formation was observed on the corresponded pneumatic spray samples (

Figure 32). The corresponding AFM data confirms these observations (see figure 31 d)

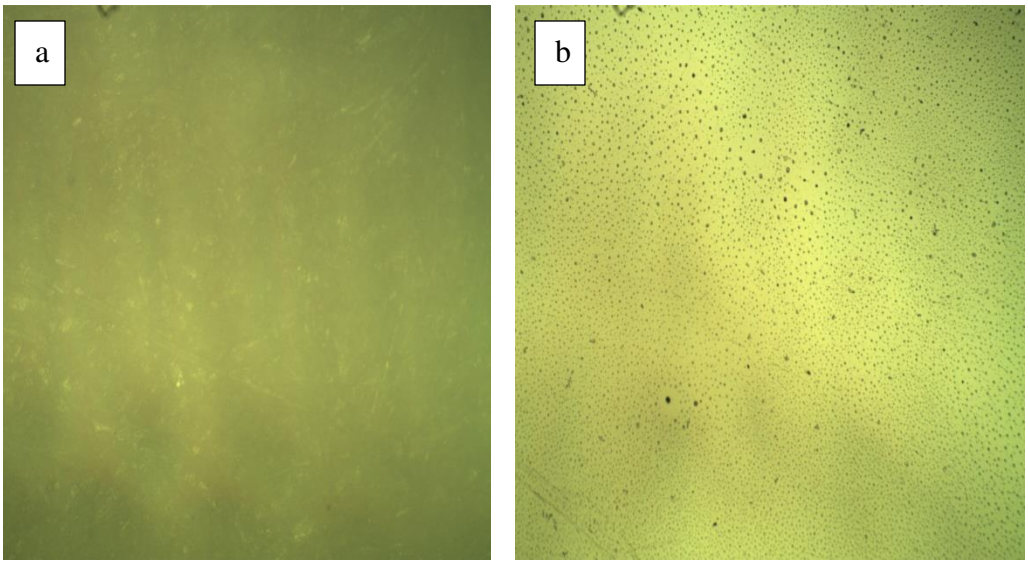

Figure 32. Optical image of deposited goat-anti E. coli O157:H7 on glass slide using two deposition techniques. (a) Pneumatic spray deposition technique, smooth film with not visible patterns at the surface. (b) ABB deposition technique, particle formation at the surface.

The avidin-biotin deposition process was divided in 5 stages with the goal to identify at what step of the avidin-biotin bridge process the aggregates starting to form. Each of the stages represented a set of steps that are associated with a main reaction step. The first stage is the cleaning of the surface with (KOH), the second stage is the silanization of the surface, the third stage is the cross-linking of the surface, the fourth stage is the addition of the protein (avidin), and the final stage is the addition of the antibody to the surface. The results of the contact angle analysis (Figure 333) of samples after each of the stages show that the surface transitioned from hydrophilic for the cleaned surface (11.35º ± 3.62) to hydrophobic after the silanization and cross-linker stages (70.88º±5.81 and 67.38º±2.98). When the avidin was added the hydrophobicity

was reduced again to 45.81°±4.46 and finally hydrophilicity (10.53°±1.13) returned after the final step of adding the antibodies.

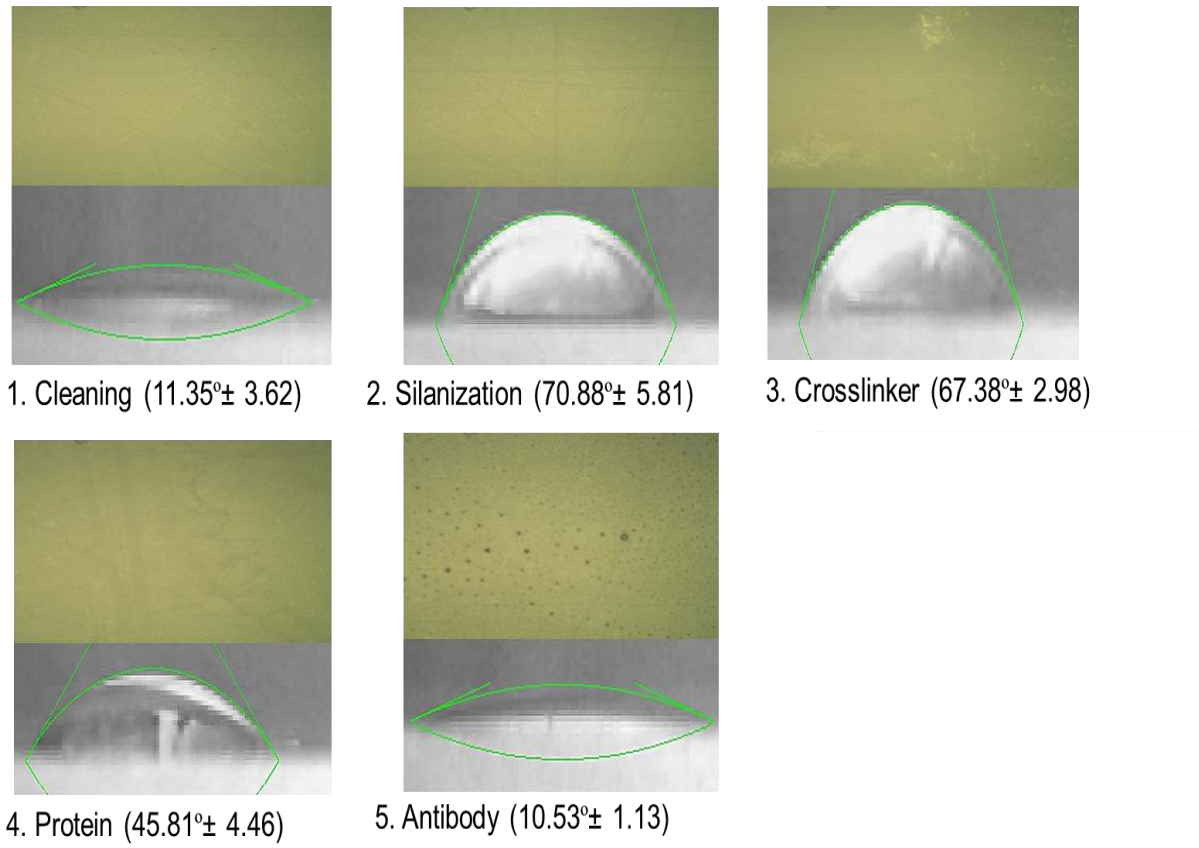

Figure 33. Optical images and contact angle analysis of each stage of the avidin-biotin bridge process.

The analysis of the surface composition using X-ray photoemission spectroscopy (XPS) confirmed and quantified the presence of antibody on the surface for both deposition techniques. In these experiments key element emissions are used as indicators for antibody immobilization. The broad C1s spectrum (Figure 34) is composed of three main peaks that are related to functional molecular groups. The three components can be identified as C-C bond related (first peak at lower binding energy), C-N bond related

(center peak) and R-C=O bond related (peak at the highest binding energy)[99, 100, 103-106].

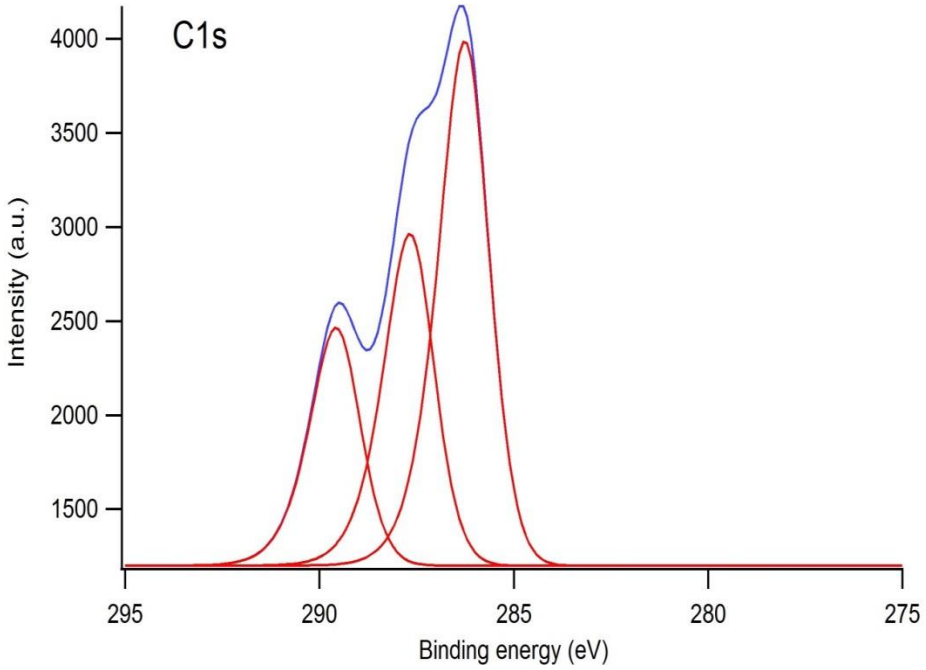

Figure 34. Deconvolution of XPS spectra C1s of pneumatic spray deposition of goat-anti E. coli O157:H7 antibody.

The peak related to the C-N as well as the N1s showed an increase in intensity from the one minute deposition (PS) to the 7 minute and then remained constant for the 10 and 14 minute deposition. The neutravidin-antibody (ABB film) showed an intensity increase of 43% relative to a film only coated with Neutravidin, which confirm the presence of antibody (Figure 35). The N1s emissions can be fitted to one component at 400 eV, which is typical for the amide nitrogen atom in the HN-C=O bonding configuration in the peptide bonds[107]. The offsets to higher binding energy observed on all XPS spectra for the PS films were due to charge building-up in the poorly conductive films.

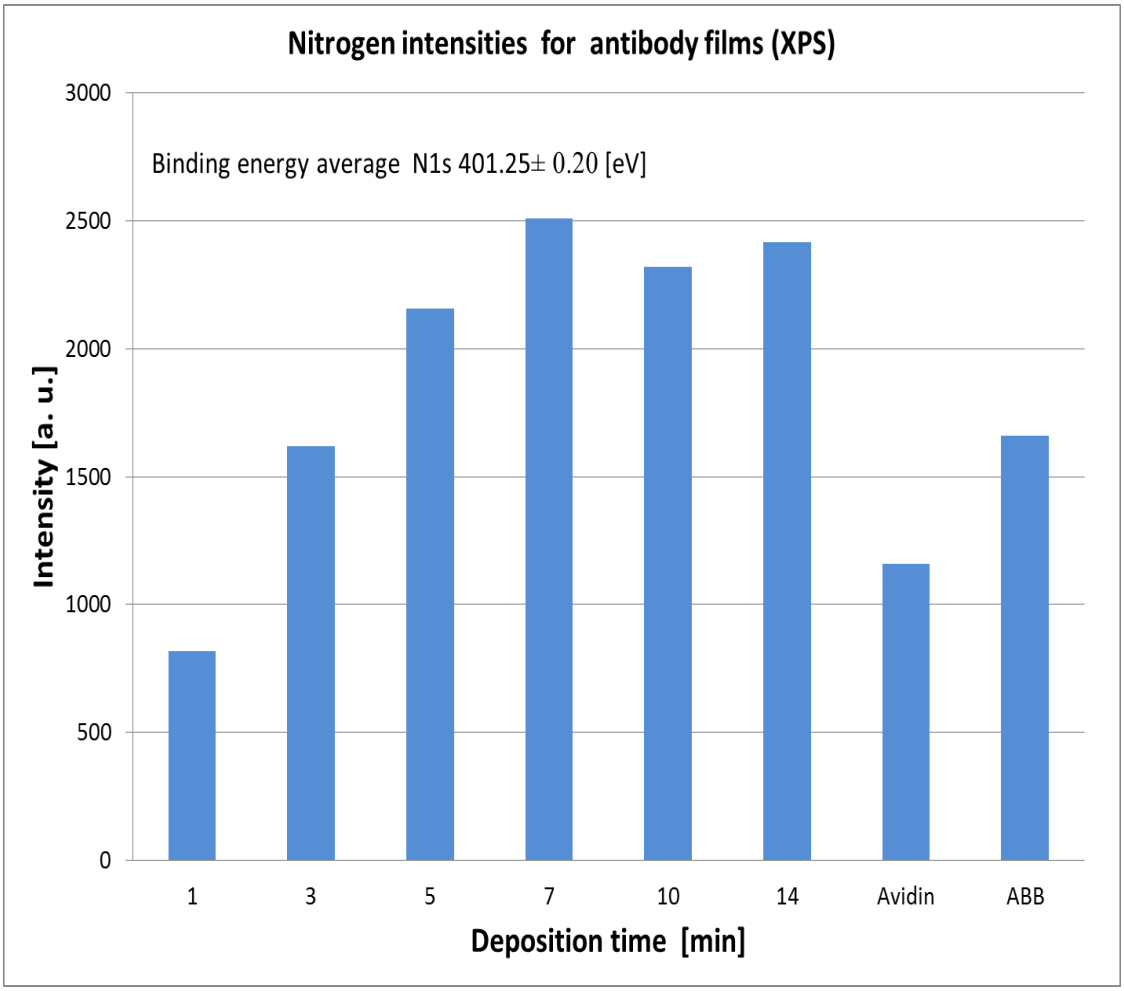

Figure 35. XPS analysis of N1s of pneumatic spray deposition of goat-anti E. coli O157:H7 antibody at different deposition times. Avidin (no antibody attached), avidin-biotin bridge film (ABB).

Figure 36 shows a graph relating contact angle to film thickness. It is obvious that the contact angle remained constant after one minute of deposition. The contact angle measurement reached at 1 minute was 60 ± 1.1. In comparison the contact angle measured on avidin-biotin bridge film was 12 ± 2.7.

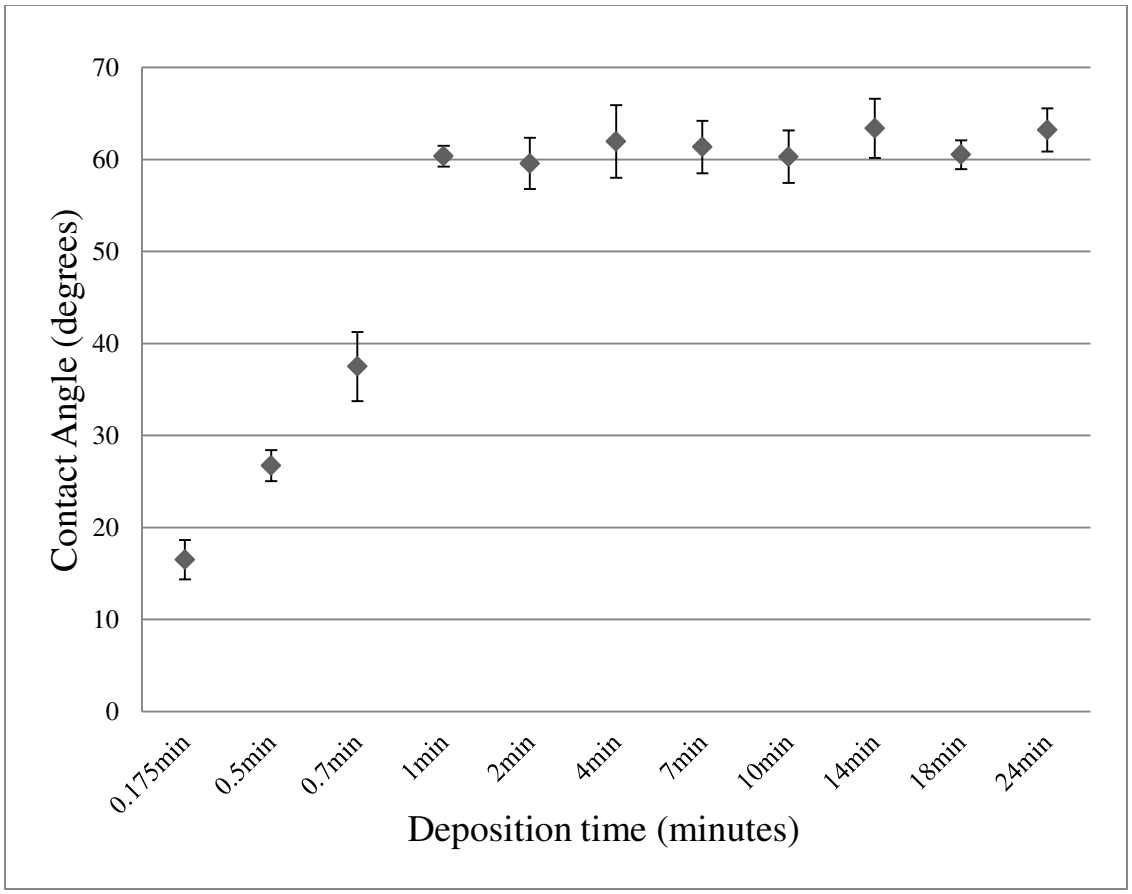

Figure 36. Contact angle measurements of pneumatic spray of goat-E.coli O157:H7 antibody films on glass slides using different deposition times. Error bars on the graphics represent the standard deviations of replicates.

4.2.3 Capture cell performance and fluorescent microscopy

Fluorescent microscopy was used to characterize the lateral distribution and localization of the analyte immobilization. In these experiments a set of pneumatic spray and avidin-biotin bridge samples was incubated with a solution of *E. coli* O157:H7 then the captured cell counted for each deposited film. Table 1 shows the concentration per area of the captured cells. The data suggested that the deposition time has no statistically significant influence on the capture density ($P > 0.05$; Dunn's multiple comparisons test),

Table 1. Assays on sprayed slides to determine the relationship of deposition time and capture cell counts. Captured E. coli O157:H7 cell counts on glass slides pneumatically sprayed with goat anti- E.coli O157:H7 IgG at different deposition times.

Deposition Time (minutes)	*Total cell captured average*	*Concentration (cells/mm^2)*
0.25	482	565.06 ± 12.62
0.50	326	382.18 ± 12.64
0.75	704	825.32 ± 13.22
1	461	540.44 ± 8.87
2	693	812.42 ± 15.79
4	532	623.68 ± 12.91
7	538	630.71 ± 17.78
10	606	710.43 ± 16.74
14	556	651.81 ± 9.79

The counts were performed in 3 slides per deposition time and in 3 different areas per slide (9 data per deposition time).

Figure 37 shows fluorescent microscopy images of representative pneumatic spray and avidin-biotin bridge samples. Image A show the deposition pattern of pneumatic spray droplets after reaching the surface and evaporating. The circular pattern left by each droplet impacting the surface indicates that the antibody is located mainly at the edge of the droplets. The same image also revealed cluster formation throughout the imaged surface as shown in Figure 37. The aggregates grew to up to 10 µm diameter over the different deposition times. The bacteria (green color) *E. coli* O157:H7 was immobilized on anti *E. coli* O157:H7 antibody (red color) with no clear pattern towards any specific area of the slide.

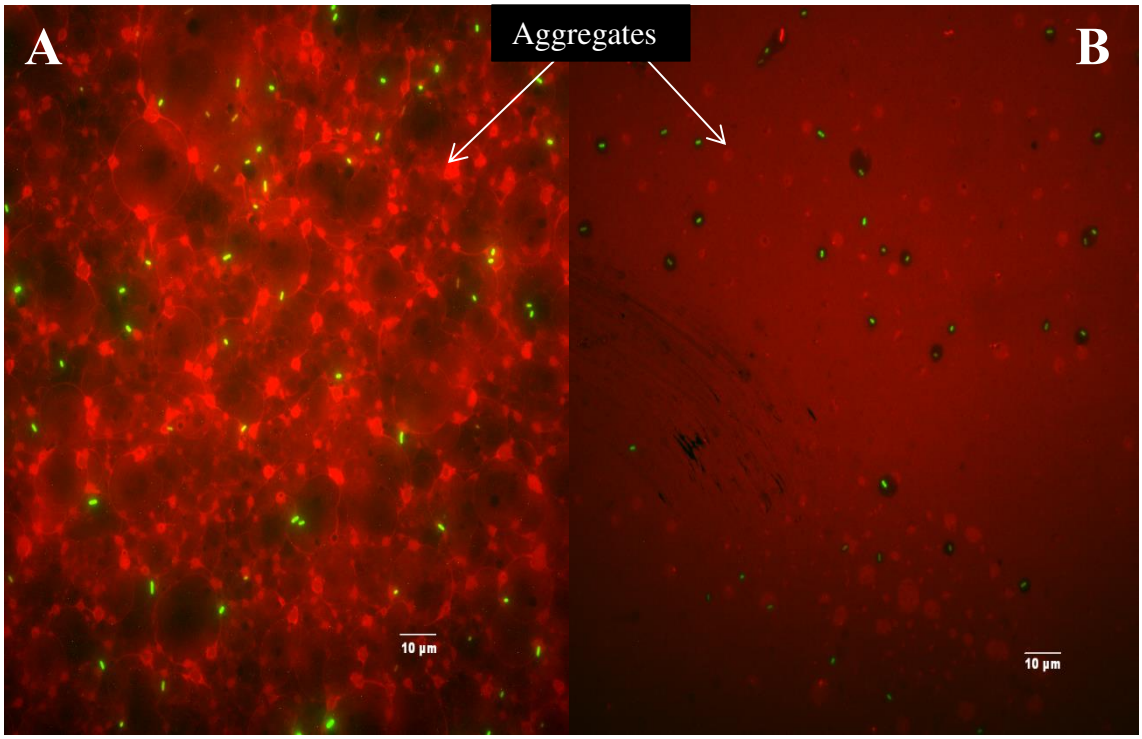

Figure 37. Fluorescence microscopy. (A) Image of pneumatic sprayed film (B) Avidin biotin bridge film. Images of immobilized GFP transformed *E. coli* O157:H7 (green particles) immobilized on a goat anti E. coli O157:H with Rhodamine red donkey anti-goat IgG.

4.3. Discussion

In the described experiments the surface morphology of representative pneumatic spray and avidin-biotin bridge samples were analyzed to gain understanding of the chemical and physical properties. The influence of the deposition technique used to immobilize antibodies on glass not only affects the stability of the film, but also the morphological properties of the surface like roughness, cluster formation and wettability. Furthermore, each step of the deposition technique influences the final surface structure and the overall capture cell performance.

4.3.1 Surface morphology, physical characteristics and capture activity

Physical adsorption of the antibodies was achieved via pneumatic spray which is a non-equilibrium deposition technique. The evaporation of the solvent from the droplet during the spray process increases with the distance from the tip of the nebulizer. Hence, the solute (i.e. antibody) concentration increases within the drop, which can potentially lead the antibody to form clusters prior to reaching the surface. However, the droplets are not completely free of solvent before reaching the surface, which allows the antibody to retain some mobility upon initial contact with the substrate. The fluorescence microscopy images confirm that the antibodies are still mobile by showing accumulation of IgG on ring-like formations throughout the films[108, 109] suggesting the evaporation of droplets after hitting the surface. As the deposition time increases, incoming droplets deposit on the top of previously deposited incompletely evaporated droplets at the surface, creating a new arrangement of the antibodies via surface diffusion processes.

The formation of aggregates or clusters at the surface via spray deposition is an unavoidable result of antibody-antibody interaction. The high concentration of antibodies in the drop before it deposits on the surface and the mobility after contact with the surface are the main factors influencing the morphology. The aggregates can be seen in the representative pneumatic spray and avidin-biotin films (Figure 37), which are randomly distributed through the entire covered surface[110]. Schramm et al. suggested that antibodies form aggregates or clusters regardless of the immobilization method and that formation is mainly caused by the properties of the antibody and not by the surface properties[111]. Large aggregate formations are visible after the 2 minute deposition in

the pneumatic spray films and these aggregates increase in diameter due to the rearrangement of antibodies at the surface. In comparison, the fluorescent microscopy images of the avidin-biotin bridge slides also showed aggregate formation at the surface. Optical microscopy images do not show the presence of aggregates on the pneumatic spray slides, but were clearly seen for the avidin-biotin bridge, result that can be explain by the low resolution of the optical microscope (both deposition techniques form aggregates). Further investigation of the avidin-biotin films (Figure 33) showed that the big particle formation was due to avidin aggregation before the biotinylated antibody was added to the surface and increase in size after the antibody is attached. Temur et al. suggested that the avidin protein forms clusters when immobilized at a solid surface[97] supporting the results found in this research. The surface roughness obtained from AFM of both sprayed and covalently immobilized antibody films showed that the avidin-biotin bridge deposited surface is magnitudes rougher than the sprayed surfaces, potentially affecting the wettability (contact angle) and the cell capture performance. Roughness and contact angle have been reported to have an inverse correlation[112, 113]. Data showed an avidin-biotin bridge surface with a roughness more than 30 times greater than pneumatic spray surface. Hence, the avidin-biotin bridge film showed a more hydrophilic surface and therefore a lower contact angle.

The results obtained from the assay of different deposition times against capture activity of the pneumatic spray films suggested that the cell capture ability of the films does not change noticeably with deposition time. In addition, the data showed that after 2 minutes deposition time the amount of antibody necessary to capture bacteria reach a

maximum, and no further cell capture improvements can be achieved with longer deposition times. Those results indicate that only the outer surface antibody layer participates in the capture process and that the antibodies in the inner layers can be regarded insignificant for capture purposes.

Fluorescent microscopy images were analyzed to determine the influence of the aggregates on the capture activity. Another focus was to see whether any patterns or trends in the immobilization of the bacteria would be influenced by the type of deposition method used. Pneumatically sprayed and avidin-biotin bridge slides (Figure 37) showed that the bacteria were immobilized randomly across the surface suggesting that the aggregates do not have a major influence in the cell capture ability of the films. This also suggests that despite the rough appearance, the entire surface is evenly coated with a homogeneous antibody surface. The low immobilization of bacteria on the aggregates can be attributed to steric hindrance produced by the crowding of antibodies, which can block some binding sites of the antibody, thereby decreasing the chances to interact with the antigen[114, 115].

The wettability of the surface (hydrophobic/hydrophilic interactions) depends on factors such as heterogeneity, density and composition of the surface[81]. The contact angle method was used to analyze the wettability of the surfaces of both immobilization methods. A set of antibody films at different deposition times was used to determine the influence of the amount of antibody at the surface on the wettability of the film. The contact angle of an avidin-biotin bridge slide and a glass slide were used as references for

comparison with the pneumatic spray samples. The data show that the contact angle of the pneumatic spray slides increased with deposition time. This indicates that the amount of the antibody changes the surface tension of the film. After one minute of deposition, the film reached the highest contact angle value making the film more hydrophobic than the avidin-biotin bridge film. Date show that when the pneumatic spray films reach a critical surface coverage point (in this case 1 minute) the contact angle reaches a plateau from 59.58 ± 2.79 to 63.39± 3.21 and no further increase in hydrophobicity was achieved by increasing the deposition time. On the other hand, the avidin-biotin bridge reference slide showed a contact angle similar to clean glass despite the fact that the sample was antibody covered.

These observations may be related to the orientation of the antibody at the surface and their surface density. Antibodies have two main regions (fragments) where one is more hydrophobic than the other (the Fc region is more hydrophobic than the Fab region[116]). Depending on the orientation of the molecule the fragment either can be preferentially exposed. The combination of randomly oriented antibodies at the surface of the sprayed films (which increased the amount of exposed Fc regions) and the higher surface density (which reduced the liquid penetration) resulted in hydrophobicity increase of the films[117].

4.3.2 Chemical and mechanical properties

The chemical and mechanical stability of the sprayed films are important factors to be analyzed to further understand the similar capture cell characteristics when

compared with the avidin-biotin bridge method. Chemical stability refers to the ability of the antibody to retain its chemical structure (protein secondary structure) unaltered. For the antibody to keep its biological activity and selectivity its secondary structure must be preserved during the immobilization process. The sprayed films were analyzed by ATR-FTIR (amide I region) which can detect any conformational changes via band shift [19, 20, 118, 119]. The results show that over the entire range of deposition times the amide I region vibration did not change significantly. This shows that the pneumatic spray procedure does not lead to denaturation of the physisorbed antibodies.

The mechanical stability summarizes the capacity of the film to keep its physical structure during rinsing and other mechanical stresses. The mechanical stability of the film was studied by determining the amount of antibody lost during rinsing process with UV-Vis spectrometry and ellipsometry. No protein was identified in the rinsing solution using the UV-Vis spectrometer and a low loss of antibody was detected by ellipsometry measurements (approximately 5% of the amount deposited on the surface). These results suggest that the films created by the spray have significant mechanical stability. Baszkin et al. mentioned in his study that after rinsing adsorbed IgG on polyethylene with buffer solution, the film showed minimal loss from the substrate due to attractive interaction with the surface[120], which is in accordance with the results obtained in our study. Another factor that plays an important role in the mechanical stability of the films is the amount of material immobilized. The surface densities calculated for the sprayed films were almost double of the value for the avidin-biotin bridge[2]. Consequently, the high surface density calculated for the sprayed antibody film and the cluster or aggregate

formation at the surface (which are more difficult to be removed from the surface as they increase in size[121]) can also be factors that influence the mechanical stability of the pneumatic spray films.

4.3.3 Film thickness and growth

The thickness of the pneumatically sprayed films was studied to understand the thin film growth mechanism in comparison with avidin-biotin bridge based films. The smallest thickness measured in the experiment was obtained at the 2 minute deposition time (55.62 ± 4.3 Å). In comparison the dimensions of an IgG molecule is approximately 85 Å x 145 Å x 40 Å[122-124]. This suggests that the deposited films consist of a mixture of antibodies in flat-on (the largest surface lying flat on the substrate) and tilted orientation (with any of the three antibody fragments tilted opposite to the surface) as was suggested by Xu et al. for antibodies adsorbed on silicon[125]. The thickness of the avidin-biotin bridge film which has oriented antibodies[14] was calculated to be 183.16 ± 8.5 Å. This value includes the cross-linkers layer plus the antibody. In comparison the pneumatic spray film thickness is purely related to the deposition of antibodies. The thickness of the films increases proportionally with the deposition time, suggesting that the pneumatic spray builds a multilayer film that grows uniformly with time. As a result the pneumatic spray can create a denser antibody film. This most likely compensates for the lack of antibody orientation via a large number of antibodies available at the surface resulting in comparable capture ability to the avidin-biotin bridge films. Vijayendran et al. tested 5 different immobilization techniques and found that randomly oriented antibodies have a surface density that is greater than achieved by techniques that produce

oriented attachment while showing comparable specific activity[126], which is in agreement with the results presented in this document.

The X-ray photoemission spectroscopy (XPS) method was used to confirm the presence of immobilized antibodies at the surface, and to elucidate the film growth mode for the pneumatic spray slides. The detection of the N1s peak in the pneumatic spray films and (increment of N1s peak) for the avidin-biotin bridge verify and quantify the presence of antibodies in both immobilization techniques. On the avidin-biotin based slides the N1s emission were present before the immobilization of the antibody due to the nitrogen content in the cross linker and the avidin protein. For the pneumatic spray films, the direct correlation in surface coverage with the deposition time was confirmed by the attenuation of the Si 2p emission from the substrate relative to the increase of the antibody-related N1s emission. The N1s peak intensity became constant after 7 minutes deposition time. That suggest that at this point thickness of the film after 7 minutes deposition time is larger than the scape depth of 70-150 Å [127] of the photoelectrons. Based on the XPS data can be reasoned that the pneumatic spray films grow as flat layers. This conclusion is supported by the ellipsometry and ATR-FTIR data, which measured similar film grow thickness.

4.4 Conclusions

The results of the surface characterization of the spray deposited antibody films suggests that the high capture activity of the films is related to the higher surface density of the antibodies that can be achieved in comparison with conventional avidin-biotin antibody films. This likely compensates for the random orientation of the antibodies in the sprayed samples. The mechanical stability of the films is also on par with the avidin-biotin prepared films. The films are able to withstand mechanical stresses with minimal loss of material. The pneumatic spray deposition technique is a non-equilibrium process, which allows loading the surface with as much antibody as desired. The higher hydrophobicity characteristic of the pneumatic spray film can be explained by their randomly oriented antibody, high surface density (thus low liquid penetration) and the low surface roughness. The hydrophobicity of the spray film is possibly aiding factor in the capture cell performance of the pneumatic sprayed films due to the trend of bacteria to attach to the more hydrophobic surfaces.

The antibody surface thickness has no mayor effect in the capture cell ability for the pneumatic spray films since only the outer layer is involved in the capturing process. In summary, the presented results show that pneumatic spray films have chemical and mechanical functional properties comparable to avidin-biotin based films, which make the technique a good alternative for immobilizing antibodies on solid surfaces.

REFERENCES

[1] Moulin AM, O'Shea SJ, Badley RA, Doyle P, Welland ME. Measuring Surface-Induced Conformational Changes in Proteins. Langmuir 1999;15:8776-9.

[2] Batall P, Fuentes M, Grazu V, Mateo C, Fernandez-Lafuente R, Guisan. JM. Oriented Covalent Immobilization of Antibodies on Physically Inert and Hydrophilic Support Surfaces through Their Glycosidic Chains. Biomacromolecules. 2008;9:719-23.

[3] Anderson GP, Jacoby MA, Ligler FS, King KD. Effectiveness of protein A for antibody immobilization for a fiber optic biosensor. Biosens Bioelectron. 1997;12:329-36.

[4] Mozaz SR, Alda MJLd, Marco MP, Barcelo´ D. Biosensors for environmental monitoring: A global perspective. Talanta. 2005;65:291-7.

[5] Mozaz SR, Marco MP, Alda MJLd, Barceló D. Biosensors for environmental applications: Future development trends. Pure Appl Chem. 2004;76:723–52.

[6] Alocilja EC, Radke SM. Market analysis of biosensors for food safety. Biosens Bioelectron. 2003;18:841-6.

[7] Lim DV, Simpson JM, Kearns EA, Kramer. MF. Current and Developing Technologies for Monitoring Agents of Bioterrorism and Biowarfare. Clin Microbiol Rev. 2005;18:583-607.

[8] Hutchinson AM. Evanescent wave biosensors. Mol Biotechnol. 1995;3:47-54.

[9] Taitt CR, Anderson GP, Ligler FS. Evanescent wave fluorescence biosensors. Biosens Bioelectron. 2005;20:2470-87.

[10] Shriver-Lake LC, PT C, Taitt CR. Immobilization of biomolecules onto silica and silica-based surfaces for use in planar array biosensors. Methods Mol Biol. 2009;504:419-40.

[11] Shriver-Lake LC, Donner B, Edelstein R, Kristen Breslin, Bhatia SK, Ligler FS. Antibody immobilization using heterobifunctional crosslinkers. Biosens Bioelectron. 1997;12:1101-6.

[12] Golden J, Shriver-Lake L, Sapsford K, Ligler F. A "do-it-yourself " array biosensor. Methods 2005;37:65-72.

[13] Taitt CR, Shriver-Lake LC, Ngundi MM, Ligler FS. Array Biosensor for Toxin Detection: Continued Advances. Sensors 2008;8:8361-77.

[14] Bhatia SK, Shriver-Lake LC, Prior KJ, Georger JH, Calvert JM, Bredehorst R, et al. Use of Thiol-Terminal Silanes and Heterobifunctional Crosslinkers for Immobilization of Antibodies on Silica. Anal Biochem. 1989;178:408-13.

[15] Narang U, Anderson GP, Ligler FS, Burans J. Fiber optic-based biosensor for ricin. Biosens Bioelectron. 1997;12:937–45.

[16] Ikeda T, Hata Y, Ninomiya K-i, Ikura Y, Takeguchi K, Aoyagi S, et al. Oriented immobilization of antibodies on a silicon wafer using Si-tagged protein A. Anal Biochem 2009;385:132-7.

[17] Lin J-N, Herron J, D.Andrade J, Marius B. Characterization of Immobilized Antibodies on Silica Surfaces. IEEE T Bio-med Eng. 1988;35:466-71.

[18] Ahluwalia A, Rossi DD, Ristori C, Schirone A, Serra G. A comparative study of protein immobilization techniques for optical immunosensors. Biosens Bioelectron. 1992;7 207-14.

[19] Chittur KK. FTIR/ATR for protein adsorption to biomaterial surfaces. Biomaterials. 1988;19:357-69.

[20] Plowman TE, Durstchi JD, Wang HK, Christensen DA, Herron JN, Reichert WM. Multiple-Analyte Fluoroimmunoassay Using an Integrated Optical Waveguide Sensor. Anal Chem 1999;71:4344-52.

[21] Anderson GP, Lingerfelt BM, Rowe-Taitt C. Eight Analyte Detection Using a Four-Channel Optical Biosensor. Sensor Letters 2004;2:18-24.

[22] Bernard A, Michel B, Delamarche E. Micromosaic Immunoassays. Anal Chem. 2001;73:8-12.

[23] Goldman ER, Pazirandeh MP, Mauro JM, King KD, Frey JC, Anderson GP. Phage-displayed peptides as biosensor reagents. J Mol Recognit. 2000;13:382-7.

[24] Ulbrich R, Golbik R, Schellenberger A. Protein adsorption and leakage in carrier-enzyme systems. Biotechnol Bioeng 1991;37:280-7.

[25] Sportsman RJ, Wilson GS. Chromatographic Properties of Silica-Immobilized Antibodies. Anal Chem. 1980;52:2013-8.

[26] Spaeth K, Brecht A, Gauglitz G. Studies on the Biotin–Avidin Multilayer Adsorption by Spectroscopic Ellipsometry. J Colloid Interface Sci

1997;196:128-35.

[27] Martin K, Ekeroth J, Elwing H, Carlsson U. Reduction of Irreversible Protein Adsorption on Solid Surfaces by Protein Engineering for Increased Stability. J Biol Chem. 2005;280 25558–64.

[28] Hlady V, Buijs J. Protein adsorption on solid surfaces. Curr Opin Biotech. 1996;7:72-7.

[29] Miller R, Aksenenko EV, Fainerman VB, Pison U. Kinetics of adsorption of globular proteins at liquid/fluid interfaces. Colloid Surface A 2001;183-185:381-90.

[30] Almagro B, Ganan-Calvo M, Hidalgo M, Canals A. Behaviour of a flow focusing pneumatic nebulizer with high total dissolved solids solution on radially and axially viewed inductively coupled plasma atomic emission spectrometry. J Anal At Spectrom. 2006;21:1072-5.

[31] Jakubowski N, Feldmann I, Stuewer D. Analytical improvement of pneumatic nebulization in ICP-MS by desolvation. Spectrochim Acta B. 1992;47:107-18.

[32] Geertsen V, Lemaitre P, Tabarant M, Chartier F. Influence of design and operating parameters of pneumatic concentric nebulizer on micro-flow aerosol characteristics and ICP-MS analytical performances. J Anal At Spectrom 2012;27:146-58.

[33] Kniseley RN, Amenson H, Butler CC, Fassel VA. An Improved Pneumatic Nebulizer for Use at Low Nebulizing Gas Flows. Appl Spectrosc. 1974;28:285-6.

[34] Todolí JL, Mermet JM. Sample introduction systems for the analysis of liquid microsamples by ICP-AES and ICP-MS. Spectrochim Acta B. 2006;61:239-83.

[35] Sharp BL. Pneumatic Nebulisers and Spray Chambers for Inductively Coupled Plasma Spectrometry. J Anal At Spectrom. 1988;3:939-63.

[36] Thomas R. A Beginner's Guide to ICP-MS. Spectroscopy. 2001;16:56-60.

[37] Otto K, Katerski A, Mere A, Volobujeva O, Krunks M. Spray pyrolysis deposition of indium sulphide thin films. Thin Solid Films 2011;519:3055-60.

[38] Otto K, Katerskia A, Volobujeva O, Merea A, Krunks M. Indium sulfide thin films deposited by chemical spray of aqueous and alcoholic solutions. Energy Procedia. 2011;3:63-9.

[39] Shindov PC. CdO Thin Films Deposited By Spray Pyrolysis. Electronics. 2004:1-4.

[40] Girtan M, Cachet H, Rusu GI. On the physical properties of indium oxide thin films deposited by pyrosol in comparison with films deposited by pneumatic spray pyrolysis. Thin Solid Films 2003;427:406-10.

[41] Mooney JB, B.Radding S. Spray Pyrolysis Processing. Ann Rev Mater Sci 1982;12:81-101.

[42] Lauten EH, Pulliam BL, DeRousse J, Bhatta D, Edwards DA. Gene Expression, Bacteria Viability and Survivability Following Spray Drying of Mycobacterium smegmatis. Materials. 2010;3:2684-724.

[43] Silva J, Carvalho AS, Teixeira P, Gibbs PA. Bacteriocin production by spray-dried lactic acid bacteria. Lett Appl Microbiol. 2002;34:77-81.

[44] Yao J, Scott JR, Young MK, Wilkins CL. Importance of Matrix:Analyte Ratio for Buffer Tolerance Using 2,5-Dihydroxybenzoic Acid as a Matrix in Matrix-Assisted Laser Desorption/ Ionization-Fourier Transform Mass

Spectrometry and Matrix-Assisted Laser Desorption/Ionization-Time of Flight. J Am Soc Mass Spectrom. 1998;9:805-13.

[45] Hess DH. Nebulizers: Principles and Performance. Respir Care. 2000;45:609-22.

[46] Rao SV, Anderson KW, Bachas LG. Oriented Immobilization of Proteins. Mikrochim Acta. 1998;128:127-43.

[47] Turkova J. Oriented immobilization of biologically active proteins as a tool for revealing protein interactions and function. J Chromatogr B. 1999;722:11-31.

[48] Wang W, Singh S, Zeng DL, King K, Nema S. Antibody Structure, Instability, and Formulation. J Pharm Sci. 2007;96:1-26.

[49] Davies DR, Metzger H. Structural Basis of Antibody Function. Annu Rev Immunol. 1983;1:87-117.

[50] Male DK, Brostoff J, Roth D, Roitt I. Immunology. 7 ed. Canada: Elsevier Science Health Science Division; 2006. p. 564.

[51] Hennes KP, Suttle CA. Direct Counts of Viruses in Natural Waters and Laboratory Cultures by Epifluorescence Microscopy. Limnol Oceanogr. 1995;40:1050-5.

[52] Lunau M, Lemke A, Walther K, Martens-Habbena W, Simon M. An improved method for counting bacteria from sediments and turbid environments by epifluorescence microscopy. Environ Microbiol. 2005;7:961-8.

[53] Squirrell DJ, Price RL, Murphy MJ. Rapid and specific detection of bacteria using bioluminescence. Anal Chim Acta. 2002;457:109-14.

[54] Gehring AG, Albin DM, Bhunia AK, Reed SA, Tu S-I, Uknalis J. Antibody Microarray Detection of Escherichia coli O157:H7: Quantification, Assay Limitations, and Capture Efficiency. Anal Chem. 2006;78:6601-7.

[55] Tu S-i, Uknalis J, Yamashoji S, Gehring A, Irwin P. Luminescent methods to detect viable and total Escherichia Coli O157:H7 in ground beef. P J Rapid Methods Autom Microbiol. 2005;13:57-70.

[56] DeMarco DR, Lim DV. Direct detection of Escherichia coli O157:H7 in unpasterized apple juice with an evanescent wave biosensor. J Rapid Methods Autom Microbiol. 2001;9:241-57.

[57] Graber DJ, Zieziulewicz TJ, Lawrence DA, Shain W, Turner JN. Antigen Binding Specificity of Antibodies Patterned by Microcontact Printing. Langmuir 2003 19:5431-4.

[58] Merritt JH, Kadouri DE, O'Toole GA. Growing and Analyzing Static Biofilms. Cur Prot Microbiol. 2011;22:1-18.

[59] Kulagina NV, Shaffer KM, Anderson GP, Ligler FS, Taitt CR. Antimicrobial peptide-based array for Escherichia coli and Salmonella screening. Anal Chim Acta 2006;575:9-15.

[60] Kulagina NV, Shaffer KM, Anderson GP, Ligler FS, Taitt CR. Antimicrobial Peptides for Detection of Bacteria in Biosensor Assays. Anal Chem 2005;77:6504-8.

[61] Simpson-Stroot JM, Kearns EA, Stroot PG, Magaña S, Lim. DV. Monitoring biosensor capture efficiencies: Development of a model using GFP-expressing Escherichia coli O157:H7. J Microbiol Methods. 2008;72:29-37.

[62] Wang H, Sharpe A. An immuno-capturing and concentrating procedure for Escherichia coli O157:H7 and its detection by epifluorescence microscopy. Food Microbiol. 1998;14:559-65.

[63] DeMarco DR, Saaski EW, McCrae DA, V.Lim D. Rapid detection of Escherichia coli O157:H7 in ground beef using a fiber-optic biosensor. J Food Prot. 1999;62:711-7116.

[64] Demarco DR, Lim DV. Direct detection of Escherichia Coli 0157:H7 in unpsteurized apple juice with an evanescent wave biosensor. J Rapid Methods Autom Microbiol. 2001;9: 241–57.

[65] Green JH, JR. SBG, Harrell WK. Stability of Fluorescent Antibody Conjugates Stored Under Various Conditions. J Clin Microbiol. 1976:1-4.

[66] Daims H, Lucker S, Wagner M. Daime, a novel image analysis program for microbial ecology and biofilm research. Environ Microbiol. 2006;8:200-13.

[67] Skoog DA, Holler FJ, Crouch SR. Signal and noise. In: Brooks T, editor. Prin Instru Anal. 6 ed. Canada: David Harris; 2007.

[68] Elwing H. Protein absorption and ellipsometry in biomaterial research. Biomaterials. 1998;19:397-406.

[69] Martin M. Ellipsometry studies of protein layer adsorbed at hydrophobic surfaces. J Colloid Interface Sci. 1994;166:333-42.

[70] Herberhold H, Marchal S, Langer R, Scheyhing C, Vogeir F, Winter R. Characterization of the pressure-induced intermediate and unfolded state of red-shifted green fluorescent protein: A static and kinetic FTIR, UV/VIS and fluorescence spectroscopy study. J Mol Biol 2003;330:1153-64.

[71] Mansur H, Oréfice R, Pereira M, Lobato Z, Vasconcelos W, Machado L. FTIR and UV-vis study of chemically engineered biomaterial surfaces for protein immobilization. Spectroscopy. 2002;16:351-60.

[72] Kazarian SG, Chan KLA. Applications of ATR-FTIR spectroscopic imaging to biomedical samples. BBA Biomembranes. 2006;1758:858-67.

[73] Green RJ, Hopkinson I, Jones RAL. Unfolding and Intermolecular Association in Globular Proteins Adsorbed at Interfaces. Langmuir. 1999;15:51025110.

[74] Schuck P. Protein Interactions: Biophysical Approaches for the Study of Complex Reversible Systems In: Atassi MZ, editor.: Springer-Verlag New York, LLC; 2007. p. 544.

[75] Ertl G, Kuppers J. Low energy electrons and surface chemistry. Germany: VCH Publishers; 1985.

[76] Graf N, gen EY, Lippitz A, Treu D, Wirth T, Unger WES. Optimization of cleaning and aminosilanization protocols for Si wafers to be used as platforms for biochipmicroarrays by surface analysis (XPS, ToF-SIMS and NEXAFS spectroscopy). Surf Interface Anal. 2008;40:180-3.

[77] Israelachvili JN. Intermolecular and surface forces with application to colloidal and Biological Systems. London: Harcourt Brace Jovanovich; 1985.

[78] Young T. An Essay on the Cohesion of Fluids. Phil Trans R Soc Lond. 1805;95:65-87.

[79] Li D, Neumann AW. Applied Surface Thermodynamics. Dekker, New York1996.

[80] Xu L-C, Siedlecki CA. Effects of surface wettability and contact time on protein adhesion to biomaterial surfaces. Biomaterials 2007;28:3273–83.

[81] de-Morais LC, Bernardes-Filho R, Assis OBG. Wettability and bacteria attachment evaluation of multilayer proteases films for biosensor application. World J Microbiol Biotechnol 2009;25:123-9.

[82] Rowe CA, Tender LM, Feldstein MJ, Golden JP, Scruggs SB, MacCraith BD, et al. Array Biosensor for Simultaneous Identification of Bacterial, Viral, and Protein Analytes. Anal Chem. 1999;71:3846-52.

[83] Abràmoff MD, Magalhães PJ, Ram SJ. Image Processing with ImageJ. P Soc Photo-Opt Ins2004. p. 36-42.

[84] Figueroa J, Magaña S, Lim DV, Schlaf R. Antibody immobilization using pneumatic spray: Comparison with the avidin–biotin bridge immobilization method. J Immunol Methods. 2012;386:1-9.

[85] O'Toole G, Kaplan HB, Kolter R. Biofilm Formation as Microbial Development. Annu Rev Microbiol. 2000;54:49-79.

[86] Richter A, Smith R, Ries R. Growth and morphology of biological thin films. Appl Surf Sci. 1999;144:419-24.

[87] Butler JE, Ni L, Nessler R, Joshi KS, Suter M, Rosenberg B, et al. The physical and functional behavior of capture antibodies adsorbed on polystyrene. J Immunol Methods. 1992;150:77-90.

[88] Arora P, Sindhu A, Dilbaghi N, Chaudhury A. Biosensors as innovative tools for the detection of food borne pathogens. Biosens Bioelectron 2011;28:1-12.

[89] Zhu P, Shelton DR, Jeffrey SK, Sundaram A, Li S, Amstutz P, et al. Detection of water-borne E. coli O157 using the integrating waveguide biosensor. Biosens Bioelectron. 2005;21:678-83.

[90] Peluso P, Wilson DS, Do D, Tran H, Venkatasubbaiah M, Quincy D, et al. Optimizing antibody immobilization strategies for the construction of protein microarrays. Anal Biochem. 2003;312:113-24.

[91] Perez-Luna VH, O'Brien MJ, Opperman KA, Hampton PD, Lopez GP, Klumb LA, et al. Molecular Recognition between Genetically Engineered Streptavidin and Surface-Bound Biotin. J Am Chem Soc. 1999;121:6469-78.

[92] Feijter JAD, Benjamins J, Veer. FA. Ellipsometry as a Tool to Study the Adsorption Behavior of Synthetic and Biopolymers at the Air-Water Interface. Biopolymers. 1978;17:1759-72.

[93] Iconaru SL, Ungureanu F, Costescu A, Costache M, Dinischiotu A, Predoi D. Characterization of Sucrose Thin Films for Biomedical Applications. J Nanomater. 2011:1-6.

[94] Giacomelli CE, Bremer MGEG, Norde W. ATR-FTIR Study of IgG Adsorbed on Different Silica Surfaces. J Colloid Interface Sci. 1999;220:13-23.

[95] Kolusheva S, Kafri R, Katz M, Jelinek R. Rapid Colorimetric Detection of Antibody-Epitope Recognition at a Biomimetic Membrane Interface. J Am Chem Soc 2001;123:417-22.

[96] Kalele SA, Ashtaputre SS, Hebalkar NY, Gosavi SW, Deobagkar DN, Deobagkar DD, et al. Optical detection of antibody using silica–silver core–shell particles. Chem Phys Lett 2005;404:136-41.

[97] Temur E, Boyacı İH, Tamer U, Unsal H, Aydogan N. A highly sensitive detection platform based on surface-enhanced Raman scattering for Escherichia coli enumeration. Anal Bioanal Chem. 2010;397:1595-604.

[98] Syguda A, Kerstan A, Ladnorg T, Stüben F, Wöll C, Herrmann C. Immobilization of Biotinylated hGBP1 in a Defined Orientation on Surfaces Is Crucial for Uniform Interaction with Analyte Proteins and Catalytic Activity. Langmuir 2012;28:6411−8.

[99] Hamadi F, Latrache H, Zahir H, Abed SE, Ellouali M, Saad IK. The Relation Between the Surface Chemical Composition of Escherichia coli and their Electron donor/Electron Acceptor (Acid-base) Properties. Res J Microbiol. 2012;7:32-40.

[100] Lu B, Xie J, Lu C, Wu C, Wei Y. Oriented Immobilization of Fab' Fragments on Silica Surfaces. Anal Chem 1995;67:83-7.

[101] Corso CD, Dickherber A, Hunt WD. An investigation of antibody immobilization methods employing organosilanes on planar ZnO surfaces for biosensor applications. Biosens Bioelectron. 2008;24:805-11.

[102] Lee D, Cui T. An electric detection of immunoglobulin G in the enzyme-linked immunosorbent assay using an indium oxide nanoparticle ion-sensitive field-effect transistor. J Micromech Microeng. 2012;22:1-9.

[103] Vermette P, Gengenbach T, Griesser HJ, Divisekera U, Kambouris PA, Meagher L. Immobilization and surface characterization of NeutrAvidin biotin-binding protein on different hydrogel interlayers. JColloid Interface Sci. 2003;259:13-26.

[104] Flink S, Veggel FCJMV, Reinhoudt DN. Functionalization of Self Assambled Monolayers on Glass and Oxidized Silicon Wafers by surface Reactions J Phys Org Chem 2001;14:407-15.

[105] Ouyang R, Lei J, Ju H, Xue Y. A Molecularly Imprinted Copolymer Designed for Enantioselective Recognition of Glutamic Acid. Adv Funct Mater 2007;17:3223-30.

[106] Lowe RD, Szili EJ, Kirkbride P, Thissen H, Siuzdak G, Voelcker NH. Combined Immunocapture and Laser Desorption/ Ionization Mass Spectrometry on Porous Silicon. Anal Chem. 2010;82:4201-8.

[107] Darain F, Gan KL, Tjin SC. Antibody immobilization on to polystyrene substrate on-chip immunoassay for horse IgG based on fluorescence. Biomed Microdevices. 2009;11:653-61.

[108] Hu H, Larson RG. Evaporation of a Sessile Droplet on a Substrate. J Phys Chem B 2002;106: 1334-44.

[109] Deegan RD, Bakajin O, Dupont TF, Huber G, Nagel SR, Witten TA. Contact line deposits in an evaporating drop. Physical Review E. 2000;62:756-65.

[110] Caruso F, Rodda E, Furlong DN. Orientational Aspects of Antibody Immobilization and Immunological Activity on Quartz Crystal Microbalance Electrodes. J Colloid Interface Sci. 1996;178:104-15.

[111] Schramm W, Paek S-H. Antibody-Antigen Complex Formation with Immobilized lmmunoglobulins. Anal Biochem. 1992;205:47-56.

[112] Ohwaki TT, Yasunori. Changes in hydrophobic properties of glass surfaces by ion implantation. Journal of Vacuum Science & Technology A. 1990;8:2173-6.

[113] North SH, Lock EH, King TR, Franek JB, Walton SG, Taitt CR. Effect of Physicochemical Anomalies of Soda-Lime Silicate Slides on Biomolecule Immobilization. Anal Chem. 2010;82:406-12.

[114] Poumbourios P, Brown LE, White DO, Jackson DC. The stoichiometry of binding between monoclonal antibody molecules and the hemagglutinin of influenza virus. Virology. 1990;179:768-76.

[115] Oreskes I, Mandel D. Reactivity of sized thermal aggregates of immunoglobulin G with IgM rheumatoid factor. Immunology. 1984;51:115-21.

[116] Tronin A, Dubrovsky T, Nicolini C. Comparative Study of Langmuir Monolayers of Immunoglobulines G Formed at the Air-Water Interface and Covalently Immobilized on Solid Supports. Langmuir. 1995;11:385-9.

[117] Dubrovsky T, Tsai J, Salamone SJ. Immobilization of Monolayers of Fc-binding Receptors on Planar Solid Supports. Clin Chem 1999;45:1675-6.

[118] Schwinte´ P, Voegel JC, Picart C, Haikel Y, Schaaf P, Szalontai B. Stabilizing Effects of Various Polyelectrolyte Multilayer Films on the Structure of Adsorbed/Embedded Fibrinogen Molecules: An ATR-FTIR Study. J Phys Chem B 2001;105:11906-16.

[119] Kong J, Yu S. Fourier Transform Infrared Spectroscopic Analysis of Protein Secondary Structures. Acta Biochim Biophys Sin. 2007;39:549–59.

[120] Baszkin A, Boissonnade MM, Kamyshny A, Magdassi S. Adsorption of Native and Hydrophobically Modified Human Immunoglobulin G on Polyethylene Solid Films: Specific Recognition of Adsorbed Layers. J Colloid Interface Sci. 2001;244:18-23.

[121] Davies J, Dawkes AC, Haymes AG, Sunderland RF, Edwards JC. Scanning tunnelling microscopy and dynamic contact angle studies of the effects of partial denaturation on immunoassay solid phase antibody. J Immunol Methods. 1995;186:111-23.

[122] LaGraff JR, Chu-LaGraff Q. Scanning Force Microscopy and Fluorescence Microscopy of Microcontact Printed Antibodies and Antibody Fragments. Langmuir. 2006;22:4685-93.

[123] Preininger C, Clausen-Schaumann H, Ahluwalia A, Rossi DD. Characterization of IgG Langmuir–Blodgett films immobilized on functionalized polymers. Talanta 2000;52:921–30.

[124] Klein JS, Gnanapragasam PNP, Galimidi RP, Foglesong CP, West AP, Bjorkmanb PJ. Examination of the contributions of size and avidity to the neutralization mechanisms of the anti-HIV antibodies b12 and 4E10. PNAS. 2009;106:7385–90.

[125] Xu H, Zhao X, Grant C, Jian RL. Orientation of a Monoclonal Antibody Adsorbed at the Solid/Solution Interface: A Combined Study Using Atomic Force Microscopy and Neutron Reflectivity. Langmuir 2006;22:6313-20.

[126] Vijayendran RA, Leckband DE. A Quantitative Assessment of Heterogeneity for Surface-Immobilized Proteins. Anal Chem 2001;73:471-80.

[127] Iucci G, Polzonetti G, Infante G, Rossi L. XPS and FT-IR spectroscopy study of albumin adsorption on the surface of a p-conjugated polymer film. Surf Interface Anal. 2004;36:724-8.

APPENDIX A: COPYRIGHT APPROVAL

Subject: Permission
Rudy Schlaf schlaf@mail.usf.edu
To: Jhon Figueroa jhonfigueroa@mail.usf.edu
Wed, Jun 12 2013 at 9:08 PM

absolutely…;-)

Rudy

-------- Original message --------
Subject: Permission
From: Jhon Figueroa <jhonfigueroa@mail.usf.edu>
To: "Schlaf, Rudy" <schlaf@mail.usf.edu>
CC:

On Jun 12, 2013, at 1:50 PM, Jhon Figueroa <jhonfigueroa@mail.usf.edu> wrote:

Dr Schlaf:

As you being a co-author, I would like to ask for your permission to use the following published articles in my dissertation:

J. Figueroa, S. Magaña, D.V. Lim, R. Schlaf. *Antibody immobilization using pneumatic spray: Comparison with the avidin–biotin bridge immobilization* method. J. Immunol. Methods 386, 1-9 (2012)

Thank you for granting you permission

Sincerely
--
Jhon Figueroa
University of South Florida
Surface Science Laboratory
3720 Spectrum Blvd., Suite 201
Tampa, FL 33612
Email: jhonfigueroa@mail.usf.edu
Phone: +1-813-974-9687
Fax +1-813-974-5250
Mobile: +1-813-298-7560
Office: IDRB 202 B

Appendix A (Continued)

Subject: Permission
Lim, Daniel lim@usf.edu
To: Figueroa, Jhon jhonfigueroa@mail.usf.edu
Wed, June 12, 2013 at 6:54 PM

You have my permission.

-------- Original message --------
Subject: Permission
From: Jhon Figueroa <jhonfigueroa@mail.usf.edu>
To: "Lim, Daniel" <lim@usf.edu>
CC:

Dr. Lim:

As you being a co-author, I would like to ask for your permission to use the following published articles in my dissertation:

J. Figueroa, S. Magaña, D.V. Lim, R. Schlaf. Antibody immobilization using pneumatic spray: Comparison with the avidin–biotin bridge immobilization method. J. Immunol. Methods 386, 1-9 (2012)

Thank you for granting you permission

Sincerely
--
Jhon Figueroa
University of South Florida
Surface Science Laboratory
3720 Spectrum Blvd., Suite 201
Tampa, FL 33612
Email: jhonfigueroa@mail.usf.edu
Phone: +1-813-974-9687
Fax +1-813-974-5250
Mobile: +1-813-298-7560
Office: IDRB 202 B

Appendix A (Continued)

Subject: Permission
Magana, Sonia <smagana@usf.edu>
To: Figueroa, Jhon jhonfigueroa@mail.usf.edu
Wed, June 12, 2013 at 2:08 PM

Jhon Figueroa, you have my permission to use the published article (data in article) for your dissertation.

Sincerely,

Sonia Magaña

-------- Original message --------
Subject: Permission
From: Jhon Figueroa <jhonfigueroa@mail.usf.edu>
To: "Magana, Sonia" <smagana@usf.edu>
CC:

Sonia Magana:

As you being a co-author, I would like to ask for your permission to use the following published articles in my dissertation:

J. Figueroa, S. Magaña, D.V. Lim, R. Schlaf. *Antibody immobilization using pneumatic spray: Comparison with the avidin–biotin bridge immobilization* method. J. Immunol. Methods 386, 1-9 (2012)

Thank you for granting you permission

Sincerely
--
Jhon Figueroa
University of South Florida
Surface Science Laboratory
3720 Spectrum Blvd., Suite 201
Tampa, FL 33612
Email: jhonfigueroa@mail.usf.edu
Phone: +1-813-974-9687
Fax +1-813-974-5250
Mobile: +1-813-298-7560
Office: IDRB 202 B

Appendix A (Continued)

Permissions Helpdesk <permissionshelpdesk@elsevier.com>
To: Jhon Figueroa <jhonfigueroa@mail.usf.edu>
Wed, Jun 12, 2013 at 2:05 PM

Dear Jhon:

Permission is covered by the rights you retain as an Elsevier journal author as outlined at http://www.elsevier.com/wps/find/authorsview.authors/rights, which include **Inclusion in a thesis or dissertation,** provided that proper acknowledgement is given to the original source of publication. Should you require any further clarification, please let me know. Best of luck with your dissertation.

Regards,

Hop Wechsler
Permissions Helpdesk Manager
Global Rights Department
Elsevier
1600 John F. Kennedy Boulevard
Suite 1800
Philadelphia, PA 19103-2899
Tel: +1-215-239-3520
Mobile: +1-215-900-5674
Fax: +1-215-239-3805
E-mail: h.wechsler@elsevier.com

Jhon Figueroa <jhonfigueroa@mail.usf.edu>
To: permissionshelpdesk@elsevier.com
Wed, Jun 12, 2013 at 2:02 PM

Good afternoon

My name is Jhon Figueroa and I would like to have a permission to use the following published articles in my dissertation:

J. Figueroa, S. Magaña, D.V. Lim, R. Schlaf. *Antibody immobilization using pneumatic spray: Comparison with the avidin–biotin bridge immobilization* method. J. Immunol. Methods 386, 1-9 (2012).

Thank you for your help

Jhon Figueroa
University of South Florida
Surface Science Laboratory
3720 Spectrum Blvd., Suite 201
Tampa, FL 33612
Email: jhonfigueroa@mail.usf.edu
Phone: +1-813-974-9687
Fax +1-813-974-5250
Mobile: +1-813-298-7560
Office: IDRB 202B

APPENDIX B: PUBLICATION 1: ANTIBODY IMMOBILIZATION USING PNEUMATIC SPRAY: COMPARISON WITH THE AVIDIN-BIOTIN BRIDGE IMMOBILIZATION METHOD

Note to Reader

Reprinted with permission from J. Immunol. Methods. 386, (2012) 1-9.

Appendix B (Continued)

Journal of Immunological Methods 386 (2012) 1–9

Contents lists available at SciVerse ScienceDirect

Journal of Immunological Methods

journal homepage: www.elsevier.com/locate/jim

Research paper

Antibody immobilization using pneumatic spray: Comparison with the avidin–biotin bridge immobilization method

Jhon Figueroa [a,1], Sonia Magaña [c,1], Daniel V. Lim [c], Rudy Schlaf [b,*]

[a] Department of Chemistry, University of South Florida, 4202 E. Fowler Ave., Tampa, FL 33620-5250, United States
[b] Department of Electrical Engineering, University of South Florida, 4202 E. Fowler Ave., Tampa, FL 33620-5101, United States
[c] Department of Cell Biology, Microbiology and Molecular Biology, University of South Florida, 4202 E. Fowler Ave., Tampa, FL 33620-7115, United States

ARTICLE INFO

Article history:
Received 6 June 2012
Received in revised form 3 August 2012
Accepted 6 August 2012
Available online 15 August 2012

Keywords:
Biosensors
Avidin–biotin bridge
Pneumatic spray
Thin films

ABSTRACT

The formation of a thin antibody film on a glass surface using pneumatic spray was investigated as a potential immobilization technique for capturing pathogenic targets. Goat-*Escherichia coli* O157:H7 IgG films were made by pneumatic spray and compared against the avidin–biotin bridge immobilized films by assaying with green fluorescent protein (GFP) transformed *E. coli* O157:H7 cells and fluorescent reporter antibodies. Functionality, stability, and immobilization of the films were tested. The pneumatic spray films had lower fluorescence intensity values than the avidin–biotin bridge films but resulted in similar detection for *E. coli* O157:H7 at 10^5–10^7 cells/ml sample concentrations with no detection of non-*E. coli* O157:H7 strains. Both methods also resulted in similar percent capture efficiencies. The results demonstrated that immobilization of antibody via pneumatic spray did not render the antibody non-functional and produced stable antibody films. The amount of time necessary for immobilization of the antibody was reduced significantly from 24 h for the avidin–biotin bridge to 7 min using the pneumatic spray technique, with additional benefits of greatly reduced use of materials and chemicals. The pneumatic spray technique promises to be an alternative for the immobilization of antibodies on glass slides for capturing pathogenic targets and use in biosensor type devices.

1. Introduction

The use of biosensors for the detection of pathogens in food and for monitoring bioterrorism pathogens has been a priority in recent years stimulating a growing interest to develop sensor devices to protect customers, military personnel and first responders (Lim et al., 2005; Arora et al., 2011). One of the most researched and developed field is the evanescent wave fluorescence biosensor (Taitt et al., 2005; Leung et al., 2007). Various devices or versions implementing the evanescent wave technology exist but share the common characteristic of immobilization of a recognition biomolecule onto an optical fiber, capillary, or planar waveguide (Taitt et al., 2005). The recognition biomolecule has affinity to a specific target, and when it comes in contact with the target, will bind to it or capture it. A detector or reporter biomolecule then binds to the captured target. The fluorophore on the detector biomolecule is excited by the evanescent wave and emits a fluorescent signal which is registered and processed by the biosensor device.

Most of the immunoassays developed for evanescent wave fluorescence biosensors use antibodies as the capture biomolecule. The antibodies are immobilized by a biotin–avidin intermediate layer covalently attached to the surface (Demarco and Lim., 2001; Golden et al., 2005; Zhu et al., 2005) indirect physical adsorption where avidin is directly adsorbed to the surface followed by a biotin conjugated antibody (Lim et al., 2005), or direct adsorption (Taitt et al., 2005). The physical adsorption method offers the advantage of simplicity, where fewer steps are performed and less

* Corresponding author.
E-mail address: schlaf@eng.usf.edu (R. Schlaf).
[1] These authors contributed equally to the work.

0022-1759/$ – see front matter © 2012 Published by Elsevier B.V.
http://dx.doi.org/10.1016/j.jim.2012.08.007

Appendix B (Continued)

reagents or chemicals are used. Often stated unwanted characteristics of the physical adsorption method are non-specific adsorption, denaturation on the surface at distinct pH, the probability that adsorbed proteins can leach or wash off from the surface if the coated substrate is exposed to a high liquid flow, and ionic strength of the buffers (Ulf et al., 1985a, 1985b; Lin et al., 1988). Some studies also have suggested that the physical adsorption of proteins can lead to denaturation of the biomolecule through surface–protein interactions resulting in non-specific binding of the antibodies to the target molecule (Moulin et al., 1999; Peluso et al., 2003; Karlsson et al., 2005). Most of these potential issues appear not to be a problem with the biotin–avidin covalent bridge method.

Optimization studies to the capture surface of various biosensors have been performed with the goal of improving sensitivity and reproducibility of the antibody capture surface but not all have been successful (Anderson et al., 1997; Plowman et al., 1999; Sapsford et al., 2001; Vijayendran and Leckband., 2001; Vermette et al., 2003; Cui et al., 2003; Gehring et al., 2006; Ngundi and Anderson, 2007; Batalla et al., 2008; Ikeda et al., 2009; Feng et al., 2011). In addition, requirement of trained personnel, extra protocol steps and reagents increase preparation time and material usage. This makes it harder to design and implement mass fabrication assay techniques. Alternative methods with potential for mass fabrication of waveguides incorporate technologies such as nanolithography and ink and laser printing (Borini et al., 2007; Lisboa el al., 2010; Sharma et al., 2010).

In this study, the possibility of using spray deposition of antibodies as an alternative to waveguide fabrication was investigated. The method presented here was demonstrated using goat anti-*Escherichia coli* O157:H7 antibody for the deposition onto glass waveguides through direct physical adsorption using a low flow concentric pneumatic nebulizer. The characteristics of the spray process offer advantages that include the fast deposition of waveguide films, an almost chemical free process, consistent coverage of the sprayed surface, and easy set up for manufacturing purposes. Additional potential benefits for a manufacturing environment are low cost and maintenance of the equipment. This makes the pneumatic spray an inexpensive and efficient immobilization technique.

2. Materials and methods

2.1. Materials

Plain microscopy glass slides were purchased from Globe Scientific Inc. (Paramus, NJ). The primary antibodies used for the immobilization processes were unlabeled goat anti-*E. coli* O157:H7 IgG (pneumatic spray process) and biotinylated labeled goat anti-*E. coli* O157:H7 IgG (avidin–biotin bridge process). Both antibodies were purchased from Kirkegaard & Perry Laboratories, Inc. (Gaithersburg, MD). The reporter antibody for the bacterial immunoassays, goat anti-*E. coli* O157:H7, was labeled with AlexaFluor 647 (AF647) using the AF647 protein labeling kit from Invitrogen (Eugene, OR) and following the manufacturer's instructions. AF647 labeled donkey anti-goat IgG (reporter secondary antibody) was purchased from Invitrogen (Eugene, OR) and Rhodamine Red conjugated AffiniPure donkey anti-goat IgG (reporter secondary antibody) was purchased from Jackson ImmunoResearch (West Grove, PA). The antibodies were rehydrated and stored according to the manufacturer's instructions. Luria–Bertani and Tryptic Soy media (Becton Dickinson Company, Sparks, MD) were used for the growth of the bacteria.

2.2. Bacteria

E. coli O157:H7 ATCC 35130 transformed to express green fluorescent protein (GFP) has been previously described (Simpson-Stroot et al., 2008) and was used for this study. GFP-*E. coli* O157:H7 was grown on Luria–Bertani media containing 100 μg/ml ampicillin and 5 mg/ml arabinose (LBAA) at 37 °C for 18–24 h. *E. coli* K12 ATCC 23590, *E. coli* O124:H7 CDC 3836-65, *Salmonella enterica* Typhimurium ATCC 19585, *Shigella flexneri* ATCC 12022, and *Staphylococcus aureus* ATCC 25923 were grown on Tryptic Soy Agar (TSA) at 37 °C for 18–24 h. Cell suspensions were prepared in 10 mM sodium phosphate/10 mM sodium chloride (NaPCl) buffer and diluted ten-fold. Direct counts were performed with Cellometers (Nexcelom Bioscience, Lawrence, MA) to approximate cell concentrations followed by spread plating on LBAA agar plates (for GFP-*E. coli* O157:H7) or TSA (all other bacteria) in triplicate to determine viable cell concentrations.

2.3. Immobilization of antibody via pneumatic spray

The pneumatic spray deposition process utilized a commercially-available concentric nebulizer with a low flow rate (3–10 μl/min) (Nebulizer Model DS-5, CETAC, Omaha, NE), which was placed into an in-house constructed apparatus to hold the nebulizer and a slide (Fig. S-1). A pressure regulated N_2 gas line was connected at the top of the nebulizer. A syringe pump (Pump 11 PicoPlus Harvard Apparatus, Holliston, MA) with a 1 ml syringe was connected to the back of the nebulizer. The glass slides were immersed in a solution of 10% KOH in methanol and incubated for 30 min followed by extensive rinsing with deionized water and dried in a flow of N_2 prior to spraying. A slide was placed on the slide assembly and positioned at a certain distance away from the nebulizer. The syringe was then filled with unlabeled goat anti-*E. coli* O157:H7 IgG solution. The parameters that were explored were the antibody concentration (100 or 200 μg/ml), the outflow N_2 pressure (20–60 PSI), the spraying time (2–32 min), the distance of the slide to the nebulizer (30–70 mm), and rotational rate of the glass slide (7.5–17 RPM). The only parameter that did not change was the syringe pump speed, which was set to 4 μl/min. After varying these parameters in a set of tests, a well-defined antibody film pattern was established using a 25×75 mm metal mask with fifteen 1×9 mm rectangular openings (rows). All pneumatic spray slides for experiments were prepared with the following parameters: 200 μg/ml antibody, 30 PSI outflow N_2 pressure, 7 min spraying time, 30 mm distance of the slide to the nebulizer, and 12 RPM. These parameters yielded at least 6 rows of immobilized antibody on the glass slides. The prepared slides were stored at 4 °C until further use.

Appendix B (Continued)

2.4. Immobilization of antibody via an avidin–biotin bridge

The procedure used to covalently immobilize antibody via an avidin–biotin bridge onto glass slides has previously been described (Rowe et al., 1999). Briefly, the glass slides were immersed in a solution of 10% KOH in methanol for 30 min, rinsed with deionized water and dried with nitrogen. The slides were treated for 1 h (under nitrogen) with a 2% solution of (3-mercaptopropyl) triethoxysilane in toluene followed by a 30 min incubation in 2.1 mM, 4-maleimidobutyric acid N-hydroxysuccinimide ester in 200 proof ethanol. The slides were rinsed with deionized water and incubated in 33 mM NeutrAvidin in NaPCl buffer at 27 °C for 2 h. The slides were rinsed with NaPCl buffer and placed in patterning templates, each consisting of a plexiglass holder and a polydimethylsiloxane (PDMS) flow module. A solution of 10 μg/ml biotinylated goat anti-*E. coli* O157:H7 IgG in NaPCl buffer was injected into 6 rows of the flow chamber. The slides were incubated for 18–22 h at 4 °C and rinsed using NaPCl with 0.5% Tween 20 (NaPClT) buffer. Slides were dried with nitrogen and used for assays or stored at 4 °C until further use.

2.5. Slide assays

Slides to be assayed with bacteria were tempered to 21 °C and placed inside plexi-glass holders with silicon gaskets. The gaskets had a 17.4×16.8 mm open area (292.32 mm^2) for sample application. One hundred microliters of the sample solution was added to the 292.32 mm^2 area and incubated for 30 min at 21 °C on a Belly Dancer Shaker (Stovall Life Science, Greensboro, NC). The slides were then rinsed 3× with 0.5 ml NaPClT buffer. Half a milliliter of 10 μg/ml AF647 anti-*E. coli* O157:H7 reporter solution was added and incubated for 15 min at 21 °C on the shaker. Each slide was subsequently rinsed 3× with 0.5 ml NaPClT buffer, removed from the plexi-glass holder and air dried.

2.6. Visualization of films and GFP bacteria

Slides prepared by pneumatic spray and avidin–biotin bridge were processed for visualization of antibody films in the following manner: 1 ml of a 5 μg/ml Rhodamine Red anti-goat IgG solution was added to each slide surface and incubated for 15 min at 21 °C. The slides were then rinsed 3× with NaPClT buffer and dried. Slides were examined on an Olympus BX60 Epifluorescent microscope (Olympus America Inc., Center Valley, PA) with UPlanFl 10× and UIS2 LUCPlan FLN 40× objectives and a Cy3 filter (Excitation 535–550, Emission 610–675, Beam splitter 565; Olympus America Inc., Center Valley, PA). Digital images were captured with an attached SPOT Flex color CCD camera (Diagnostic Instruments Inc., Sterling Heights, MI) and measurements made with the SPOT Advanced version 4.6 software.

Assayed slides with detector antibody were read using a biosensor array reader apparatus as described by (Golden et al., 2005). Each slide was illuminated using a 635 nm laser and emitted light from the AF647 fluorophores was captured as an image with a Peltier-cooled CCD camera.

Slides assayed with GFP bacteria were subjected to observation and imaging with epifluorescence microscopy using a U-MWIBA filter (Excitation 475–490, Emission 515–550, Dichroic 500; Olympus America Inc., Center Valley, PA) to determine GFP cell counts and calculate percent capture efficiencies.

2.7. Reproducibility and functionality of pneumatic spray antibody films

After establishing optimized pneumatic spray parameters, ten prepared slides were treated with reporter secondary antibody to check for pattern reproducibility of the immobilized antibody films. The slides were placed horizontally on a slide holder. One milliliter of 5 μg/ml AF647 donkey anti-goat IgG solution was added to the surface of each slide and incubated for 15 min at 27 °C. The slides were rinsed 3× with NaPClT buffer and air dried. Slides were read as described above.

The functionality of the pneumatic spray antibody films was then tested and compared against avidin–biotin bridge slides in various experiments. Slides were assayed with GFP-*E. coli* O157:H7 and non-target bacteria to determine the sensitivity and specificity, respectively, of the immobilized antibody. Five assay replicate experiments were performed in which each experiment consisted of three slides of each deposition method (overall total of 30 slides). For each experiment, one slide of each deposition method was assayed with GFP-*E. coli* O157:H7 at 1.2–4.6×10^5, 1.2–4.6×10^6, or 1.2–4.6×10^7 cells/ml. Slides from 3 different experiments (3 sets) were then subjected to the procedure for visualization of the antibody films with Rhodamine Red reporter secondary antibody. A different set of slides was assayed with non-target bacteria following the same assay procedure: *E. coli* K12, *E. coli* O124:H7, *S. enterica* Typhimurium, *S. flexneri*, and *S. aureus* suspensions at 10^7 cells/ml were used per slide.

In further testing of antibody functionally, 12 slides were prepared via the pneumatic spray process on the same day (day 0) and stored at 4 °C. On day 1 (24 h after slide prep) one slide was assayed with a GFP-*E. coli* O157:H7 sample at 10^7 cells/ml. One slide was then assayed at the same concentration each week for 12 weeks.

2.8. Data analysis

The images captured with the CCD camera were analyzed with the HLAB 5000 analysis software (Hanson Technologies, Inc., Carlisle, PA). Relative fluorescence intensities (RFU) were generated for 6 antibody rows per slide, termed regions of interest (ROI; 4.37 mm^2) and for the non-target areas to the top and bottom of the ROI (area between the rows), designated as the top and bottom backgrounds (1.09 mm^2 each) using a 1×6 array grid. Mean and standard deviation RFU values for each slide were calculated using the 6 replicates. Signal to noise ratios (SNR) were determined by subtracting the mean background fluorescence intensity from the mean intensity of the ROI and then dividing the results by the background standard deviation. Antibody rows with SNR≥3 were considered positive detection in the bacterial assays.

Percent capture efficiencies for each slide was determined by placing each GFP-*E. coli* O157:H7 assayed slide on the

Appendix B (Continued)

epifluorescence microscope and generating a digital image of the ROI for each row (total of 6 values per slide). The area imaged was 0.09486 mm^2. GFP-*E. coli* O157:H7 cells in the imaged area were counted using DAIME 1.31 software (Daims et al., 2006). The percent capture efficiency was calculated by dividing the number of GFP cells counted per image by the theoretical number of GFP cells per image and multiplying by 100. The theoretical number was calculated by dividing the number of cells applied by the antibody film area in contact with each cell sample. Each antibody film row for the pneumatic spray slides was estimated (based on mask dimensions) to be 16.80 mm^2 and 14.94 mm^2 for the avidin–biotin bridge slides.

Differences in pneumatic spray and avidin–biotin bridge fluorescence intensity values, SNR, and percent capture efficiencies were analyzed with the unpaired *t*-test or the Mann–Whitney test for sample groups with non-Gaussian distributions (GraphPad InStat v3.0, GraphPad Software, Inc., La Jolla, CA). Differences were considered statistically significant for *P* values less than or equal to 0.05 (95% confidence level). Error bars on the graphics represent the standard deviations of replicates.

2.9. Thin film analysis

The thickness of the pneumatic spray and avidin–biotin bridge antibody films were analyzed by ellipsometry (Null point Ellipsometer, Rudolph AutoEL III) with a single wavelength of 632.8 nm and a resolution of 3–10 Å at a fixed angle of 70°. Substrates for the process were prepared in the following manner: 2.5×4 cm silicon wafers were immersed in a solution of 10% KOH in methanol and incubated for 30 min followed by extensive rinsing with deionized water and subsequently dried with N_2. Ten silicon wafers were pneumatically sprayed with goat anti-*E. coli* O157:H7 as described in the pneumatic spray process. Each wafer was sprayed in duplicate using different deposition times of 2, 4, 7, 10 and 14 min. Two silicon wafers were used to immobilize anti-*E. coli* O157:H7 IgG via the avidin–biotin bridge process. A clean silicon wafer without immobilized antibodies was retained as a reference for each of the two immobilization techniques. The measurements were performed on silicon wafer due to its highly reflective characteristics and an index of refraction far from the region of biological transparent films allowing an accurate measurement of the films.

3. Results and discussion

3.1. Characteristics of antibody films

Figs. 1 and 2 display representative images of the immobilized antibody films visualized with a 635 nm laser/CCD camera apparatus and epifluorescence microscopy, respectively, for both pneumatic spray and avidin–biotin bridge prepared slides. Initial testing did not include addition of cells but rather direct visualization to determine pattern reproducibility of the pneumatic sprayed films (Fig. 1, A1). This was accomplished as all ten slides assayed in the reproducibility experiment had defined immobilized films with at least 6 defined rows for. Two slides had high AF647 background values as indicated by the higher residual fluorescence between the rows as seen in Fig. 1, A1. Some of the antibody films were slightly off-centered but adjusted in subsequent tests and some rows were slightly thicker than other rows. With this data and further observations, it was determined that the positioning, tightening, and slight deformity of the aluminum mask caused an uneven seal between the mask and slides allowing for thicker rows and sprayed antibody to enter underneath the mask and immobilized between the rows. This caused a low-density antibody coating in these areas with resultant antigen capture capability during the functionality tests (Figs. 1, B1–B2 and 2, E2). Overall, however, all slides had immobilized multi-row films that were suitable for bacterial assay testing.

When the antibody films were treated with Rhodamine Red detector IgG and viewed with fluorescence microscopy, images revealed a difference in surface morphology between the pneumatic spray and avidin–biotin bridge prepared slides (Fig. 2). The pneumatic sprayed films had a grainy, less homogeneous surface morphology than the avidin–biotin bridge films. The differences observed are explained by the way both immobilization procedures work. During the pneumatic spray process, the nebulizer head creates an aerosol containing small droplets of antibody solution. These droplets decrease in volume size with the distance traveled from the nebulizer to the surface of the glass as the water evaporates, resulting in an increase in antibody concentration within the droplet forcing the IgG molecules to get closer to each other. Furthermore, the pH of the antibody solution influences aggregation. The isoelectric point of IgG is between 6.1 and 6.5 (Cheng et al., 2011) but the pH of the solution before spraying was 4.8±0.1. Hence, the antibody had a net positive charge in the solution. Majhi et al. (2006) suggested that the protein aggregation is driven mainly by electrostatic attractive forces and that the net charges produced under non denaturing conditions are not relevant. Moreover, it was found that maximum aggregation actually occurs at a pH level where the net charge is positive. It can be hypothesized that two main factors for aggregate formation on the pneumatic spray films are an increase in antibody concentration within the droplet and enhanced electrostatic attraction due to the high antibody density. The antibody droplets are immobilized randomly and overlap each other on the surface; this creates the non-uniform, grainy film seen on the Rhodamine Red detector images. The covalently attached film produced a much more homogeneous result with some circular spots on the surface; an explanation to these circular spots is unknown.

The data obtained from the ellipsometer showed a linear behavior between the thickness of the antibody film made by pneumatic spray and the deposition time with a linear regression of 0.9874. The average thickness calculated for the avidin–biotin bridge technique was 183.16±8.54 Å, whereas the standard deposition time of 7 min for the pneumatic spray process showed an average thickness of 155.25±11.78 Å. The thickness values of both films were similar. However, the thickness of the sprayed slides corresponds entirely to the sprayed antibody, whereas in the case of the avidin–biotin bridge films, the thickness is a result of the covalent linked bridge (silane, cross-linker, avidin, and biotin conjugated antibody). This suggests that

Appendix B (Continued)

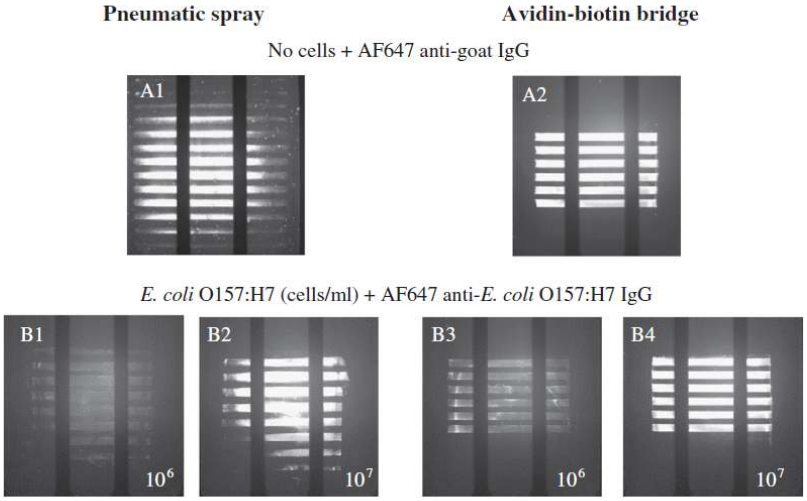

Fig. 1. Visualization of immobilized antibody film patterns using AlexaFluor 647 (AF647) labeled IgG as the reporter antibody, a 635 nm laser, and Peltier-cooled CCD camera. Fluorescence obtained in the images was due to the emitted light from AF647 excited by the 635 nm laser. Images displayed (approximately 90 mm^2 of slide area) are representative of slides prepared with pneumatic spray (A1, B1, B2) and avidin–biotin bridge (A2, B3, B4) antibody immobilization. Slides represented in images A1 and A2 show the fluorescence response after being subjected to AF647 labeled anti-goat IgG (secondary reporter antibody) which bound to the immobilized goat anti-*E. coli* O157:H7 IgG. Slides represented in images B1–B4 show the fluorescence response after addition of GFP-*E. coli* O157:H7 cells at 10^6 (B1, B3) and 10^7 cells/ml (B2, B4) followed by AF647 labeled goat anti-*E. coli* O157:H7 IgG (primary reporter antibody).

the sprayed films have a higher antibody density than the avidin–biotin bridge attached films. The corresponding mass of the deposited antibody was calculated to be around 31.69 ng/mm^2 for the pneumatic spray films, while the deposited mass for the avidin–biotin bridge has been reported to be between 2.2 ng/mm^2 (Moulin et al., 1999; Batalla et al., 2008) and 4.74 ng/mm^2 (Anderson et al., 1997; Gehring et al. 2006). This is not surprising since the spray process is a non-equilibrium technique, whereas the covalent attachment in solution is equilibrium controlled. In other words, the spray technique can load the surface with antibodies at any desired density, while the chemical attachment in solution has a maximum density that is governed by the rate constants of the participating chemical reactions.

3.2. Sensitivity and specificity of pneumatic spray assayed slides

Fig. 3A and B graphs the mean fluorescence intensities for the ROI and background areas in relative fluorescence units (RFU) as measured for *E. coli* O157:H7 samples assayed on the pneumatic spray and avidin–biotin bridge prepared slides. The mean ROI RFU at 10^5 cells/ml were similar for both slide immobilization processes with no significant difference ($P=0.1581$), but were significantly different at 6 ($P=0.0072$) and 10^7 cells/ml ($P=0.0104$) in which the avidin–biotin bridge slides had higher values. Mean SNR values (Fig. 3C) yielded no detection at 10^5 cells/ml for pneumatic spray and avidin–biotin bridge slides, 0% and 40% detection at 10^6 cells/ml and 60% and 100% detection at 10^7 cells/ml for pneumatic spray and avidin–biotin bridge, respectively. There were no significant differences ($P=$ 0.1175) between the 10^5 cells/ml SNR values, but there were significant differences ($P<0.0001$) at the 10^6 and 10^7 cells/ml concentrations, where avidin–biotin bridge slides had higher values. This difference was a result of the slightly lower ROI RFU (Fig. 3A) in combination with higher background values (Fig. 3B) that caused lower SNR values for the pneumatic spray slides. The lower SNR values were not an indication of decreased antibody functionality within the sprayed films but a direct consequence of the spraying process. As mentioned earlier, the uneven seal between the mask and slides allowed for a low-density antibody coating between the rows, where the background readings were taken (any difference in seal tightness on a particular slide can allow more or less antibody leak under the mask and create the large standard deviation for the samples as shown in Fig. 3C). This in turn resulted in antigen capture during these tests (Figs. 1, B1–B2 and 2, E2) and caused increased background values.

In contrast, the slightly lower ROI RFU values for the pneumatic sprayed slides were likely a result of the detachment of some of the antibody from the surface during sample incubation. The representative images D1 and E1 in Fig. 2 demonstrate that the *E. coli* O157:H7 cells applied and captured on the sprayed slide surface were fluorescent after treatment with Rhodamine Red detector IgG whereas the cells on the avidin–biotin bridge slides were not. This suggests that cells immobilized on sprayed slides were coated with a certain amount of capture antibody during assay sample incubation. Once the Rhodamine Red anti-goat IgG was added, it bound to the goat anti-*E. coli* O157:H7 IgG on the cells' surfaces. This coating most likely results in blockage of some of the epitopes on the cell surface thereby

Appendix B (Continued)

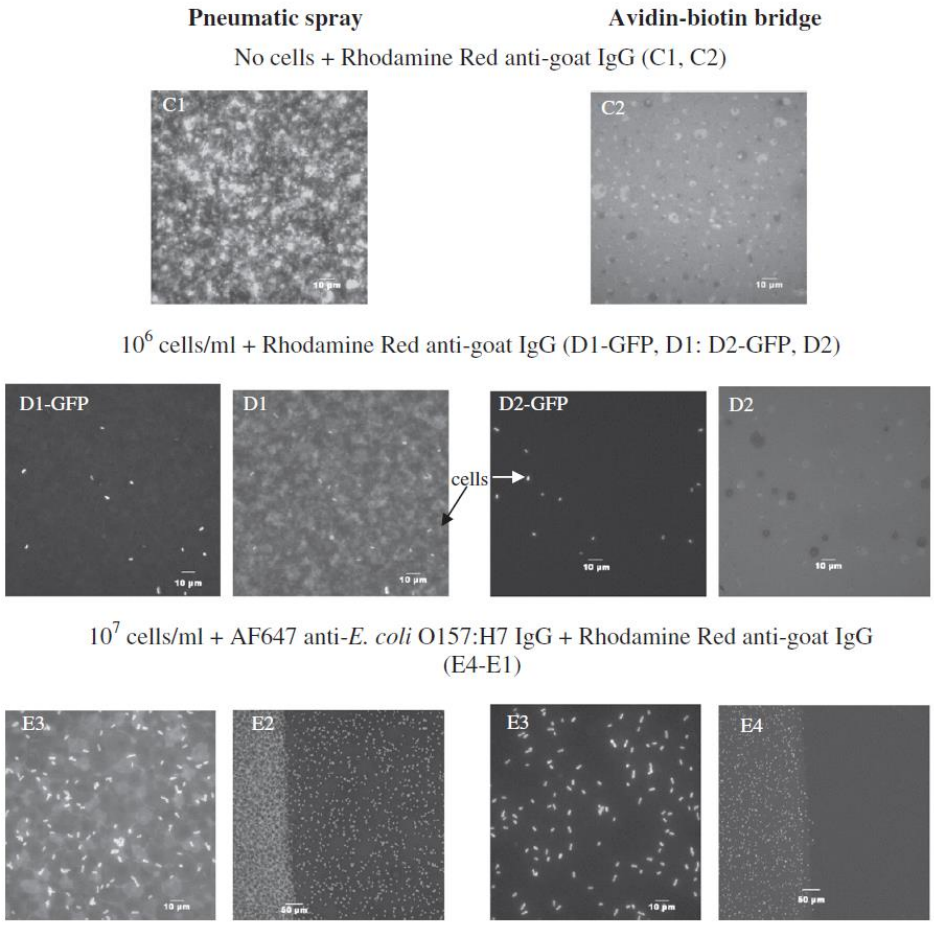

Fig. 2. Visualization of GFP-*E. coli* O157:H7 cells and immobilized antibody films by epifluorescence microscopy. A Cy3 filter (excitation 535–550, emission 610–675, beam splitter 565) and SPOT Flex CCD camera was used to obtain all images except for D1-GFP and D2-GFP where a U-MWIBA filter (excitation 475–490, emission 515–550, dichroic 500) was used to view only the GFP-*E. coli* O157:H7 cells. Images displayed are representative of slides prepared with pneumatic spray (C1, D1-GFP, D1, E1, E2) and avidin–biotin bridge (C2, D2-GFP, D2, E3, E4) antibody immobilization. Slides represented in images C1 and C2 show the fluorescence response after incubation with secondary reporter antibody, Rhodamine Red (RR) donkey anti-goat IgG (which bound to the immobilized goat anti-*E. coli* O157:H7 IgG). Slides represented in images D1-GFP (same area as D1), D1, D2-GFP (same area as D2), and D2 show the fluorescence response after incubation with GFP-*E. coli* O157:H7 cells at 10^6 cells/ml followed by RR anti-goat IgG. Slides represented in images E1–E4 show the fluorescence response after incubation with GFP-*E. coli* O157:H7 cells at 10^7 cells/ml followed by AF647 labeled goat anti-*E. coli* O157:H7 IgG (primary reporter antibody) and then RR anti-goat IgG. Color images were transformed to grayscale where white is fluorescence and black is no fluorescence but do not necessarily represent quantified fluorescence intensities.

reducing the amount of attachment of reporter antibody. As a consequence the measured fluorescence intensity is lower. This phenomenon appears absent on assays on the covalently attached films. This is a qualitative observation and further studies will need to be performed to confirm and quantify this process.

The ROI RFU values resultant from the shelf life study were 1600–4300 with no significant increase or decrease of fluorescence intensity over the 100 days of storage (Fig. S-2). The ROI RFU values were similar to those generated by the antibody functionality experiments (Fig. 3A) at the same concentration with no significant difference ($P=0.7155$). Mean SNR values (Fig. S-2) yielded positive detection of *E. coli* O157:H7 at 10^7 cells/ml, showing that there was no loss of detection for the pneumatic spray slides stored up to 100 days. There was a significant difference ($P<0.0001$) between the SNR values for the stored slides and the antibody functionality experiments (Fig. 3C). The SNR values for the stored slides were higher. This difference was due to the lower background RFU achieved for the stored slides in comparison to the significantly higher ($P<0.0001$) values for the antibody functionality experiment slides (Fig. 3B). The mean background RFU values were between 1400 and 2500 in the first 3 slides but then decreased to 900–1700 for the

Appendix B (Continued)

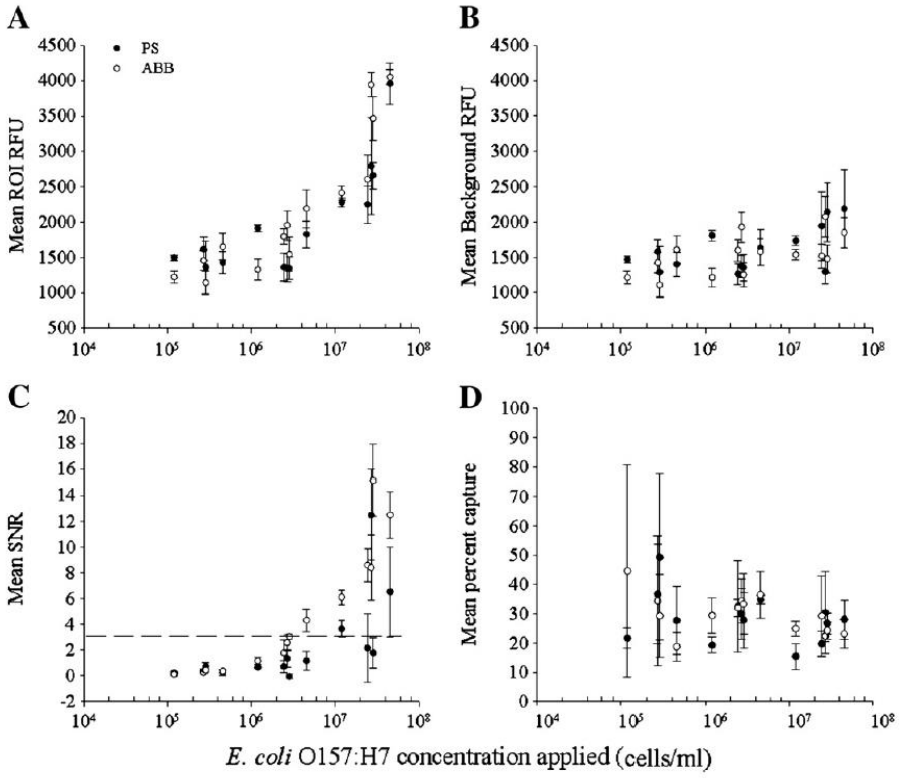

Fig. 3. *E. coli* O157:H7 assay and capture data obtained using pneumatic spray (PS) and avidin–biotin bridge (ABB) prepared slides. One sample concentration ranging from 10^5 to 10^7 cells/ml was used per slide with each slide having 6 replicate points (rows). Five slides were assayed per log concentration except for 10^5 cell/ml of which 4 were done. [A] Mean region of interest (ROI) and [B] background relative fluorescence units (RFU) for each slide assayed with *E. coli* O157:H7 and AF647 detector antibody. [C] Mean signal to noise ratios (SNR) calculated for each slide by subtracting the mean background RFU from the mean ROI RFU and then dividing by the mean background standard deviation. Sample slides with SNR ≥ 3 (displayed via the horizontal dotted line) were considered as positive detection for *E. coli* O157:H7. [D] Mean percent capture efficiencies obtained for each slide assayed with *E. coli* O157:H7. Each circle point in each graph is 1 assayed slide at 1 cell concentration with error bars representing the standard deviation of the 6 replicates.

rest of the slides. It is possible that the cause was loss of the antibody indirectly immobilized between the film rows.

The specificity experiments yielded no detection of any of the non-*E. coli* O157:H7 strains tested. The mean SNR values of all pneumatic spray and avidin–biotin bridge assayed slides were $\leq 0.2 \pm 2$. In comparison, the *E. coli* O157:H7 positive control yielded a mean SNR of 15.2 ± 10.5 for the pneumatic spray and 14.6 ± 6.4 for the avidin–biotin bridge slides.

3.3. Cell capture efficiencies of assayed slides

The mean percent capture efficiencies (Fig. 3D) were similar for both slide immobilization processes at each concentration. There were no significant differences between the two techniques at 10^5 ($P = 0.5600$), 10^6 ($P = 0.1673$), or 10^7 cells/ml ($P = 0.9964$). Mean percent capture efficiencies against time stored ranged from 11 to 73% with the median range at 10–40% (Fig. S-2D). There was no significant difference ($P = 0.6599$) between these percent capture efficiencies and those generated by the antibody functionality experiments.

The similarity of the results suggests a compensatory process between antibody density and antibody orientation. The sprayed prepared slides have a higher antibody density with randomly immobilized antibody on the surfaces whereas the avidin–biotin bridge prepared slides have less antibody but clearly have a higher degree of orientation (Gehring et al., 2006). Studies suggest that random orientation reduces the ability of the antibody to react with the antigen due to the impact of steric hindrance generated by the arbitrary alignment of the antibodies (Lu et al., 1996; Xu and Zhao et al., 2006b). However, a reduction on antigen binding activity is not just related to randomly oriented films, because (Spitznagel et al. (1993) suggested that, despite the favorable orientation of the antibody at the surface of covalently attached films, molecular crowding can denature the fragment antigen binding (Fab) region making it necessary to find an optimal maximal coverage, which is not necessarily achieved by the avidin–biotin bridge method.

Appendix B (Continued)

Peluso et al. (2003) found an average increase of 33% in antigen binding activity for specifically oriented antibodies when compared with randomly oriented antibodies with the same antibody density at the surface. At this point, it would seem likely that the avidin–biotin bridge method with orientated antibodies would supersede the sprayed method in terms of capturing cells but instead the sprayed prepared slides compensate this with antibody density.

As mentioned earlier, the pneumatic spray process creates a grainy surface morphology where antibody droplets are immobilized on top of each other or are overlapping. This creates a type of multi-layer antibody film where only the outer layer of randomly adsorbed antibody is responsible for the interaction with the antigen (Ngundi and Anderson, 2007) while the inner antibody layer acts as an attachment support by the antibody–antibody and antibody–surface interactions. (Kamyshny et al. (2001) suggested that the formation of antibody aggregates can favor the adsorption at the surface due to attachment of the aggregation unit to the surface, and that an increase in antigen binding activity is expected with a denser antibody layer. Xu and Williams et al. (2006a) noted that having a dense antibody surface reduces antibody structural unfolding and thereby increases the antigen binding capacity. Separate experiments (data not shown) confirmed this property by demonstrating that increases in antibody film thickness initially increased both capture efficiency and sensitivity, but ultimately reached thresholds after which no further improvement was achieved. Similarly, the avidin–biotin bridge film has a maximum threshold on antibody density at the surface. Peluso et al. (2003) using a gold coated glass surface, found that the oriented antibody immobilization achieved with the covalent attachment method usually resulted in a collateral decrease of the surface coverage (antibody density) when compared with random attachment.

The stability and functionality of an immobilized antibody film strongly depend on the type of substrate used, antibody density, and configuration of the antibody at the solid surface as well as its surrounding environment. In this study, immobilization of *E. coli* O157:H7 IgG on a glass surface using the pneumatic spray technique yielded a high density film with characteristics of antibody aggregation which in turn supported immobilization, stability, and potentially increased shelf life.

4. Conclusions

Polyclonal IgG antibody was successfully immobilized in a multi-row film onto glass waveguides using a pneumatic nebulizer. The results showed that the functionality of the high density, randomly immobilized antibody was similar to assays prepared with the often used avidin–biotin covalent attachment strategy. An investigation of the morphology of the pneumatic spray films suggests that about one to three compact layers of antibody are attached to the glass surface. The adherence of the layers is strong enough to withstand standard rinsing processes, allowing the efficient performance of assays. In summary, the reproducibility of the spraying method, the good stability of the films, capture efficiency, and the significant reduction in preparation time and chemical waste makes this new technique a promising alternative to traditional avidin–biotin covalent methods.

Acknowledgments

The authors are grateful to the National Science Foundation for funding this project (CBET 0854354).

Appendix A. Supplementary data

Supplementary data to this article can be found online at http://dx.doi.org/10.1016/j.jim.2012.08.007.

References

Anderson, G.P., Jacoby, M.A., Ligler, F.S., King, K.D., 1997. Effectiveness of protein A for antibody immobilization for a fiber optic biosensor. Biosens. Bioelectron. 12, 329–336.
Arora, P., Sindhu, A., Dilbaghi, N., Chaudhury, A., 2011. Biosensors as innovative tools for the detection of food borne pathogens. Biosens. Bioelectron. 28, 1–12.
Batalla, P., Fuentes, M., Grazu, V., Mateo, C., Fernandez-Lafuente, R., Guisan, J.M., 2008. Oriented covalent immobilization of antibodies on physically inert and hydrophilic support surfaces through their glycosidic chains. Biomacromolecules 9, 719–723.
Borini, S., Staiano, M., Rocchia, M., Rossi, A.M., Rossi, M., D'Auria, S., 2007. Advanced nanotechnological approaches for designing protein-based "lab-on-chips" sensors on porous silicon wafer. Recent Pat DNA Gene Seq, 1, p. 1.
Cheng, M.S., Lau, S.H., Chow, V.T., Toh, C.S., 2011. Membrane-based electrochemical nanobiosensor for Escherichia coli detection and analysis of cells viability. Environ. Sci. Technol. 45, 6453–6459.
Cui, X., Pei, R., Wang, Z., Yang, F., Ma, Y., Dong, S., Yang, X., 2003. Layer-by-layer assembly of multilayer films composed of avidin and biotin-labeled antibody for immunosensing. Biosens. Bioelectron. 18, 59–67.
Daims, H., Lucker, S., Wagner, M., 2006. Daime, a novel image analysis program for microbial ecology and biofilm research. Environ. Microbiol. 8, 200.
Demarco, D.R., Lim, D.V., 2001. Direct detection of Escherichia coli 0157:H7 in unpasteurized apple juice with an evanescent wave biosensor. J. Rapid Methods Autom. Microbiol. 9, 241–257.
Feng, B., Huang, S., Luo, G.F., Jia, D., Dai, Y., 2011. 3D antibody immobilization on a planar matrix surface. Biosens. Bioelectron. 28, 91–96.
Gehring, A.G., Albin, D.M., Bhunia, A.K., Reed, S.A., Tu, S., Uknalis, J., 2006. Antibody microarray detection of Escherichia coli O157:H7: quantification, assay limitations, and capture efficiency. Anal. Chem. 78, 6601–6607.
Golden, J., Shriver-Lake, L., Sapsford, K., Ligler, F.S., 2005. A "do-it-yourself" array biosensor. Methods 37, 65–72.
Ikeda, T., Hata, Y., Ninomiya, K., Ikura, Y., Takeguchi, K., Aoyagi, S., Hirota, R., 2009. Oriented immobilization of antibodies on a silicon wafer using Si-tagged protein A. Anal. Biochem. 385, 132–137.
Kamyshny, A., Lagerge, S., Partyka, S., Relkin, P., Magdassi, S., 2001. Adsorption of native and hydrophobized human IgG onto silica: isotherms, calorimetry, and biological activity. Langmuir 17, 8242–8248.
Karlsson, M., Ekeroth, J., Elwing, H., Carlsson, U., 2005. Reduction of irreversible protein adsorption on solid surfaces by protein engineering for increased stability. J. Biol. Chem. 280, 25558–25564.
Leung, A., Shankar, M.P., Mutharasan, R., 2007. A review of fiber-optic biosensors. Sens. Actuators B. Chem. 125, 688–703.
Lim, D.V., Simpson, J.M., Kearns, E.A., Kramer, M.F., 2005. Current and developing technologies for monitoring agents of bioterrorism and biowarfare. Clin. Microbiol. Rev. 18, 583–607.
Lin, J.N., Herron, J., Andrade, J.D., Brizgys, M., 1988. Characterization of immobilized antibodies on silica surfaces. IEEE Trans. Biomed. Eng. 35, 466–471.
Lisboa, P., Valsesia, A., Colpo, P., Rossi, F., Mascini, M., 2010. Nanopatterned surfaces for bio-detection. Anal. Lett. 43, 1556–1571.
Lu, B., Smytha, R.M., O'Kennedy, R., 1996. Oriented immobilization of antibodies and its applications in immunoassays and immunosensors. Analyst 121, 29–32.
Majhi, P.R., Ganta, R.R., Vanam, R.P., Seyrek, E., Giger, K., Dubin, P.L., 2006. Electrostatically driven protein aggregation: B-lactoglobulin at low ionic strength. Langmuir 22, 9150–9159.

Appendix B (Continued)

Moulin, A.M., O'Shea, S.J., Badley, R.A., Doyle, P., Welland, M.E., 1999. Measuring surface-induced conformational changes in proteins. Langmuir 15, 8776–8779.
Ngundi, M.M., Anderson, G.P., 2007. Failure of layer-by-layer multilayers composed of neutravidin-biotin-labeled antibody for sandwich fluoroimmunosensing. Biosens. Bioelectron. 22, 3243–3246.
Peluso, P., Wilson, D.S., Do, D., Tran, H., Venkatasubbaiah, M., Quincy, D., Heidecker, B., Poindexter, K., Tolani, N., Phelan, M., Witte, K., Jung, L.S., Wagner, P., Nock, S., 2003. Optimizing antibody immobilization strategies for the construction of protein microarrays. Anal. Biochem. 312, 113–124.
Plowman, T.E., Durstchi, J.D., Wang, H.K., Christensen, D.A., Herron, J.N., Reichert, W.M., 1999. Multiple-analyte fluoroimmunoassay using an integrated optical waveguide sensor. Anal. Chem. 71, 4344–4352.
Rowe, C.A., Tender, L.M., Feldstein, M.J., Golden, J.P., Scruggs, S.B., MacCraith, B.D., Cras, J.J., Ligler, F.S., 1999. Array biosensor for simultaneous identification of bacterial, viral, and protein analytes. Anal. Chem. 71, 3846–3852.
Sapsford, K.E., Liron, Z., Shubin, Y., S., Ligler, F.S., 2001. Kinetics of antigen binding to arrays of antibodies in different sized spots. Anal. Chem. 73, 5518–5524.
Sharma, H., Nguyen, D., Chen, A., Lew, V., Khine, M., 2010. Unconventional low-cost fabrication and patterning techniques for point of care diagnostics. Ann. Biomed. Eng. 39, 1313–1327.
Simpson-Stroot, J.M., Kearns, E.A., Stroot, P.G., Magaña, S., Lim, D.V., 2008. Monitoring biosensor capture efficiencies: development of a model using GFP-expressing Escherichia coli O157:H7. J. Microbiol. Methods 72, 29–37.
Spitznagel, T.M., Jacobs, J.W., Clark, D.S., 1993. Random and site-specific immobilization of catalytic antibodies. Enzyme Microb. Technol. 15, 916–921.
Taitt, C.R., Anderson, G.P., Ligler, F.S., 2005. Evanescent wave fluorescence biosensors. Biosen. Bioelectron. 20, 2470–2487.
Ulf, J., Magnus, M., Inger, R., 1985a. Immobilization of immunoglobulins on silica surfaces. Biochem. J. 227, 363–371.
Ulf, J., Magnus, M., Inger, R., 1985b. Immobilization of immunoglobulins on silica surfaces stability. Biochem. J. 227, 373–378.
Vermette, P., Gengenbach, T., Griesser, H.J., Divisekera, U., Kambouris, P.A., Meagher, L., 2003. Immobilization and surface characterization of NeutrAvidin biotin-binding protein on different hydrogel interlayers. J. Colloid Interface Sci. 259, 13–26.
Vijayendran, R.A., Leckband, D.E., 2001. A quantitative assessment of heterogeneity for surface-immobilized proteins. Anal. Chem. 73, 471–480.
Xu, H., Lu, J.R., Williams, D.E., 2006a. Effect of surface packing density of interfacially adsorbed monoclonal antibody on the binding of hormonal antigen human chorionic gonadotrophin. J. Phys. Chem. B. 110, 1907–1914.
Xu, H., Zhao, X., Grant, C., Lu, J.R., 2006b. Orientation of a monoclonal antibody adsorbed at the solid/solution interface: a combined study using atomic force microscopy and neutron reflectivity. Langmuir 22, 6313–6320.
Zhu, P., Shelton, D.R., Karns, J.S., Sundaram, A., Li, S., Amstutz, P., Tang, C., 2005. Detection of water-borne E. coli O157 using the integrating waveguide biosensor. Biosens. Bioelectron. 21, 678–683.

APPENDIX C: PUBLICATION 2: CHARACTERIZATION OF FULLY FUNCTIONAL SPRAY-ON ANTIBODY THIN FILMS.

Note to Reader

Document under revision in the Journal of Applied Surface Science (October 2013).